# Quantifying variation in teeth of Late Triassic vertebrates: implications for identification, palaeoecology, and biostratigraphy

Emily Keeble

Dissertation submitted to the faculty of the Virginia Polytechnic Institute and State University in partial fulfilment of the requirements for the degree of

Doctor of Philosophy

In

Geosciences

Sterling Nesbitt (Chair)

Michelle Stocker

Rachel Ried

Nicolas Campione

August 28th, 2025

Blacksburg, Virginia

Keywords: vertebrate palaeontology, teeth, variation, Archosauria, Hybodontoidea, Aetosauria

Quantifying variation in teeth of Late Triassic vertebrates: implications for identification, palaeoecology, and biostratigraphy

Emily Keeble

## ABSTRACT

The Triassic Period (~252–201.5 Ma) represents one of the most dynamic intervals in Earth's history, characterised by major evolutionary radiations following the end-Permian mass extinction, the emergence and diversification of key vertebrate lineages, and the establishment of modern terrestrial ecosystems. Whereas macrofossils tend to capture greater attention, small fossils are equally as important to reconstructing vertebrate communities of ancient ecosystems. This is especially true of fossils found from microvertebrate localities (deposits where 75% of remains are <50mm) as these record both small vertebrates and small parts of larger organisms. Tooth fossils are among the most readily preserved in these sites thanks to their relative hardness and resistance to chemical and physical weathering. However, when teeth are found isolated, it can be difficult to ascribe them to a species or even clade as many teeth come from currently unknown animals, and there is a high degree of convergence with little variation among many archosaur teeth in the Triassic Period. Different methods have been used to quantify variation and identify isolated teeth, particularly within Dinosauria, but 3D methods have been underutilised, despite the increasing availability of scanned fossils and increased information on dimensionality that can be captured by using 3D models. My dissertation quantified variation in

tooth morphologies at three different taxonomic levels: within a species, within a clade, and among clades with similar inferred diet, and employs quantitative and qualitative analyses on a broad range of taxa. The goal of this work was to test whether the variation in tooth morphology, once quantified, allows for the identification of isolated teeth of unknown taxa in microvertebrate deposits, and as an aid to determine the biostratigraphic utility of the specimens tested. In my first chapter, I looked at variation in tooth shape and discrete characters within a clade, using aetosaurs (quadrupedal terrestrial pseudosuchians with extensive armour across most of the body) and their close outgroups as an example. Interestingly, isolated aetosaur teeth are exceptionally rare in deposits where other aetosaur fossils, such as osteoderms, are common; however, it is unknown whether this is an artifact of aetosaurs generally having fewer teeth than other archosaurs or the result of the difficulty of identifying isolated aetosaur teeth. To determine if aetosaur teeth are diagnostic and can be identified apart from other Triassic Period archosaurs, I created matrices that use 3D geometric morphometrics (3DGM) and non-metric multidimensional scaling (NMDS) to both examine variation and evaluate whether these techniques could be used to help identify isolated aetosaur teeth, particularly in microvertebrate deposits. I found that, broadly, aetosaurs can be distinguished from the outgroups tested. When isolated teeth suspected to be from aetosaurs were added into the matrix, they plotted within the space of the majority of aetosaurs in the 3DGM. In the NMDS morphospace, they plotted more disparately, but still away from the outgroups, suggesting that these methods are useful in identifying isolated aetosaur teeth. My second chapter utilised the methods from my first chapter and applied them to a wider group of animals – the carnivorous archosaurs of the Triassic Period (e.g. *Coelophysis*, *Batrachotomus*, *Smilosuchus*) to test whether distantly related carnivorous taxa retain a similar tooth form, and whether it is possible to identify teeth to major clade despite

these taxa sharing the ancestral tooth shape for this clade (i.e., recurved, serrated, and laterally compressed). I found that even though some taxa (e.g. *Diandongosuchus*, *Ornithosuchus*, *Riojasuchus*) overlap greatly in dental morphospace using 3D morphometrics and within the NMDS analysis morphospace plots, dinosaurs tend to plot away from pseudosuchians in the 3DGM, implying that 3DGM may be useful in separating these two clades. My third and final chapter further addressed intraspecific tooth variation and described a new species of hybodontiform shark based on teeth from a highly productive microvertebrate locality called the 'Green Layer' near the Petrified Forest National Park, Arizona, USA. Chondrichthyan (shark) teeth can be useful for biostratigraphy, but differences in tooth shape throughout the mouth can make disentangling species from one another difficult. Additionally, specimens are also known from a second site within Petrified Forest National Park, and I examined variation between the two assemblages using NMDS and conducted a 3DGM analysis on the 'Green Layer' teeth revealing that there is limited morphological variation in this new species. When I conducted a NMDS analysis, the two assemblages strongly overlapped suggesting that these assemblages are indeed the same species and as tooth shape is highly conserved, they are a useful index taxon for the early Revueltian. My dissertation found that the two methods (3DGM and NMDS) used in each chapter are useful on a broad range of vertebrate taxa in combination, from pseudosuchians to chondrichthyans and highlights the importance of small and isolated fossils in reconstructing vertebrate communities.

Keywords: vertebrate palaeontology, teeth, variation, Archosauria, Hybodontoidea, Aetosauria

Quantifying variation in teeth of Late Triassic vertebrates: implications for identification, palaeoecology, and biostratigraphy

Emily Keeble

## GENERAL AUDIENCE ABSTRACT

The Triassic Period (~252–201.5 Ma) was an important time for the evolution of vertebrates and the establishment of modern ecosystems. Large animals are often studied, but small animals are equally important in reconstructing the composition of these ecosystems. Especially useful for this are microvertebrate sites (where 75% of remains are <50mm) as these sites record not only small animals, but also small parts, such as teeth, of larger animals. Tooth fossils are more easily preserved than most as they are hard and resist chemical and physical weathering, meaning that we find a lot of them. However, when these teeth are found isolated, it can be difficult to ascribe them to a species, or even type of animal, as they often come from previously unknown animals. Different methods have been used to quantify variation and identify isolated teeth, particularly in dinosaurs, but methods involving 3D models and methods are underutilised, despite the increasing availability of scanned fossils and the fact that more information can be captured in 3D models. My dissertation looked at variation in tooth shapes and characteristics at three different levels: within a species, within a group of related animals, and among animals from a much wider group called archosaurs that share a carnivorous diet. My goal was to test whether quantifying variation helps identify isolated teeth in microvertebrate sites, and, in turn, whether

these identifications aid in correlating rock units of the same age. In my first chapter, I looked at variation in tooth shape and features within a group, using aetosaurs (four-legged, heavily armoured reptiles) and their close relatives as an example. Aetosaur teeth are exceptionally rare in deposits where we do find other aetosaur fossils, such as their armour plates, but it is unclear whether there weren't many teeth to be found, or rather we are finding them, but they are being misidentified. To test whether aetosaur teeth can be distinguished from other archosaur teeth, I created visual plots that used techniques that show similarity of overall shape of the teeth and I used discrete characteristic (e.g. presence or absence of serrations) plots to examine variation that aid in these identifications, particularly in microvertebrate sites. I found that, broadly, aetosaurs can be distinguished from their relatives. When isolated teeth suspected to come from aetosaurs were added into the shape plots, they plotted with aetosaurs whereas in the discrete characteristic plots, isolated teeth plotted more disparately, but still away from their non-aetosaur relatives. This suggests that these methods can be used to identify isolated aetosaur teeth. My second chapter took the methods from the first chapter and applied them to a wider group of animals – the carnivorous archosaurs of the Triassic Period – to test whether it is possible to identify teeth that are all similar due to ancestry and diet. All teeth in this chapter are recurved, serrated, and narrow. I find that although many animals plotted in the same place in both analyses, dinosaurs tended to plot away from the crocodile relatives in the shape plot, thus implying that this method may be useful in separating these two groups. My third chapter examined tooth variation limits and described a new species of hybodontiform shark from a highly productive site called the 'Green Layer' near the Petrified Forest National Park, Arizona, USA. Shark teeth are useful in correlating rocks of the same age, but differences in tooth shape throughout the mouth can make disentangling species from one another difficult. Additionally,

specimens are known from a second site within Petrified Forest National Park, and I examined variation between the two populations using the methods from my first two chapters. In the discrete characteristic plot, the two populations overlap, supporting that they are indeed the same species and as tooth shape is conserved in this species, they may be a useful species for correlating a rock unit called the Sonsela Member. My dissertation found that the two methods used in each chapter are useful in quantifying variation and helping to identify some teeth of a broad range of vertebrates, from dinosaurs to sharks, and highlighted the importance of small and isolated fossils in reconstructing vertebrates in their ecosystems.

**ACKNOWLEDGEMENTS**

Before anyone else, I must thank my advisor, mentor and committee chair, Dr. Sterling Nesbitt. Through good, bad, and a lot of struggles he has supported me these last four years and helped me to grow as a scientist. I am still stunned that he took me on as a student to begin with and am forever grateful for the opportunity. Without his knowledge, help, support, and encouragement especially, none of this would have been possible. Great thanks are also given to the other members of my committee: Drs. Michelle Stocker, Rachel Reid, and Nic Campione, who together challenged me and made me think more deeply about my work and where I want to be. Thank you to Michelle for pushing me to be a better scientist, and for always looking out for me when I got overwhelmed with fieldwork. To Rachel particularly for working with and supporting me while Michelle and Sterling were away on sabbatical. To Nic for his much-appreciated help with R and coding, teaching me things I wouldn't have even thought to explore. Thank you to my whole committee for believing in me, even when I didn't.

The specimens in this dissertation come from a wide group of museums across the world, without which this work would not have been possible. Thank you to the curators and collections staff of the following museums who allowed me to and facilitated visits to their collections as part of my work, many of whom also provided scans: the American Museum of Natural History, Carnegie Museum, Mesalands Dinosaur Museum, Museum of Comparative Zoology at Harvard, Natural History Museum (London), New Mexico Museum of Natural History and Science, Petrified Forest National Park, and Texas Tech Museum of Paleontology. I also thank the faculty and staff at those institutions I was not able to visit, but who still provided materials for my work: the Institute of Vertebrate Paleontology and Paleoanthropology, Marischal College Zoology Department, Museu de Ciências Naturais, National Museum of Natural History,

National Museum of Tanzania, Paleontología Museo de Ciencias Naturales de la Universidad Nacional de La Rioja, Paleontología de Vertebrados, New Mexico Bureau of Geology Mineral Museum, Perot Museum, Ruth Hall Museum of Paleontology, South African Museum, Staatliches Museum für Naturkunde, Texas Memorial Museum, and the Zhejiang Museum of Natural History. In particular, I would like to thank those at Petrified Forest National Park for their great assistance and for hosting us during fieldwork where some of my specimens were collected: Drs Bill Parker, Adam Marsh, and Matthew Smith.

For discussion and help that greatly improved this manuscript and my presentations over the years and in some cases made this possible at all, I would like to thank Drs. Julia Desojo, Valentine Fischer, Nick Hebdon, Voltaire Paes-Neto, and Will Reyes.

I would also like to thank the Virginia Tech Department of Geosciences and the Graduate and Professional Student Senate for funding given.

From before I even got to Virginia Tech, I would like to thank the DawnDinos team, and especially Drs. John Hutchinson, Ashleigh Wiseman, and Oliver Demuth for their encouragement, help with my application, and joy when I was accepted. I would also like to thank Dr. Mike Benton for all his help during my masters and for publishing with me since – and thank you for really introducing me to my beloved aetosaurs.

For their endless support and help given, I would like to thank Dr. Leslie Lowry and Deb Jenkins.

This would not have been possible without the support and friendship of my fellow graduate students in the palaeontology research group: Helen Burch, Adam Fitch, Danielle Fitzgerald,

Mark Nohomovich, Brynden Perkins, Isaac Pugh, Prescott Vayda and honorary palaeo person Amy Hagen, and Drs. Erika Goldsmith, Devin Hoffman, Ben Kligman, Morrigan Nolan, Jack Stack, Khanh To, and Brenen Wynd. Out of them I would especially like to thank Drs. Erika Goldsmith, Khanh To, and Helen Burch and Danielle Fitzgerald for their much-appreciated attempts to keep me sane. Special thanks are given to our wonderful postdoc, Dr. Davide Foffa and his wife, Dr. Isla Simmons. I would also like to acknowledge the fantastic staff and faculty of the group: Drs. Shuhai Xiao and Pedro Monarrez, and Annamarie Fadorsen, Mariah Green, and Vicki Yarborough. And what a fantastic bunch of undergrads we have and have had – their endless enthusiasm and drive have been a light in the rough time a PhD can be.

Still in my palaeoshpere, I would like to thank the members of the palaeontology discord server I am a part of for their friendship, advice, and always having my back when searching for obscure papers.

I want to thank the "members" of the Paleo Dream Team for following along and helping by encouraging me as a woman in STEM on this journey of mine: Kathryn Abbott, Mackenzie Ballou, Lindsey Davis Blanchard, Ashley Hall, Katie Hunt, Bryce McElvogue, Kade Parsons, Myria Perez, Holly Simon, Nikki Simon, Evelyn Volmer, and Skye Walker.

Outside of palaeontology, I would like to thank my good friends, Zander Butterworth, Ashe Cook, Pauline Dunne, Caitlin Foster, Elliot Gascoyne, Tony Maycock, Will Tarrant, and Jen Thompson, for always brightening my days with jokes, heartfelt words, and for putting up with me. I am looking forward to being closer to you all once again. Special thanks go to Alex May for his love, encouragement, and always level head. I have had your "IT'S SOMETHING. KEEP

GOING.” texts printed out and hung above my desk for years now and it still makes me smile. I am looking at them now.

Thanks are given to Aileen Nicolas and the community she has created without whom the manuscript would have taken a lot longer to write.

Finally, I must thank my family, Julie, Matt, and Alex Keeble for their support in every way possible over these four years and beyond. This would not have been possible without their endless belief in me and lifelong encouragement.

# Contents

## CHAPTER 1 - Aetosaur dental variation and the identification of their isolated teeth


### ABSTRACT

The Late Triassic saw a tremendous radiation of modern tetrapod clades, exemplified by that seen in the archosaurs. Archosaurs diversified to fill many ecological niches, and underwent transitions in their diets, accompanied by changes in tooth shape. Just looking at the Aetosauria (Pseudosuchia), we see a diverse array of tooth shapes across the clade, suggesting a variety of different diets. I asked the question of how tooth shape changes across an evolutionary radiation using aetosaurs as a case study. In addition to this, I establish methods that may be useful in the identification of isolated aetosaur teeth, particularly those found in microvertebrate localities, which are rarer than expected based on osteoderm numbers found. Here, I compared aetosaurs (*Aetosauroides, Coahomasuchus, Neoeatosauroides, Paratypothorax, Stagonolepis,* and *Stenomyti*) and close relatives (*Euparkeria, Ornithosuchus, Parringtonia, Revueltosaurus,* and *Riojasuchus*) to categorize shape and variation of teeth within species and across genera throughout time and space. I also plotted multiple types of teeth (premaxillary, maxillary and dentary) from these taxa, where available, to characterize the full dentition of aetosaurian tooth morphologies. Teeth were surface, synchrotron, or CT scanned and processed using Materialise Mimics, 3-Matic, and Meshlab before being analysed with 3D geometric morphometric code in R. To complement this quantitative approach, a non-metric multidimensional scaling analysis was also carried out to visualise the differences among discrete characters; this returned generally similar results as the 3D geometric morphometric analysis. As we see that each tooth type from each genus plots together, plotting isolated aetosaur teeth into this matrix allows us to determine their broad phylogenetic position and that they belong to members of the Aetosauria. We would expect to see non-aetosaurian tetrapods plot in a more distant space from the

aetosaurian teeth and would test this as a next step. With proof of concept, we can expand this method to look at other clades to provide more confident tooth identifications from microvertebrate localities than were previously possible, thus allowing us to conduct studies of diversity, ecology and faunal change through time in much greater detail than ever before.

## INSTITUTIONAL ABBREVIATIONS

**DMNH** – Perot Museum of Nature and Science, Dallas, USA; **MCN** - Museu de Ciências Naturais, Secretaria Estadual do Meio Ambiente e Infraestrutura, Porto Alegre, Brazil; **MCZD** - Marischal College Zoology Department, Scotland, UK; **NHMUK** - The Natural History Museum, London, UK; **NMT** – New Mexico Bureau of Geology Mineral Museum, New Mexico, USA; **PEFO** – Petrified Forest National Park, Arizona, USA; **PULR** - Paleontología Museo de Ciencias Naturales de la Universidad Nacional de La Rioja, La Rioja, Argentina; **PVL** - Paleontología de Vertebrados, Tucuman, Argentina; **SAM** - South Africa Museum, Capetown, South Africa; **TMM** - Vertebrate Paleontology Laboratory, Texas Natural Science Center, Austin, Texas, USA; **TTUP** - Texas Tech University, Texas, USA

## INTRODUCTION

Across time, rapid evolutionary radiations are frequently accompanied by dietary transitions (Grant & Grant 2003, Ma et al. 2022, Wynd et al. 2022) and variation in dentition (Weishampel & Norman 1989) often originating from an ancestor with a tooth shape less specialised for any single particular diet (van Valkenburgh 1989). Exemplifying this is the

radiation of archosauromorphs in the Late Triassic (Nesbitt 2011). This radiation saw an extensive variety of diets and feeding strategies arise from an ancestral small carnivore (Sookias 2016), which over the course of the Mesozoic Era, gave rise to large carnivores (Benyoucef et al 2015, Qvarnström et al. 2019, Ma et al. 2020), herbivores (Weishampel & Norman 1989, Barrett 2014), omnivores (Barrett et al. 2011, Desojo et al. 2013), and more generalists (Xing et al. 2013). These transitions are predominantly inferred from changes in dentition. These dentition changes are especially clear in clades that transitioned to herbivory such as rhynchosaurs (Benton 1990, Sethapanichsakul et al. 2023), allokotosaurs (Nesbitt et al. 2015), some dinosaurs (Weishampel & Norman 1989, Barrett et al. 2011), and some members of the aetosaurs (Walker 1961, Parker 2016).

Aetosauria was a clade of armoured, quadrupedal pseudosuchian archosaurs with a global distribution, excluding Antarctica and Australia (Heckert and Lucas 2000, Desojo et al 2013). A homodont dentition, wherein all teeth have virtually the same shape, though may be different sizes, is present in all aetosaurs except *Typothorax* (Parker et al. 2024) wherein different tooth shapes are observed within the dentary and between the different regions of the mouth (Reyes et al. 2021). Among taxa, however, dental form is highly disparate, with a wide range of shapes, likely reflecting different diets, possibly including herbivorous (Walker 1961), insectivorous or omnivorous (Small 2002, Desojo et al. 2013) and, notably in *Coahomasuchus kahleorum,* and possibly *Aetosauroides scagliai,* even carnivorous (Parker 2016; Parker et al. 2024). These various tooth shapes may also potentially be constrained by phylogeny in addition to function.

But aetosaurs are only one component of many vertebrate communities in the Late Triassic Epoch. One way to increase our understanding of communities throughout time is to focus on teeth within microvertebrate assemblages. Microvertebrate localities, defined as sites

where 75% of remains are <50 mm (Eberth et al. 2007), preserve many, often fragmentary and disarticulated, remains of a wide range of vertebrates. Not only are small vertebrates present, but also small elements of larger vertebrates, such as teeth and osteoderms. This makes microvertebrate localities ideal for studies of ecosystem diversity, as they paint a much broader picture of the entire ecosystem than can be obtained through looking solely at macro remains. Teeth are often abundant in microvertebrate assemblages as they are more resistant to erosion and weathering than other elements and so are more likely to persevere in sediments (Bhat 2017). When using teeth as a proxy for the number of species present in a deposit, uncertainty in the identification of aetosaur teeth in microvertebrate localities may lead to a false signal that they were rarer or less speciose than in reality, thus confounding studies of diversity.

Studies of diversity require large sample sizes of confidently identified remains. Whereas microvertebrate localities often contain remains from a diversity of small and large vertebrates, those remains are often isolated, making them notoriously hard to identify to specific clades. The case of *Revueltosaurus* being assumed to be an ornithischian dinosaur for decades before a full skeleton was discovered, revealing that it was a pseudosuchian, is a prime example of the need to be cautious (Parker et al 2005; 2021). Here, I propose a new set of quantitative methods that can be used to improve identification confidence using aetosaurs as a proof of concept.

Historically, tooth identification has been accomplished through qualitative methods including direct comparison and discrete characters (Hunt & Lucas 1994, Kelner & Mader 1997, Heckert 2004). More recently, techniques such as canonical variate analysis and discriminant function analysis (Larson and Currie 2013), 2D geometric morphometrics (Calede & Glusman 2017), and even machine learning (Wills et al. 2021; 2023) have been used to apply quantitative methods to tooth identification, with good results. Another technique with promise for

quantitatively distinguishing among taxa is 3D geometric morphometrics (3DGM). This technique quantifies the shape of objects and allows comparison among them using Cartesian coordinates rather than discrete measurements (Lawing & Polly 2009). With broader availability of methods of producing 3D data such as surface scanners, 3DGM has become more accessible for a wider user base (Adams et al. 2013) and has the potential to be a powerful tool in the identification of isolated teeth.

Here, I analysed tooth evolution and shape in aetosaurs using three-dimensional geometric morphometrics (3DGM) and non-metric multidimensional scaling to create morphospace plots of aetosaur and sister taxa teeth from specimens that have been confidently identified. Although losing dimensional data in 2D is inevitable, this is not a concern in 3DGM. Much more comparative information (e.g., curvature over multiple angles, roundness, bulbousness of the whole tooth rather than two sides, angle(s) of recurvedness in 3D space - whether simply pointing distally or also angling, for example, lingually as well) can be garnered from using three dimensions.

I asked whether teeth from the different regions of the mouth (maxilla, premaxilla, and dentary) can be distinguished, and are there trends along the tooth row? Do we see changes in dentition that reveal a pattern from a more plesiomorphic tooth (recurved, serrated, laterally compressed) to a more peg-like tooth? And, ultimately, could these techniques be used to identify isolated aetosaur teeth, particularly from microvertebrate assemblages, and to how fine an affinity? I separated teeth by region of the mouth and position in the tooth row to test for variation both among species, and within the mouth of individual taxa. Isolated teeth can then be plotted in the matrix and conclusions drawn about their affinities based on where they fall.

## MATERIALS AND METHODS

### Aetosaurs

Given the wide range of morphologies across the clade of Aetosauria, a description of each study taxon is found below. Terminology follows that put forward by Hendrickx et al. (2015). These teeth all come from specimens that have been confidently identified based on skeletal features either in previous work (e.g. Paes Neto et al. 2021, Small & Martz 2013, Tarborda et al. 2021, Gower & Walker 2002, Nesbitt et al. 2017, Parker et al. 2021, Sookias & Butler 2013) or independently. Therefore, this initial matrix consists only of teeth identified to genus level. A total of 72 teeth from nine taxa of aetosaur (*Aetosauroides* (10)*, Calyptosuchus* (1)*, Coahomasuchus* (4)*, Desmatosuchus* (2)*, Longosuchus* (1)*, Neoaetosauroides* (4)*, Paratypothorax* (1)*, Staganolepis* (5)*,* and *Stenomyti* (13)) and five outgroup taxa (*Euparkeria* (12)*, Ornithosuchus* (8)*, Parringtonia* (2)*, Revueltosaurus* (4)*,* and *Riojasuchus*(5)) were used in the analysis.

It was not possible to see every specimen in person, and so many are described on the basis of scans, casts, photographs, and the published literature. As such, some features may be missing from each description (for example, few scans pick up on serrated carinae when present on teeth).

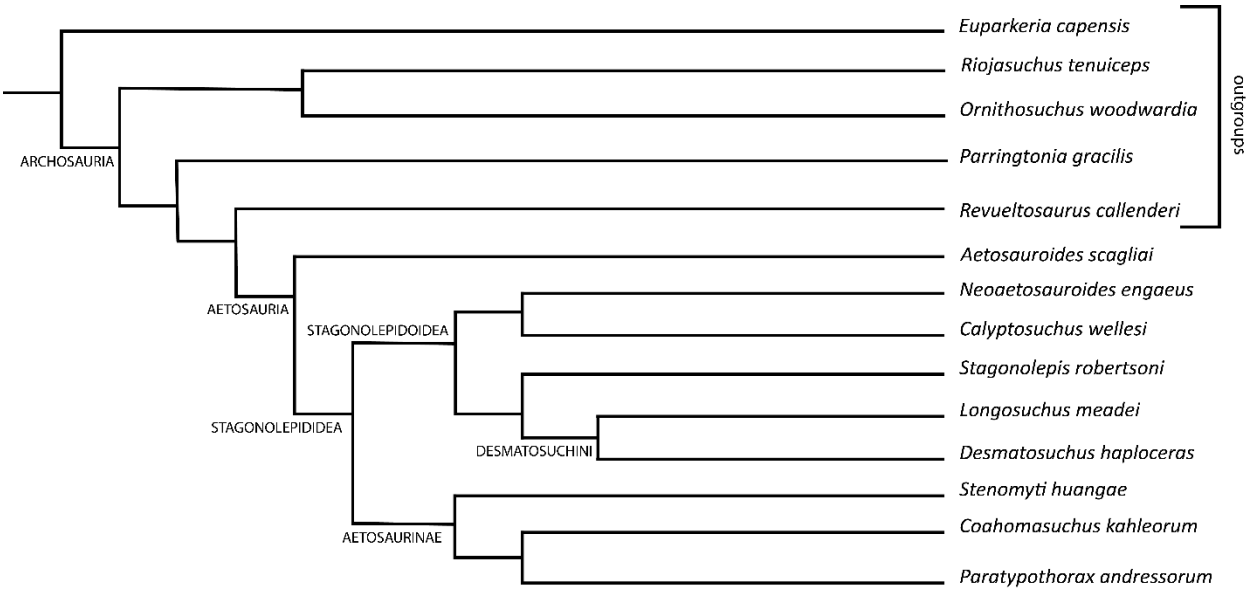


**Figure 1.** Phylogenetic tree of outgroups and aetosaurs used. Adapted from Reyes et al. 2024a and Nesbitt 2011.

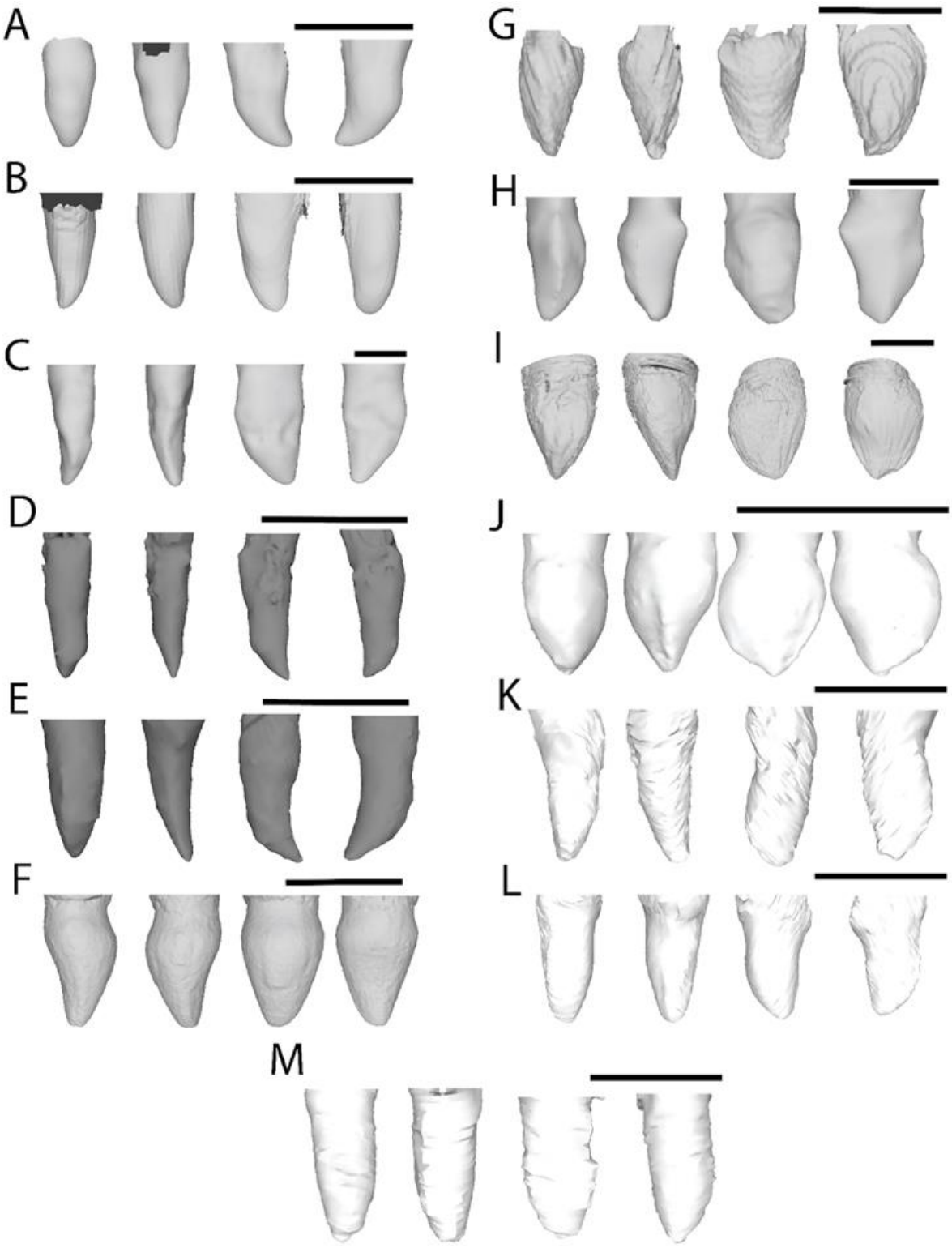
A
B
C
D
E
F
G
H
I
J
K
L
M

**Figure 2.** Three-dimensional models of each tooth type from all aetosaurs (flipped to the same direction for the analysis) from left to right in mesial, distal, labial, and lingual views. A: *Aetosauroides* left dentary tooth 11, B: *Aetosauroides scagliai* MCN 2347 right premaxillary tooth one, C: *Calyptosuchus wellesi* PEFO 49321 right maxillary tooth five, D: *Coahomasuchus kahleorum* TMM 31100-437 right dentary tooth one, E: *Coahomasuchus kahleorum* TMM 31100-437 left maxillary tooth three, F: *Desmatosuchus smalli* TTU-P 9420 dentary or maxillary tooth, G: *Longosuchus meadei* TMM 31100-1338 left dentary five, H: *Neoaetosauroides engaeus* PULR 108 left maxillary tooth three, I: *Paratypothorax andressorum* PEFO 49322 left dentary tooth three, J: *Stagonolepis robertsoni* MCZ 2 right maxillary tooth six, K: *Stenomyti huangae* DMNH 60708 left dentary tooth one, L: *Stenomyti huangae* DMNH 60708 right maxillary tooth eight, M: *Stenomyti huangae* right premaxillary tooth three. Scale bars are 1 cm.

***Aetosauroides scagliai*** (Casamiquela 1960)

**Specimen:** MCN PV 2347 consisting of an almost complete skull, the first cervical vertebrae and their corresponding osteoderms. Limited appendicular postcrania is present, and includes radius, ulna, and a femur fragment (Paes Neto et al. 2021).

**Locality and Age:** Piche site, *Hyperodapedon* Assemblage Zone, base of the Candelária Sequence, Santa Maria Supersequence, (southern Brazil near the city of São João do Polêsine (Paes Neto et al. 2021); late Carnian–early Norian, Late Triassic.

**Scan:** The skull was scanned in three parts at at the Instituto de Petróleo e dos Recursos Naturais (Laboratório de Sedimentologia e Petrologia) of Pontifícia Universidade Católica do Rio Grande

do Sul in a Bruker SkyScan 1173 microtomograph with voltage of 130 kV and current of 61 uA). The slices were segmented manually with Avizo 7.1 (Paes Neto et al. 2021). The 3D file used for this study was much larger than life, and so was scaled down in PrusaSlicer before being treated the same as the other taxa in Meshlab and Landmark.

**Description:** *Aetosauroides* had five teeth in each premaxilla (Biacchi Brust et al. 2018), at least seven in the maxilla, though this is likely to be closer to 10-12 based on closely related species (Paes Neto et al 2021), and 12 in each dentary (Paes Neto et al. 2021, Parker et al. 2024). When using the higher estimates of alveoli count, this gives a likely total tooth count of 58 teeth. The teeth are recurved at their tips in the dentary and maxilla, and those in the maxilla bear fine serrations (unquantified denticles per mm) on the length of the distal carinae, and towards the tip of the mesial carinae (Biacchi Brust et al. 2018). In MCN PV 2347, whereas no teeth are preserved in the maxillae, one tooth from the right premaxilla, two from the right dentary and six from the left dentary were used in this analysis. These teeth exhibit differences in morphology between the dentary and the premaxillary tooth, counter to other studies that only consider *Typothorax* as the heterodont aetosaur (Reyes et al. 2021).

The dentary teeth of MCN PV 2347 are recurved, though have a more rounded apex and are shorter than the recurved teeth of other taxa such as *Coahomasuchus*. They are slightly constricted at the base of the crown, and are somewhat laterally compressed. The wider base of the crown constricts at approximately the mid-point to two thirds of the way to the apex from the cervix where the angle of recurvature becomes more dramatic.

The premaxillary tooth of MCN PV 2347 is far more simple and peg-like. The tooth is almost completely apicobasally straight with only a slight distal curvature, and lacks surface features or serrations. A small heel is present towards the base of the crown on the lingual side of

the tooth and there is some labiolingual compression. The apex is more rounded than that of the dentary teeth, and the maxillary teeth of other specimens (Biacchi Brust et al. 2018).

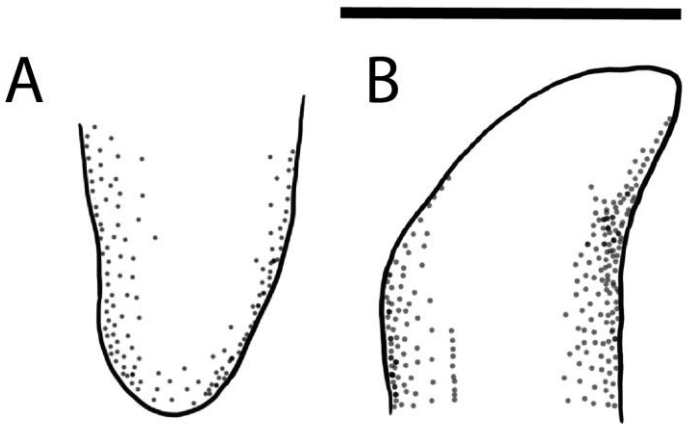


**Figure 3.** Selected teeth of *Aetosauroides scagliai* in lateral view: A left premaxillary tooth; B right dentary tooth in position 11. (MCN 2347). Scale bar is 1 cm.

***Calyptosuchus wellesi*** (Long & Ballew 1985)

**Specimen:** PEFO 49321 is a right maxilla with a single tooth preserved.

**Location and Age:** Blue Mesa Member, Chinle Formation (Parker 2018, Reyes et al. 2024b) of Petrified Forest National Park (PEFO), Arizona, USA. Norian, Late Triassic.

**Scan:** Surface scanned on an Artec Spider scanner at Virginia Tech.

**Description:** PEFO 49321 has six alveoli, though it is missing some of the anteriormost section (Reyes 2024). A partial right dentary (UCMP 27225) is known and contains nine alveoli (Parker 2018). However, it is missing the anterior portion, though what is preserved is edentulous (Parker 2018), suggesting that nine would have been the true number of teeth.

The single exposed preserved maxillary tooth from PEFO 49321 is used in this study (Fig. 4). It is mediolaterally compressed, slightly constricted at the base, and apically pointed with a curved mesial carina and straight distal carina, both unserrated.

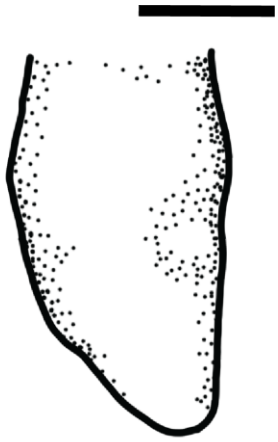

**Figure 4** Tooth of *Calyptosuchus wellesi* in lateral view: right maxillary tooth in position 5. **(**PEFO 49321). Scale bar is 1 cm.

***Coahomasuchus kahleorum*** (Heckert & Lucas 1999)

**Specimen:** TMM 31100-437 is a partial skeleton of *Coahomasuchus kahleorum* consisting of the incomplete skull and various postcranial elements including trunk vertebrae, many paramedian, lateral, ventral, and appendicular osteoderms, and limb elements. (Parker 2016, Parker et al. 2024).

**Locality and Age:** Otis Chalk Quarry 3, Colorado City Formation from the Dockum Group of western Texas, USA Dockum Group, Late Triassic of Texas, USA (Sawin 1947, Parrish 1994); Otischalkian, Late Triassic (Stocker et al. 2016).

**Scan:** MicroCT scanned at the University of Texas High Resolution X-ray CT Facility with source voltage of 120 kV and a current of 0.18 mA. (Parker et al. 2024)

**Description:** There are at least 11 alveoli present in the dentary of TMM 31100 437; however, neither dentary is complete (Parker et al. 2024). Nonetheless, based on other aetosaur dentaries, this number is not likely to be higher than 12. Seven alveoli are present in the maxilla (Parker et al. 2024). The premaxilla is not preserved in TMM 31100-437 and so no tooth count estimates can be made for this bone. Excluding the premaxilla, this gives an estimated tooth count of 36.

The teeth of *Coahomasuchus,* along with *Aetosauroides*, are the most "carnivorous" in appearance out of all the aetosaurs used here (Murry & Long 1996, Parker 2016, Parker et al. 2024) and are the most reflective of the hypothesised plesiomorphic archosaur tooth, though with some key differences. Whereas mediolaterally compressed, they are much rounder in cross section than other teeth of carnivorous archosaurs of the Late Triassic such as the loricatans (~'rauisuchians'), or early dinosaurs. The teeth are tall, strongly recurved wherein the apex extends past the body of the crown, and come to a narrow apex, with denticles on the distal side (Parker et al. 2024). There is no constriction at the base of the crown as in some other aetosaurs such as *Stagonolepis* and *Neoaetosauroides*. Out of twelve teeth segmented, four were included in the present analysis because of their superior preservation: three left maxillary teeth from alveolar positions one, three and four, and one right dentary tooth from alveolus one. Many others were broken, making them unsuitable for 3D geometric morphometric analysis.

Of those teeth preserved, there is little variation across the tooth row in the maxilla. It seems the first tooth has a more gradual curvature compared to the other teeth present; however, this may be the result of better preservation of the first maxillary tooth, and how it is more easily

segmented from CT scans. The entire labial surface is free of matrix and sits on top of the other three preserved teeth of the maxilla. Teeth three and four (Fig. 5) seem to have a point where the angle of the distal curvature of the mesial side changes to be more acute that is not observed on the first tooth.

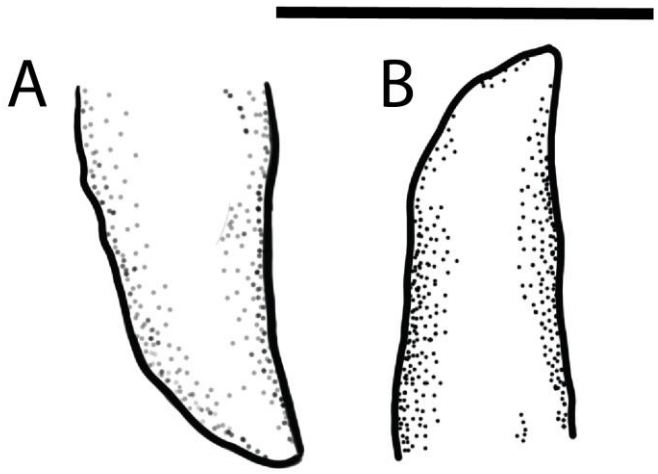


**Figure 5.** Selected teeth of *Coahomasuchus kahleorum* in lateral view: A left maxillary tooth in position four; B left dentary tooth in position seven. **(**TMM 31100-437). Scale bar is 1 cm.

***Desmatosuchus haploceras***

**Specimen:** TTU-P 9420, a partially disarticulated, but mostly complete skull (Small 2002).

**Locality and Age:** Post Quarry, Cooper Canyon Formation (Dockum Group) in Garza County, Texas, USA. Early-middle Norian (Adamanian), Late Triassic (Martz et al. 2012).

**Scan:** Photogrammetry via the Abound (formerly Metascan) application for iPhone. Scanned at Texas Tech University.

**Description:** The maxilla of *Desmatosuchus haploceras* contains 10-13 teeth, and the dentary six-seven (Small 2002) giving an estimated range for total tooth count of between 32 to 40 teeth in the mouth. This range of potential tooth counts is the result of variation between individuals of *D. haploceras* (Small 2002). A pattern similar to that in the dentition of *Stagonolepis robertsoni* is observed in the variation of alveoli size in the maxilla of *D. haploceras* where the alveoli start smaller and increase in size until alveolus six, approximately the middle tooth of the maxilla, then decrease in size posteriorly (Small 2002). There is only one skull known with teeth in situ in the skull, TTU-P 9420, which is used here. However, these teeth are not used in this study because of difficulty in surface scanning these teeth without obstruction, and poor preservation. Three of the teeth that were discovered in the matrix around the skull are used here (Fig. 6). As such, information on the position of these teeth in the skull is not known other than they are maxillary or dentary teeth, given the edentulous condition of the premaxilla of *Desmatosuchus* (Small 2002).

The crowns are bulbous, with a constricted base that expands outwards in all directions before narrowing again to a blunt point, most similar in gross shape to those of *Neoaetosauroides*. The teeth have a heel at the base of the lingual side and are somewhat laterally compressed, particularly above this point. Denticles are present on one tooth and are described by Small (2002) as being “almost imperceptible”. These may have been present on the other teeth but were not observed in study of the original material here. The teeth possess faint fluting, though this seems worn down, either by preparation or taphonomy, on some of them.

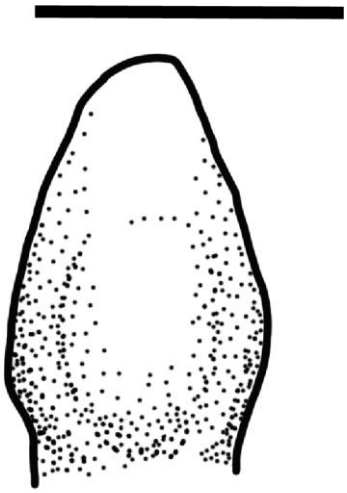

**Figure 6.** Tooth of *Desmatosuchus smalli* tooth from unknown position. (TTU-P9420). Scale bar is 1 cm.

***Longosuchus meadei*** (Sawin 1947)

**Specimen:** TMM 31100-1338, an undescribed left dentary.

**Locality and Age:** Otis Chalk Quarry 3, Colorado City Formation from the Dockum Group of western Texas, USA (Sawin 1947, Parrish 1994); Otischalkian, Late Triassic (Stocker et al. 2016).

**Scan:** MicroCT scanned at the University of Texas High Resolution X-ray CT Facility

**Description:** The premaxilla in *L. meadei* is seemingly edentulous; however, Parrish 1994 described a single tooth preserved on the broken premaxilla of TMM 31185-84B, the skull of which is missing much of the anterior portion. Seven alveoli are preserved on the dentary, which is virtually complete in TMM 31185-84B, and the anterior portion is edentulous. There would have been at least ten teeth in the maxilla, though this number may have been greater in life than

can be discerned here because of incomplete preservation of the anterior portion of the maxilla. This gives an estimated minimum total tooth count of 34.

The teeth of *Longosuchus* are not known to be serrated and are simple (Parrish 1994). The tooth used in this study is from position five of the dentary of TMM 31100-1338 (Fig. 7), and slightly expands both mesiodistally and labiolingually, particularly lingually out from the base of the crown. There is a slight heel at the base of the crown as this expansion on the lingual side reduces around a third of the way apicobasally from the cervix. It is fairly conical otherwise, and is not recurved. The tip of the crown used in this analysis is broken, but I assessed this to be minor, and the tooth to still be suitable for both 3D geometric morphometrics and NMDS analysis. As only one tooth is preserved in TMM 31100-1338, comparisons across the tooth row cannot be drawn.

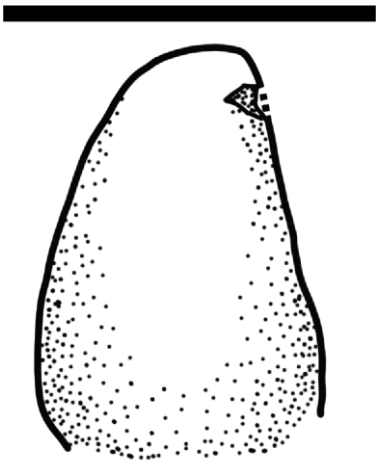

**Figure 7.** Tooth of *Longosuchus meadei* in lateral view: left dentary tooth in position five. **(**TMM 31100-1338). Scale bar is 1 cm.

***Neoaetosauroides engaeus*** (Bonaparte 1967)

**Specimen:** PULR 108 is the only natural cast used in this study. It consists of casts of the lower jaw and internal skull anatomy (von Backzo et al. 2018, Taborda et al. 2021).

**Locality and Age:** Los Colorados Formation, La Rioja, Argentina (Tarborda et al. 2021); Norian, Late Triassic.

**Scan:** Scanned on a medical 64 channel axial tomography multi-slicer at the Clínica la Sagrada Familia in Buenos Aires at 140 kV and 200mA.

**Description:** Based on PULR 108 and other skulls (PVL 4363, PVL 5698), Taborda et al (2021) found *Neoaetosauroides* to have four premaxillary teeth, eight maxillary and eight dentary teeth, giving a total tooth count of 40 teeth.

The teeth are bulbous - expanding further out than the cervix before narrowing again - and slightly curved labiolingually towards the lingual side in a conical scoop shape. The premaxillary teeth are dramatically smaller than the maxillary teeth, though none were able to be included here because of poor preservation. From PULR 108, the four best preserved maxillary teeth were used in this analysis from alveolar positions 2, 3, 4, and 5 (Fig. 8). Tooth size in the maxilla decreases posteriorly along the tooth row, but the shape of teeth remains consistent.

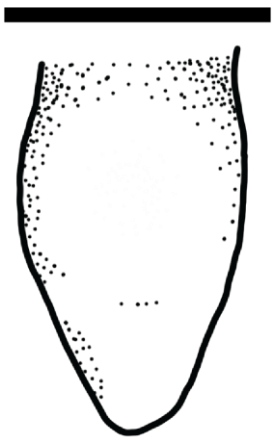

**Figure 8.** Tooth of *Neoaetosauroides engaeus* in lateral view: left maxillary tooth in position four. **(**PULR 108). Scale bar is 1 cm.

***Paratypothorax andressorum*** (Long & Ballew 1985)

**Specimen:** PEFO 49322 a partial skeleton, currently undescribed.

**Location and Age:** Chinle Formation of Petrified Forest National Park (PEFO), Arizona, USA; Norian, Late Triassic.

**Scan:** CT-scanned at the Shared Materials Instrumentation Facility at Duke University using a Nikon XTH 225 ST.

**Description:** There are four teeth in the premaxilla, which are smaller in size than those in the dentary or maxilla (Schoch & Desojo 2016). The maxilla houses ten teeth, however, an accurate tooth count of the dentary teeth is not possible with SMNS 19003 as this is occluded with the maxilla, and not all alveoli are exposed (Schoch & Desojo 2016). PEFO 49322 contains seven alveoli, but the posterior portion is missing and so there may have been more originally. This gives a minimum total tooth count of 42 for the entire mouth.

In the dentary of PEFO 49322, there is one partially erupted tooth in alveolus three that is preserved well and is used in this analysis (Fig. 9). No other teeth are preserved. The tooth expands mesiodistally out from the base of the crown where the labial and lingual sides are always narrower than the width of the base. The labial side shows a series of grooves that emanate from the apex and taper out towards the cervix.

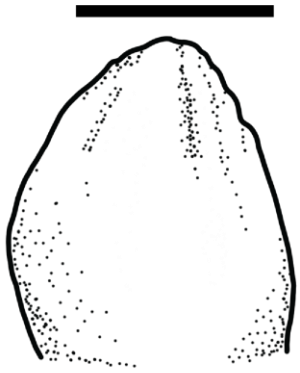

**Figure 9.** Tooth of *Paratypothorax andressorum* in lateral view: left dentary tooth in position three. (PEFO 49322). Scale bar is 1 cm.

***Stagonolepis robertsoni*** (Agassiz 1844)

**Specimen:** MCZD 2 is made up of seven blocks from the Lossimouth Sandstone of Scotland containing cranial and postcranial material preserved predominantly as bone, but also natural moulds (Gower & Walker 2002) with the snout used here consisting of bone. Most of the skull is preserved, though it is crushed.

**Location and Age:** Lossimouth Sandstone from Elgin, Scotland, UK. Carnian – early Norian, Late Triassic.

**Scan:** Scanned at the XTM Facility, Palaeobiology Research Group, University of Bristol on a Nikon XTH 225ST machine.

**Description:** Four alveoli are known in the premaxilla from other *Stagonolepis* specimens (Parker 2018, Reyes et al. 2021) with nine or ten in the maxilla and at least eight in the dentary, giving a total tooth count for the whole mouth of 44/46. I used six maxillary teeth from MCZD 2

from positions one - four, six, and seven along the tooth row.

The teeth of MCZD 2 are the most typically bulbous in the study (Fig. 10) with the widest part of the crown extending labiolingually and mesiodistally outwards from the cervix creating a "waist" at the base of the crown (Walker 1961). They are not recurved and do not possess any denticles, with no surface features such as fluting. The curvature of the labial and lingual sides of the crown is relatively equal, leading to a round tooth in cross section. The teeth maintain their shape across the maxillary tooth row, but increase in size from the first through to the fourth tooth, then decrease in size again after that. As the fifth tooth is missing, it is not possible to say whether this was smaller, larger, or equal in size to the fourth maxillary tooth.

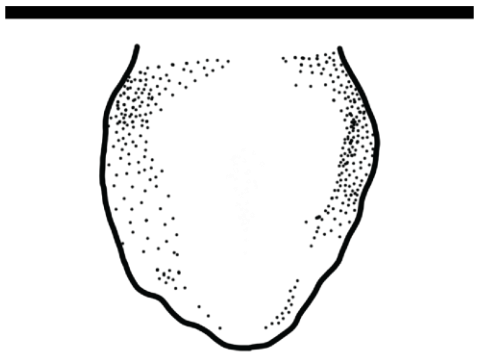

**Figure 10.** Selected tooth of *Stagonolepis robertsoni* in lateral view: right maxillary tooth in position seven **(**MCZD 2). Scale bar is 1 cm.

***Stenomyti huangae*** (Small & Martz 2013)

**Specimen**: DMNH 60708 (holotype) consisting of a virtually complete skull, and much of the postcrania, which is largely disarticulated, but associated. The postcranial material includes

osteoderms (dorsal, lateral, ventral, and appendicular), vertebrae, ribs, pelvic elements, right hindlimb, and fragmentary forelimbs. (Small & Martz 2013).

**Locality and Age:** Chinle Formation, of Colorado, USA (Small & Martz 2013); Revueltian (correlated as being mid-late Norian with biostratigraphy), Late Triassic.

**Scan**: Synchrotron scan created at the ANSTO Research Facilities in Melbourne, Australia at 80 keV.

**Description:** There are three alveoli on either side of the premaxilla, nine in each maxilla, and at least nine in each dentary, giving a total tooth count of 42 for the entire mouth. Currently, no undamaged dentaries are known and so there may have been more teeth in life. In this analysis, two premaxillary (one from each side, both from position three), five maxillary (all from the right maxilla, positions one, two, and six-eight), and six dentary teeth (the first two from the left and the first four from the right dentary – tooth positions given here start from the known tooth sockets of *Stenomyti* and ignore potential missing alveoli) were used, being the best preserved and only ones suitable for the 3D geometric morphometrics portion of this study. These teeth came from the left premaxilla, alveolus three; right premaxilla, alveolus three; left dentary, alveoli one and two; right dentary, alveoli one - four; and right maxilla, alveoli one, two, and six - eight.

The teeth somewhat reflect those of TMM 31100-437 *Coahomasuchus kahleorum*, being tall and pointed, though not as recurved (Fig. 11). The teeth are slightly bulbous – mesiodistally and labiolingually expanded from the cervix (though not to the extent of *Neoaetosauroides* or *Stagonolepis*). The labial side is far more convex in comparison with the lingual side in both

maxillary and dentary teeth. The surfaces are simple, with no serrations, fluting, crenulations, or ridges (Small & Martz 2013).

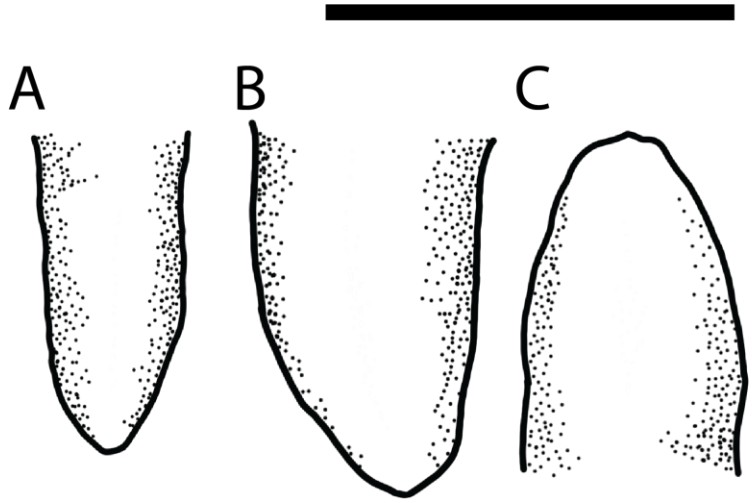


**Figure 11.** Selected teeth of *Stenomyti huangae* in lateral view: A right premaxillary tooth in position three; B right maxillary tooth in position eight; C right dentary tooth in position three (DMNH 60708). Scale bar is 1 cm.

**Outgroup Taxa**

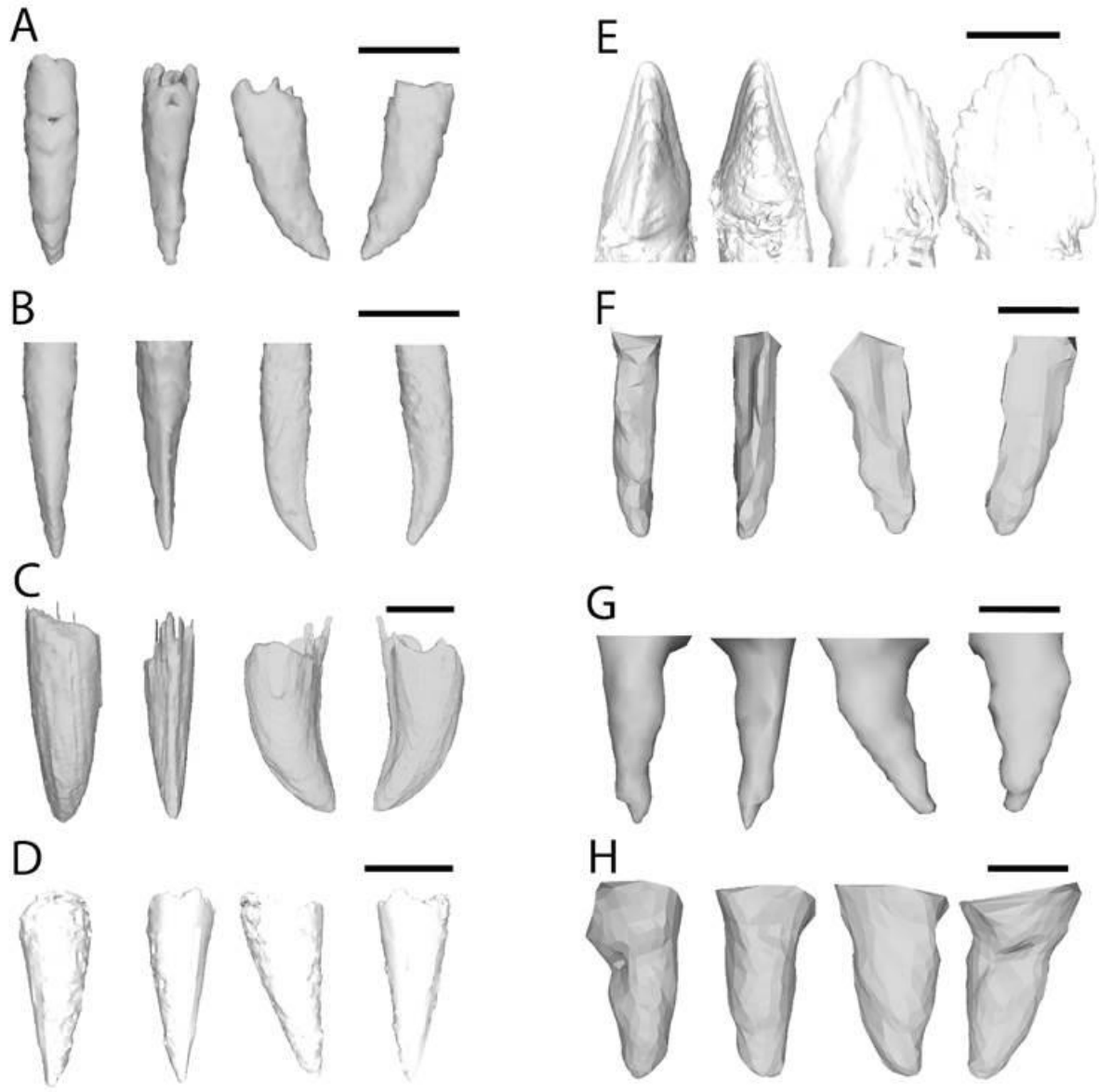


**Figure 12** 3D models of each tooth type from all outgroup taxa (flipped to the same direction for the analysis) from left to right in mesial, distal, labial, and lingual views. Scale bars are 5 mm. A: *Euparkeria capensis* SAM PK 5867 left dentary tooth 11, B: *Euparkeria capensis* SAM PK 5867 right maxillary tooth 12, C: *Ornithosuchus woodwardia* NHMUK R 3143 left dentary tooth (unknown position), D: *Parringtonia gracilis* NMT RB 426 premaxillary tooth (unknown position), E: *Revueltosaurus callenderi* PEFO 34561 left dentary tooth two, F: *Riojasuchus*

*tenuiceps* PVL 3827 right dentary tooth one, G: *Riojasuchus tenuiceps* PVL 3827 right maxillary tooth six, H: *Riojasuchus tenuiceps* PVL 3827 left premaxillary tooth two.

***Euparkeria capensis*** (Broome 1913)

**Specimen:** SAM PK 5867 (holotype) consists of an articulated and almost complete skull and partial skeleton. The postcranial material includes much of the axial skeleton except the caudal series, girdles, and limb material. (Sookias & Butler 2013).

**Locality and Age:** *Cynognathus* Zone of the Karoo of South Africa; Anisian, Middle Triassic (Senter 2003, Sookias & Butler 2013).

**Scan:** CT scanned at the Evolutionary studies Institute at the University of the Witwatersrand, Johannesburg, South Africa using a Nikon X Tek HMX ST 225 machine with a tungsten target and 70Kv, 140 μA, 1000 ms, 57.50 μm voxel size with a 1.8 mm aluminium filter (Sookias et al. 2020).

**Description:** The premaxilla of *Euparkeria* contains four tooth positions, and the maxilla and dentary both contain thirteen alveoli (Sookias et al. 2020), giving a total tooth count for the mouth of 60. There seems to be an alternating repeating pattern with larger teeth followed by smaller teeth along the tooth row, however, this could be from an alternating pattern of tooth replacement (Sookias 2020). Out of these teeth, those of the left dentary and right maxilla were best preserved in SAM PK 5867, and teeth from positions three, four, six, eight, 10, and 12 were used from the maxilla; and those from positions one, three, five, seven, nine, and 11 were taken from the dentary. Only the posterior portion of the premaxillae are present in SAM PK 5867, and

of those teeth preserved, they were not deemed suitable to be included in the geometric morphometrics here because of poor preservation. Although small teeth are present on the pterygoid, palate, and vomer (Sookias & Butler 2013, Sookias et al. 2020), these are not included here because of their absence in the other taxa considered in this study.

The teeth of *Euparkeria* are thought to be representative of the ancestral archosaur tooth condition and are recurved, serrated on both mesial and distal edges (apart from those of the premaxilla), and mediolaterally compressed (Fig. 13). Those of the premaxilla are rounder in cross section than those of the maxilla or dentary, being less laterally compressed. Only the right most posterior tooth of the premaxilla of SAM PK 5867 seems to be serrated, though the matrix may be obscuring the other teeth rather than a true lack of serrations (Sookias et al. 2020). Whereas the teeth of the dentary are generally smaller, they mirror the features of the maxillary teeth, which are virtually indistinguishable from each other by eye (Sookias et al. 2020).

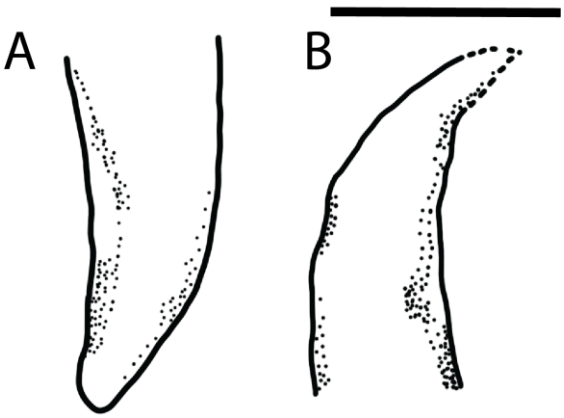


**Figure 13.** Selected teeth of *Euparkeria capensis* in lateral view: A right maxillary tooth in position four; B left dentary tooth in position three. (SAM PK 5867). Scale bar is 1 cm.

***Ornithosuchus woodwardia*** (Newton 1894)

**Specimen:** NHMUK R 3143 is the holotype of *Ornithosuchus woodwardia* and comprises the anteriormost portion of the skull, including premaxilla, maxilla, and dentary.

**Locality and Age:** Lossimouth Sandstone from Elgin, Scotland, UK. Carnian-early Norian, Late Triassic.

**Scan:** Taken on a Nikon HMX ST 225 at the Natural History Museum, London.

**Description:** *Ornithosuchus* is described as having three premaxillary teeth, nine maxillary teeth, and around ten dentary teeth (Walker 1964) giving an estimated total tooth count of 44.

With the exception of one premaxillary tooth, all teeth of *Ornithosuchus* are recurved where the apex of the tooth extends more distally than the distal edge of the crown (Fig. 14). Teeth are smooth and lack features such as ridges, fluting etc. The maxillary teeth often display curvature on the labial and lingual sides that is equal to the other, whereas the other teeth show an unequal curvature. No teeth are found to exhibit any degree of "bulbousness" and all sides taper inwards from the cervix. Denticles are present on all teeth where this could be scored from observation of the specimen and digital models. These are found on the mesial and distal of the dentary and maxillary teeth with those of the distal edge extending further down the tooth than those on the mesial edge. Denticles are only noted on one side each of the premaxillary teeth studied, though this may be because of poor preservation or loss during preparation, and it is expected that they would have been present on both sides in life.

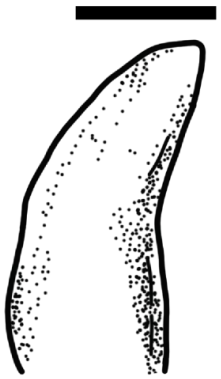

**Figure 14.** Selected tooth of *Ornithosuchus woodwardia* in lateral view: left dentary tooth from an unknown position. **(**NHMUK R 3143). Scale bar is 1 cm.

***Parringtonia gracilis*** (Huene 1939)

**Specimen:** NMT RB426 is the most complete specimen of *Parringtonia* comprising a nearly complete skeleton with most of the skull intact (Nesbitt et al. 2017).

**Locality and Age:** Lifua Member of the Manda Beds in the Ruhuhu Valley of southwestern Tanzania; Middle Triassic (Nesbitt & Butler 2013).

**Scan:** CT-scanned at the Shared Materials Instrumentation Facility at Duke University using a Nikon XTH 225 ST.

**Description:** The maxilla of *P. gracilis* has five maxillary alveoli, whereas the maxilla is incomplete, the teeth are restricted to the anterior portion and so seems accurate (Nesbitt & Butler 2013). Whereas no maxillary teeth are used in this study, one was discovered on CT scanning for Nesbitt & Butler 2013 of the holotype NHMUK R8646 and is described as having a round cross section, no serrations, and being slightly recurved, similar to the teeth of *Erpetosuchus*. The premaxillary teeth are also round in cross section and are gently recurved and

are slightly mesiodistally compressed, being wider at the base on the labiolingual axis. No information could be accessed regarding the teeth of the dentary.

**Figure 15.** Selected tooth of *Parringtonia gracilis* (NMT RB426) in lateral view: premaxillary tooth from an unknown position. Scale bar is 1 cm.

***Revueltosaurus callenderi*** (Hunt 1989)

**Specimen:** PEFO 34561 consists of a virtually complete skull and associated postcranial elements (Parker et al 2005). The dentary has been scanned and is the material used here.

**Locality and Age:** *Revueltosaurus* Quarry (PFV 297), Petrified Forest National Park, Arizona, USA; Revueltian, middle to late Norian, Late Triassic (Parker et al 2021).

**Scan:** Surface scanned with an Artec Spider scanner at PEFO.

**Description:** There are five teeth within the premaxilla, nine within the maxilla, and ten or eleven in the dentary (Parker et al 2021) giving a total tooth count of 48 or 50. The left dentary

of PEFO 34561 contains six teeth, the best preserved four of which are used in this study, from alveoli two, four, five, and six.

The teeth are highly distinctive within the Chinle Formation assemblage, but reflect those of later ornithischian dinosaurs, being leaf shaped to cone shaped with cusps on the mesial and distal carinae, resulting in confusion as to the affinity of *Revueltosaurus* in the past (Parker et al. 2005). Focussing on the teeth of the dentary used here, they have a ridge on the midline of the lingual side that extends apicobasally from cervix to apex (Fig. 16). The ridge is cone shaped, being wider at the bottom and coming to a point at the apex. Aside from this, the lingual side is typically flat to slightly convex and bears no other features such as fluting, crenulations etc. The labial side is rounded more typically, and has no ridges or other features on it. The mesial and distal carinae can expand outwards from the cervix, however, this is not typically seen on the labial or lingual sides, making them not truly bulbous.

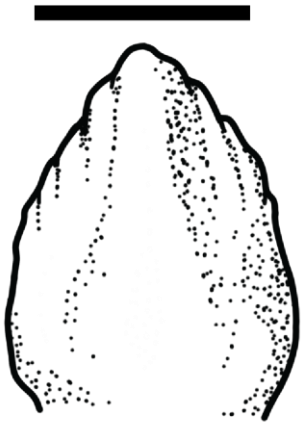

**Figure 16.** Selected tooth of *Revueltosaurus callenderi* in lateral view: left dentary tooth in position four. (PEFO 34561). Scale bar is 1 cm.

***Riojasuchus tenuiceps*** (Bonaparte 1967)

**Specimen:** PVL 3827 (holotype) a complete skull and virtually complete postcrania.

**Locality and Age:** Los Colorados Formation, La Rioja, Argentina (Bonaparte 1967); Norian, Late Triassic.

**Scan:** Scanned on a medical 64 channel axial tomography multi-slicer at the Clínica la Sagrada Familia in Buenos Aires at 120 kV and 279 mA.

**Description:** *Riojasuchus* has three premaxillary teeth, seven maxillary teeth, and nine dentary teeth (von Baczko & Desojo 2016) giving a total tooth count of 38. Teeth are generally large with some denticles on the maxillary and dentary teeth. Whereas no denticles are observable on the premaxillary teeth, this may be the result of overpreparation of the surface rather than the original condition (von Baczko & Desojo 2016). Three maxillary (positions one and four from the left maxilla, position six from the right maxilla), one premaxillary (left premaxilla position two) and one dentary tooth (right dentary position one) were used in this study from PVL 3827.

The maxillary teeth of PVL 3827 are strongly recurved (Fig. 17). In contrast, dentary tooth one is straight and conical. The premaxillary teeth fall between these two extremes and are weakly recurved. The teeth have no visible features on the surfaces of the crowns, but again, this may be the result of overpreparation described in von Baczko & Desojo (2016). These teeth are the lowest resolution in the study, but still capture gross overall shape.

**Figure 17.** Selected tooth of *Riojasuchus tenuiceps* in lateral view: right maxillary tooth in position six. **(**PVL 3827). Scale bar is 1 cm.

**3D Geometric Morphometrics**

Morphometrics were used to compare the gross shape of the teeth with each other to tease out groupings in a principal component analysis. 3DGM was chosen over 2D GM as it gives a greater idea of overall shape (Srikant et al. 2019).

I used the threshold tool in Mimics 22 (https://www.materialise.com/en/healthcare/mimics) to segment CT files. Auto-separation when possible, and then cleaning or defining individual slices. Teeth were fully segmented out of the jaws focusing on the crowns necessary for analysis. In Meshlab, some CT scanned teeth were Laplacian smoothed to prevent the analysis from focusing on jagged edges as a result of the scan slices rather than the actual morphology of the tooth. This also brought them closer in line with the resolution of the surface scanned teeth.

The resulting models were placed into morphospace using the method described by Fischer et al. (2022) and described in brief here. All teeth were oriented to face the same direction, that of the teeth in the left maxilla. Those that were in the opposite orientation were flipped using the Transform: Flip and/or Swap Axis function in Meshlab. A .ply file of each tooth in ASCII format had five fixed landmarks applied using the single point function in IDAV Landmark on the apex, the mesial edge, the distal edge, the labial side, and the lingual side, following that order each time. The latter four points were placed as close as could be distinguished to the cervix where the crown meets the root. In isolated teeth, it was simple to compare with in situ teeth and to look at the angle of recurvedness, i.e. how the apex pointed distally, and morphology of the tooth to determine orientation. This method works well where 3D data is of varying quality as landmarks are easy to consistently place on the centre of each side and dense semi-landmarks are objectively draped over based on the five fixed landmarks, rather than needing to be hand placed. The .ply and .pts files were loaded into the code provided by Fischer et al. (2022) and had semi-landmarks draped over them by a template disk. Teeth were normalised as part of a Procrustes analysis. They were plotted as a principal components analysis (PCA). Thin plate splines were created for the minimum and maximum ends of the first three PCs using the package geomorph in R (Baken et al. 2021, Adams et al. 2025).

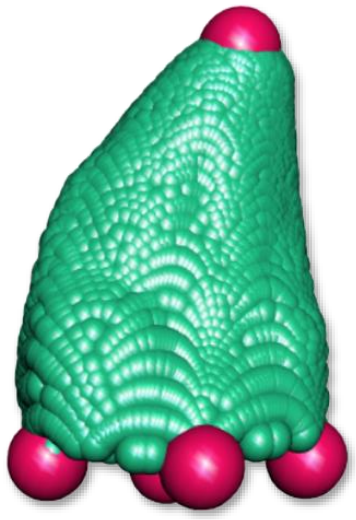

**Figure 18**. Landmarks on *Calyptosuchus wellesi* PEFO 49321 right maxillary tooth five. Fixed landmarks are in red and larger. Semilandmarks are in green and smaller.

**NMDS**

A non-metric multidimensional scaling analysis was used to capture qualitative data using discrete shape details, such as those utilised in a phylogenetic analysis, to complement the morphometric analysis. A total of 14 characters were used to score teeth. The majority of these characters were taken from Hoffman et al. (2019), and the remainder were modified from characters from Brocklehurst & Benson (2021) to be more applicable to isolated teeth and to make some characters binary. Taxa were further subdivided by tooth type where this was applicable as there can be significant variation in tooth characters among the premaxilla, maxilla, and dentary of an individual. For the characters that could only be scored in teeth with denticles, teeth without these were scored with a "?". Characters were scored in Mesquite before being copied to palaeontological statistics (PAST) (Hammer et al. 2001) to conduct the analysis. In

PAST, the NMDS analysis was conducted using a Gower similarity index as this copes well with missing information that is typical of fossil data (Gower 1971).

**Table 1**: Tooth characters used in NMDS.

| | |
|---|---|
| 1 | Tooth apex, location, relative to the distal margin of the tooth base: tip mesial to or in the same vertical plane as the distal edge (0) or tip is located more distal than the distal edge (1)<br><br>From Hoffman et al. 2019 |
| 2 | Tooth lingual/labial, surfaces: texture is smooth (lack of crenulations, ridges, etc.) (0) or surface texture possess a series of parallel ridges from tooth apex to base (= fluted) (1).<br><br>From Hoffman et al. 2019 |
| 3 | Tooth labial/lingual, shape: crown curvature unequal (one side expanded relative to other) (0) or equal labial and lingual curvature (1).<br><br>From Hoffman et al. 2019 |
| 4 | Mesial tooth margin, shape: curvature angles change gradually (0) or angle changes abruptly at a single discrete point along mesial edge (1).<br><br>From Hoffman et al. 2019 |

| | |
|---|---|
| 5 | Tooth crown, size: labiolingual widths dorsal to the tooth crown base are all less than the crown base width (0) or a crown labiolingual width dorsal to the tooth crown base is greater than the crown base width (1).<br><br>From Hoffman et al. 2019 |
| 6 | Denticles, mesial edge: absent (0) or present (1)<br><br>Modified from Brocklehurst and Benson 2021 |
| 7 | Denticles, distal edge: absent (0) or present (1)<br><br>Modified from Brocklehurst and Benson 2021 |
| 8 | Mesial/distal crown margins, surfaces: denticle caudae (= grooves on crown surface from between individual denticles) are absent (0) or present (1)<br><br>From Hoffman et al. 2019, originally from Abler, 1992 |
| 9 | Mesial margin, length: mesial denticle row ends at a point sub-equal with distal denticle row (0) or mesial denticle row ends significantly further apically on crown than distal row (1). Can only be scored for teeth with both mesial and distal denticle series.<br><br>From Hoffman et al. 2019 |
| 10 | Mesial/distal margins, denticle density: number of mesial and distal denticles is <3 per mm (0), or >3 per mm (1). Measurements are taken near the middle of the carina.<br><br>From Hoffman et al. 2019 |

| | |
|---|---|
| 11 | Mesial margin, location: vertical axis of the mesial carina is in line with the mesial-distal long axis (0) or laterally offset from the mesial distal long axis (1).<br><br>From Hoffman et al. 2019 |
| 12 | Mesial/distal margins, size: average size of mesial and distal denticles are the same (0) or the average size of the mesial and distal denticles is different (1)<br><br>From Hoffman et al. 2019 |
| 13 | Mesial/distal margins, shape: lateral profile shape of mesial and distal denticles remains constant (0) or denticles lateral profile changes shape (e.g., rounded to square) (1).<br><br>From Hoffman et al. 2019 |
| 14 | Lingual side: heel (=cingulum) on teeth: absent (0); present (1)<br><br>Modified from Brocklehurst and Benson 2021 |

**Statistical Tests**

A non-parametric analysis of variance test (ANOVA) was used to test for significant differences among the genera in the PCA. This was done through the R package geomorph (Baken et el. 2021, Adams et al. 2025). A pairwise test was used to test for significant differences between paired taxa.

**RESULTS**

## 3D Geometric Morphometrics

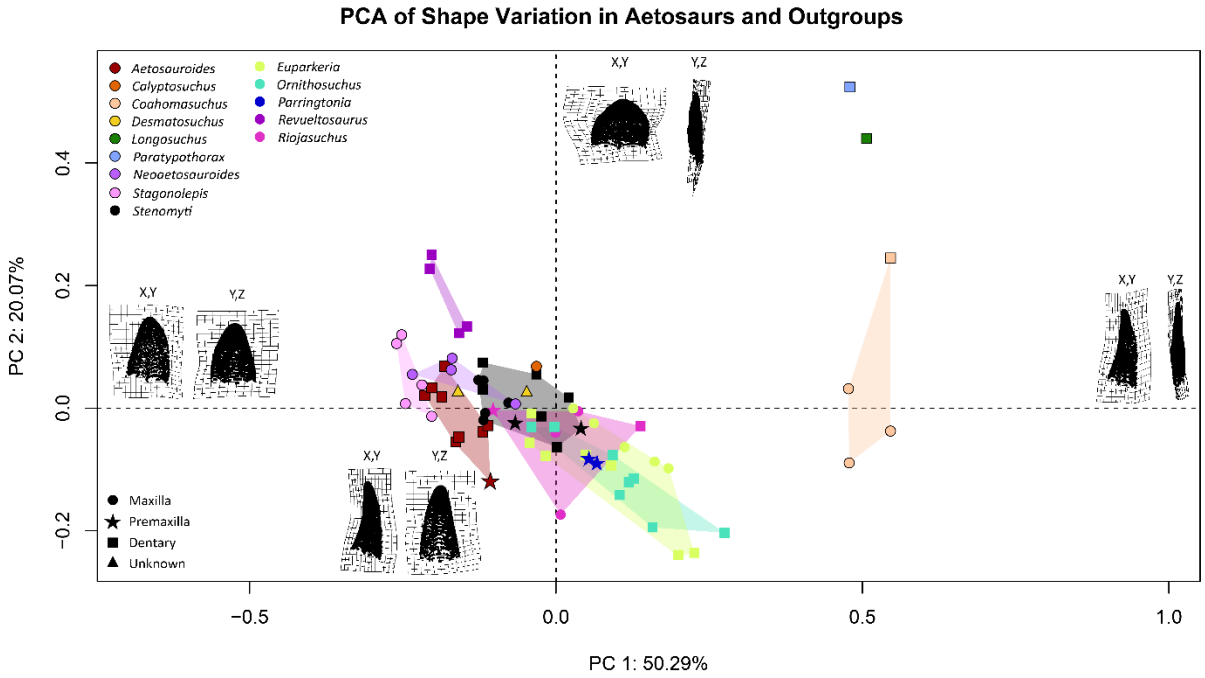


**Figure 19.** Morphospace occupation of aetosaur and outgroup teeth from the first two axes of the PCA. Points represent individual teeth. Coloured transparent polygons represent the convex hulls of morphospace occupied by each taxon. Thin plate splines show deformation of teeth at the extremes of each axis

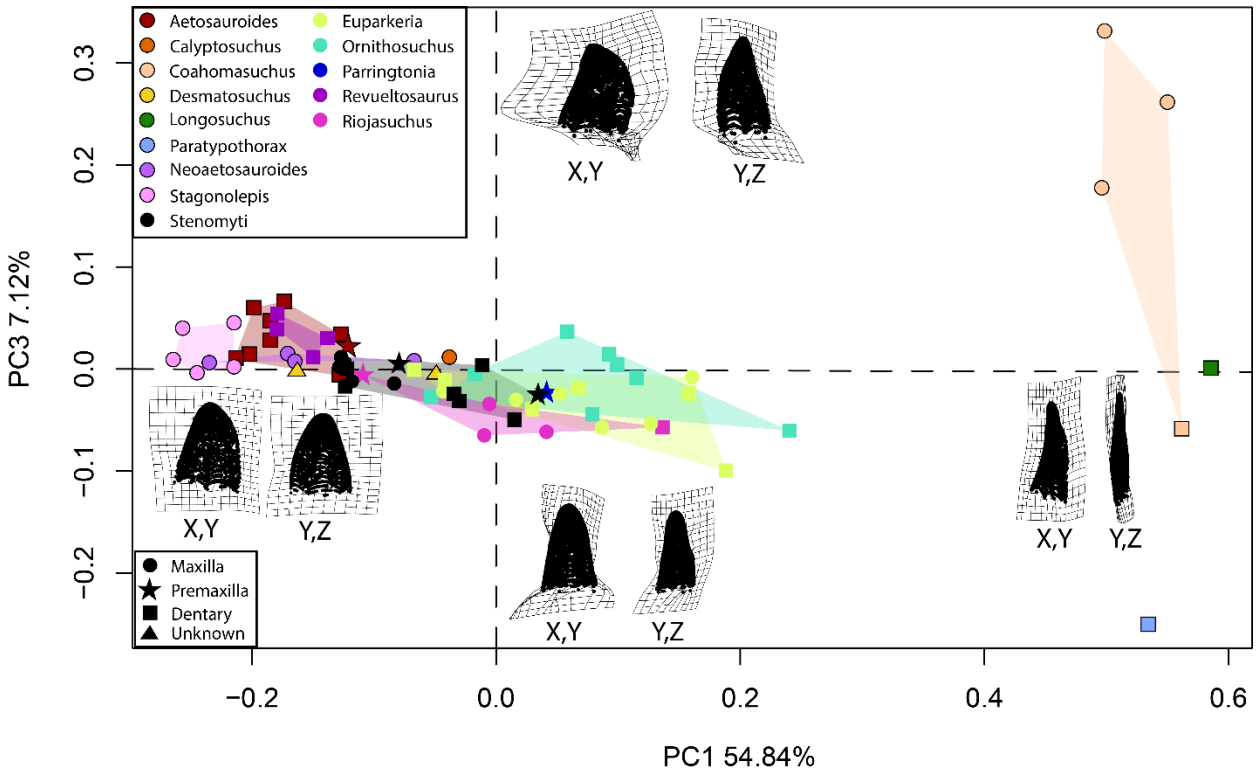


**Figure 20.** Morphospace occupation of aetosaur and outgroup teeth from PCs one and three of the PCA. Points represent individual teeth. Coloured transparent polygons represent the convex hulls of morphospace occupied by each taxon. Thin plate splines show deformation of teeth at the extremes of each axis

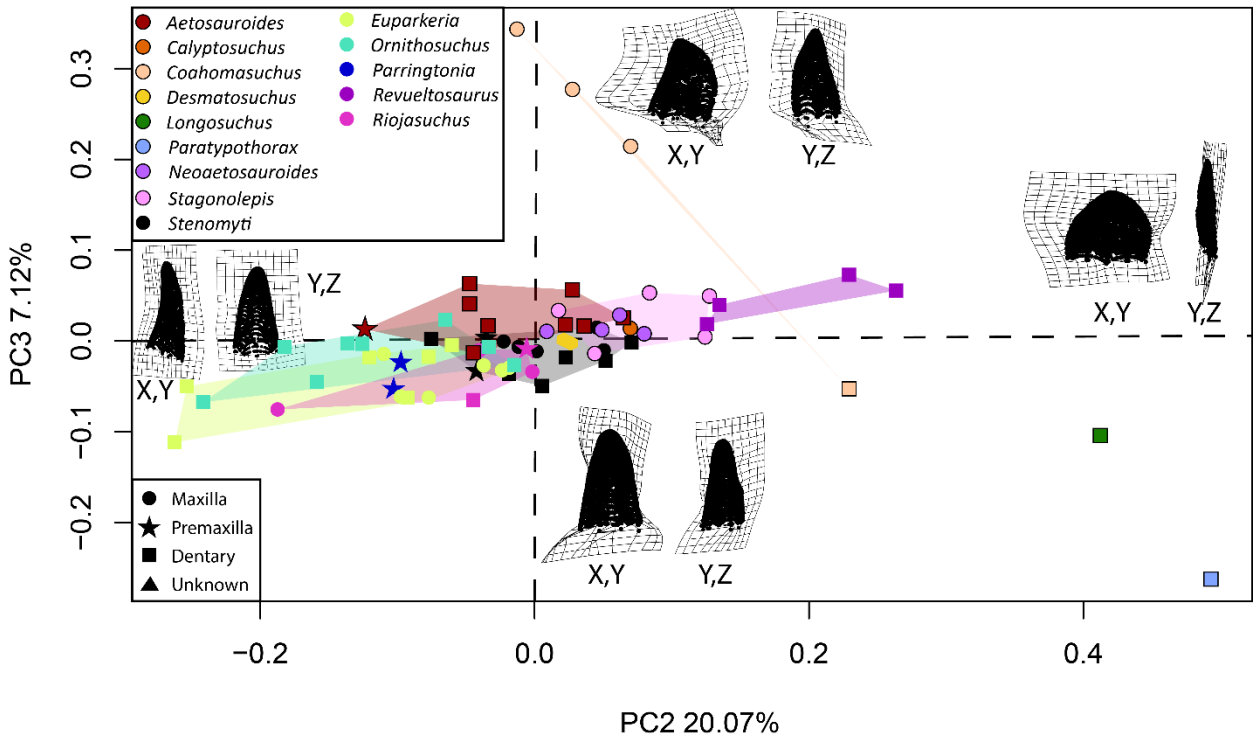


**Figure 21.** Morphospace occupation of aetosaur and outgroup teeth from PCs two and three of the PCA. Points represent individual teeth. Coloured transparent polygons represent the convex hulls of morphospace occupied by each taxon. Thin plate splines show deformation of teeth at the extremes of each axis

Together, PC1, PC2, and PC3 explain 78.31% of the variance seen in the 3DGM. From thin plate spline grids, we see that PC1, accounting for 50.29% of variance, appears to show a slightly recurved and labiolingually narrow tooth at the positive end, and a wider tooth with a round base at the negative end (Figs. 19, 20). PC2, accounting for 20.9% of variance, corresponds with a mesiodistally wide and apicobasally short, but flat tooth positively and a narrowing of the tooth and a significant increase in recurvedness and height negatively (Figs. 19, 21). PC3, accounting for 7.12% of variation, goes from a straight tooth at the minimum, to a

more curved and wider tooth at the maximum (Figs. 20,21). We see the outgroup taxa *Euparkeria*, and *Ornithosuchus* which have strongly recurved teeth, at the lowest negative of PC2 and midway along PC1, and aetosaurs *Paratypothorax,* and *Longosuchus,* and the sister group taxon, *Revueltosaurus*, all of which are not recurved, at the highest positive of PC2 (Fig. 19).

Looking at PC1 vs PC2 (Fig. 19), most taxa form a cluster around the centre of PC1 and PC2 when looking at these two axes, though outgroup taxa, save *Revueltosaurus*, tend to be on the negative side of PC2, and the aetosaurs and *Revueltosaurus* on the positive side. Most outgroup taxa also fall on the positive side, or around 0 on PC1, whereas the aetosaurs, apart from some outliers (*Coahomasuchus, Longosuchus,* and *Paratypothorax*), generally fall on the negative side or also around 0. Taxa for which more teeth were analysed take up greater areas in morphospace. Teeth from individuals form smaller clusters, regardless of which region of the mouth they come from.

*Coahomasuchus*, the "carnivorous aetosaur", groups together at the higher end of PC1 (Fig.19), and the maxillary teeth also do this on PC3 (Figs. 20,21), far from the main aetosaur/outgroup cluster. Its teeth differ from the outgroups showing the plesiomorphic condition by having a much rounder cross section and a more "hooked" tip, which is likely setting them apart.

The ANOVA test on genus (Table 2) performed showed a highly significant result (P: <0.001) and explains 73% of variance ($R^2$: 0.73089). This means that the generic diversity of aetosaurs explains much of the difference between tooth shape and tooth shape is not random.

Tooth shape is clearly different between each taxon. A pairwise comparison (Table 3) shows that out of all taxa, *Coahomasuchus* has the most significant differences between it and other taxa.

| | df | Sum Sq | Mean Sq | F-value | P-value | Sig. |
|---|---|---|---|---|---|---|
| Genus | 13 | 4.0194 | 0.309184 | 11.908 | 0.001 | *** |
| Residuals | 57 | 1.4799 | 0.26911 | | | |

**Table 2**. Table of ANOVA results where significance cut-offs are "." 0.1>p>0.05, "*" 0.05>p>0.01, "**" 0.01>p>0.001, "***" p<0.001

| | Calyp | Coa | Des | Eup | Long | Neo | Ornith | Para | Parr | Rev | Rio | Stag | Steno |
|---|---|---|---|---|---|---|---|---|---|---|---|---|---|
| Aeto | 0.710 | 0.001 | 0.677 | 0.003 | 0.002 | 0.743 | 0.004 | 0.001 | 0.194 | 0.115 | 0.062 | 0.298 | 0.212 |
| Calyp | | 0.064 | 0.911 | 0.492 | 0.101 | 0.845 | 0.421 | 0.061 | 0.576 | 0.584 | 0.669 | 0.479 | 0.923 |
| Coa | | | 0.003 | 0.001 | 0.080 | 0.001 | 0.001 | 0.058 | 0.006 | 0.001 | 0.001 | 0.001 | 0.001 |
| Des | | | | 0.244 | 0.021 | 0.955 | 0.191 | 0.007 | 0.0524 | 0.413 | 0.474 | 0.519 | 0.964 |
| Eup | | | | | 0.022 | 0.024 | 0.900 | 0.005 | 0.936 | 0.004 | 0.439 | 0.003 | 0.026 |
| Long | | | | | | 0.007 | 0.022 | 0.466 | 0.030 | 0.017 | 0.018 | 0.001 | 0.017 |
| Neo | | | | | | | 0.025 | 0.002 | 0.230 | 0.498 | 0.196 | 0.623 | 0.622 |

| | | | | | | | | | | | | | |
|---|---|---|---|---|---|---|---|---|---|---|---|---|---|
| Ornith | | | | | | | | 0.011 | 0.759 | 0.006 | 0.408 | 0.004 | 0.019 |
| Para | | | | | | | | | 0.014 | 0.003 | 0.009 | 0.001 | 0.003 |
| Parr | | | | | | | | | | 0.063 | 0.672 | 0.092 | 0.451 |
| Rev | | | | | | | | | | | 0.026 | 0.319 | 0.061 |
| Rio | | | | | | | | | | | | 0.033 | 0.251 |
| Stag | | | | | | | | | | | | | 0.81 |

**Table 3**. Summary of p-values of the pairwise comparison results for the ANOVA in Table 2. Aeto – *Aetosauroides*, Calyp – *Calyptosuchus*, Coa – *Coahomasuchus*, Des – *Desmatosuchus*, Eup – *Euparkeria*, Long – *Longosuchus*, Neo – *Neoaetosauroides*, Ornith – *Ornithosuchus*, Para – *Paratypothorax*, Parr – *Parringtonia*, Rev – *Revueltosaurus*, Rio – *Riojasuchus*, Stag – *Stagonolepis*, Steno - *Stenomyti*

The bone from which the teeth come, however, does not seem to be significant in where the teeth plot. In an ANOVA analysing this (Table 4), the p-value was 0.586. This also explains little of the variation, with a very low $R^2$ of 0.03299.

| | df | Sum Sq | Mean Sq | F-value | P-value | Sig. |
|---|---|---|---|---|---|---|
| Tooth Type | 3 | 0.1814 | 0.060466 | 0.7618 | 0.586 | . |
| Residuals | 67 | 5.3179 | 0.96701 | | | |

**Table 4**. Table of ANOVA results looking at the bones each tooth comes from (Tooth Type) where significance cut-offs are "." 0.1>p>0.05, "*" 0.05>p>0.01, "**" 0.01>p>0.001, "***" p<0.001

The clade of each taxon also seems to play a significant role in where they plot (Table 5). Aetosaurs were separated into *Aetosauroides* as the earliest diverging aetosaur, Stagonolepidoidea, and Aetosaurinae. Outgroups were separated into *Euparkeria* as our outgroup archosauriform, Ornithosuchidae, Erpetosuchidae, and *Revueltosaurus* as the sister taxon to aetosaurs.

| | df | Sum Sq | Mean Sq | F-value | P-value | Sig. |
|---|---|---|---|---|---|---|
| Clade | 7 | 2.0577 | 0.293958 | 0.37417 | 0.001 | *** |
| Residuals | 63 | 3.4416 | 0.054629 | | | |

**Table 5.** Table of ANOVA results looking at the clade of each taxa where significance cut-offs are "." 0.1>p>0.05, "*" 0.05>p>0.01, "**" 0.01>p>0.001, "***" p<0.001

There is a weaker significant difference between the two major groups of aetosaurs and outgroups (Table 6), however, the $R^2$ value is very loe ($R^2$: 0.06132).

| | df | Sum Sq | Mean Sq | F-value | P-value | Sig. |
|---|---|---|---|---|---|---|
| Group | 1 | 0.3372 | 0.33723 | 04.5076 | 0.003 | ** |
| Residuals | 69 | 5.1621 | 0.07481 | | | |

**Table 6:** Table of ANOVA results comparing between aetosaurs and outgroups where significance cut-offs are "." 0.1>p>0.05, "*" 0.05>p>0.01, "**" 0.01>p>0.001, "***" p<0.001

**NMDS**

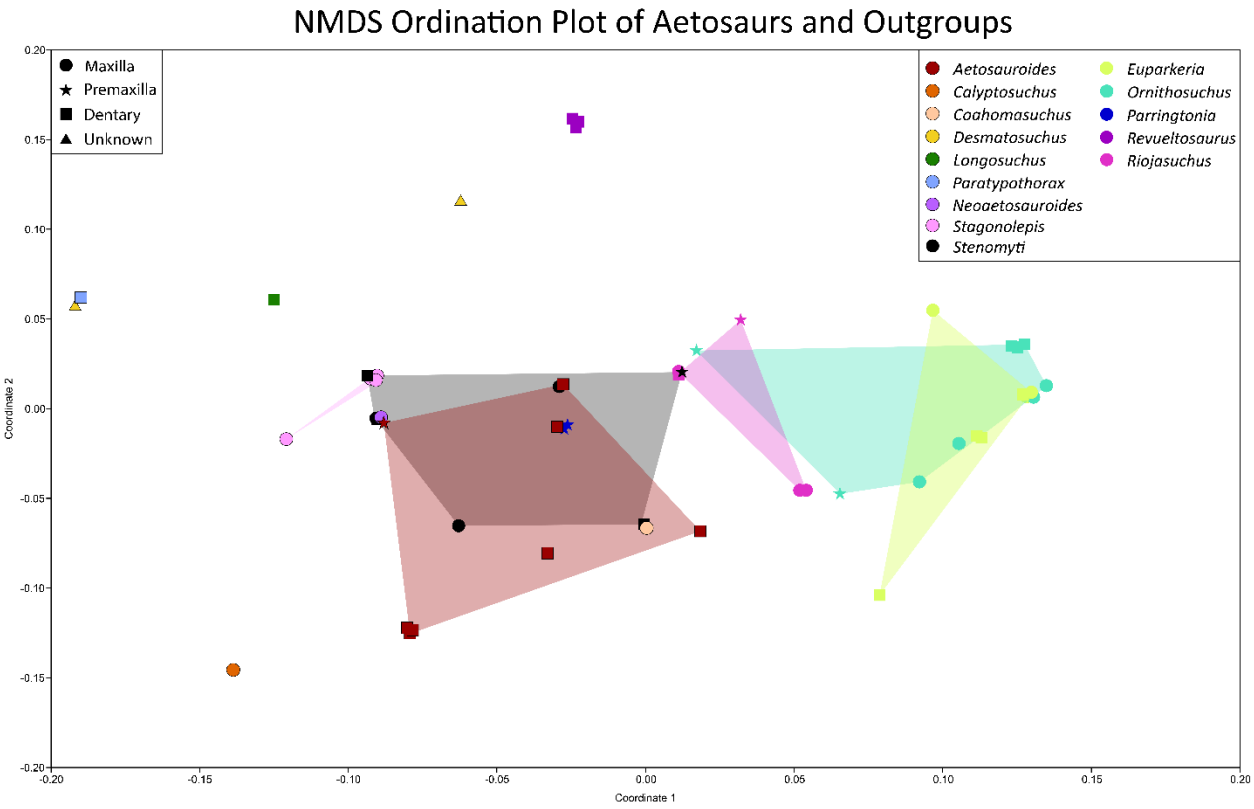


**Figure 22.** Ordination plot of the first two NMDS coordinates. Points represent individual teeth. Coloured transparent polygons represent the convex hulls of morphospace occupied by each taxon

The NMDS results generally show more of a separation between aetosaurs and outgroup taxa. *Revueltosaurus* forms a grouping at the extreme positive of coordinate 2, and most plesiomorphic outgroup taxa (*Euparkeria, Ornithosuchus,* and *Riojasuchus*) fall more in the positive of coordinate 1 than all aetosaurs (Fig. 22). The plesiomorphic outgroup exception is *Parringtonia*, which falls within the space of *Aetosauroides* and *Stenomyti*. Only a handful of teeth of *Aetosauroides* and *Stenomyti* stray into the positive of coordinate 1. Again, we generally

see those taxa with more teeth plotting over a wider area, in the case of *Aetosauroides* and *Stenomyti*, this is more pronounced in the NMDS. It is worth noting that some teeth, particularly those of the same species, shared the exact same character profile and so plotted on top of each other.

**Isolated Teeth**

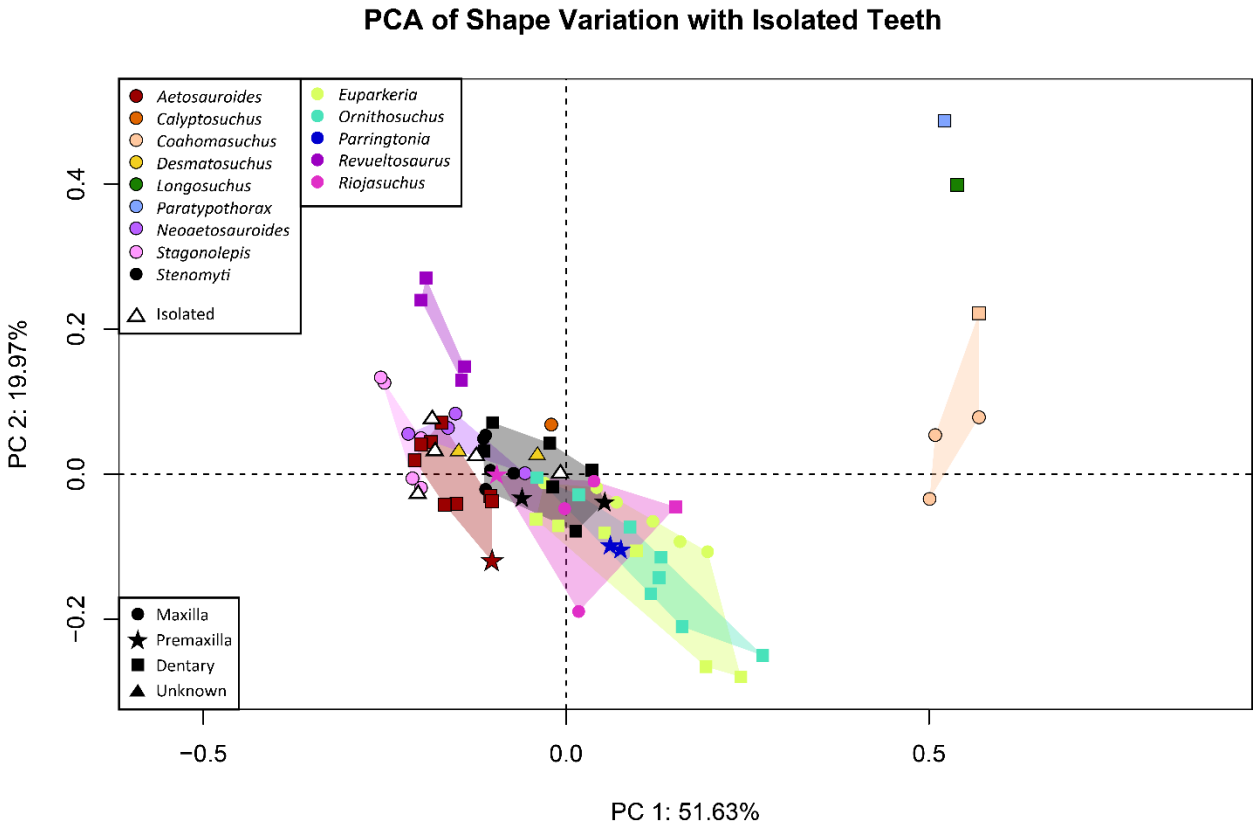


**Figure 23.** Morphospace occupation plot showing all known taxa with the isolated teeth in the white hexagons. Points represent individual teeth.

When isolated teeth, thought to be from stagonolepids, from the Tecovas Formation are added to the 3DGM analysis (Fig. 23), the majority plot near this group, particularly *Desmatosuchus, Neoaetosauroides* and *Stagonolepis.* However, one tooth (TTU-P 24191) plots a

little further away towards the positive end of PC1, within the *Stenomyti* cluster, and close to the edge of the outgroup taxa. For the majority, my results confirm they are aetosaurs and may be within the Stagonolepidoidea.

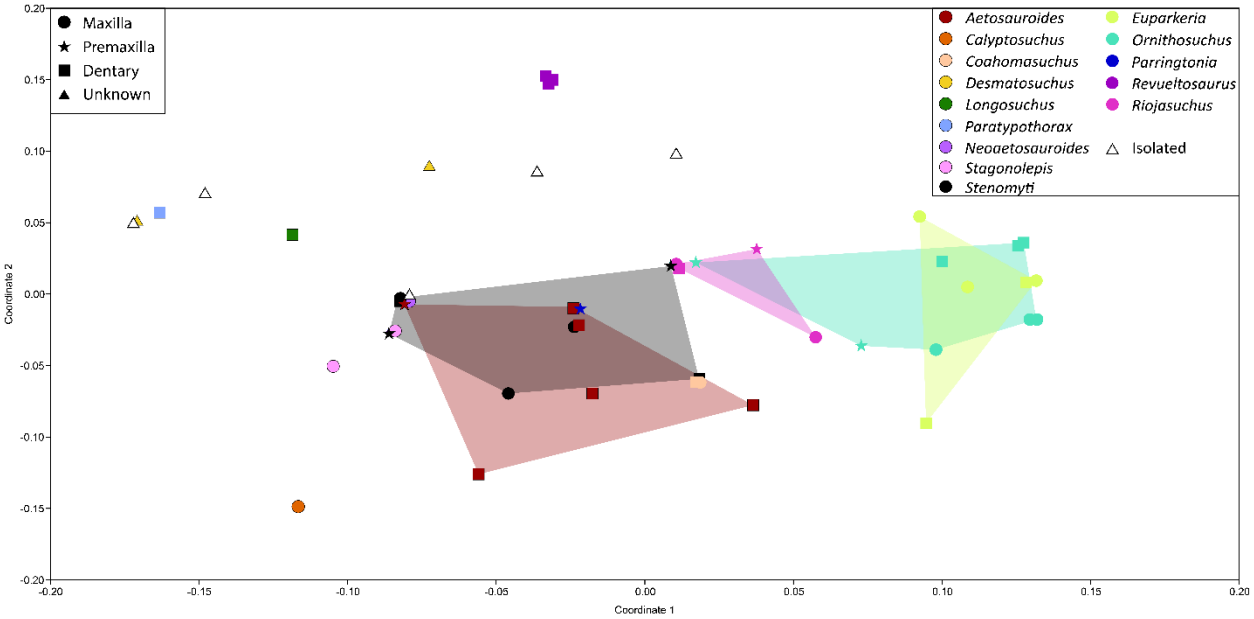


**Figure 24.** Ordination plot showing the known taxa and the isolated teeth in white hexagons. Points are individual teeth.

There is a greater spread of the isolated teeth in the NMDS analysis (Fig. 24), though some still plot near *Desmatosuchus*, *Stagonolepis*, *Aetosauroides*, and *Neoaetosauroides*. However, as these points are very spread out and several do not plot near their suspected clade, it seems that the NMDS is less helpful in identifying isolated aetosaur teeth although they do still plot away from the outgroups and so can be distinguished as likely aetosaurs.

## DISCUSSION

**Overall discussion of outgroups vs aetosaurs**

In the 3D GM, the outgroups tend to cluster together, with little overlap from aetosaurs, except for *Stenomyti*, which straddles both the main aetosaur cluster, and the edge of the outgroup (excluding *Revueltosaurus*) taxa clump (Fig. 19). *Euparkeria* and *Ornithosuchus* in particular virtually sit on top of one another. The majority of outgroup taxa cluster around 0 and the negative side of PC2, and the lower positives of PC1, which is likely to do with their being taller and more recurved than the majority of aetosaur teeth, as similar shapes are found at these ends of the axis. This pattern is reflected in the NMDS analysis (Fig.22), where the majority outgroup taxa showing the plesiomorphic condition form a cluster that is largely separate from any aetosaur taxa, with only a small overlap. This shows that these teeth are picked up as distinctly different from those of the aetosaurs and this can be confirmed both by looking quantitatively at shape and via discrete characters.

*Revueltosaurus* is the only exception to this out of the outgroup taxa in both the 3DGM and the NMDS analysis, which was to be expected as its teeth are different from those plesiomorphic teeth in the main clusters, and it is the outgroup most closely related to the aetosaurs. It plots even more positively along PC2 than most aetosaurs in the 3DGM, with only *Longosuchus* and *Paratypothorax* plotting higher, and slightly out of the aetosaur cluster (Fig. 19). *Revueltosaurus* and *Paratypothorax* have superficially similar dental features, (e.g. cusps, ridges), though these are much less pronounced in *Paratypothorax* which has a far rounder base, explaining the significant distance between them. In the NMDS analysis, it is again separate from any other taxon. These teeth are generally distinct from others in microvertebrate deposits

and are instantly recognisable, with many distinguishing characteristics (e.g. the large cusps that are not seen on any other taxon in this study) (Hunt 1989).

**Overall discussion of early diverging aetosaurs vs other aetosaurs**

The earliest-diverging aetosaur, *Aetosauroides*, strays down into the negative of PC2 possibly suggesting a more faunivorous diet than some other aetosaurs (as was also suggested in Paes Neto et al. 2021), as this falls in line with the main outgroup taxa cluster, but also has points that only just overlap with *Desmatosuchus, Stagonoleips* and *Neoaetosauroides.* Its premaxillary tooth is the furthest in the negative of PC2, which is similar to *Stenomyti* with its premaxillary teeth being two of the furthest negative of the taxon suggesting some slight shape heterodonty.

The Aetosaurinae are extremely disparate across morphospace, with none of them plotting especially close together. *Stenomyti* plots around the 0 point of both axes, whereas *Coahomasuchus* and *Paratypothorax* are much further along the positive side of PC1. However, these two genera are greatly separated across PC2, with the more recurved teeth of *Coahomasuchus* falling closer to or around 0 of PC2. In the NMDS, the opposite is true of *Stenomyti* and *Coahomasuchus*, the latter of which plots on the edge of the hull and virtually on top of some of the teeth of the former.

The teeth of Stagonolepidoidea plot much more closely together, excepting *Longosuchus*, and form the bulk of taxa in the main aetosaur cluster. Again, the opposite is true in the NMDS analysis: the majority of these taxa plot disparately due to a wider variety of discrete characters than shapes. This suggests that isolated teeth that plot in the main aetosaur cluster in the 3DGM may be able to be more specifically identified with the use of the NMDS, which generally gives a great degree of separation among each taxon.

There does not appear to be any pattern when it comes to the ages of each aetosaur in the 3DGM. The Carnian aetosaurs (*Aetosauroides, Coahomasuchus, Longosuchus,* and *Stagonolepis*) do not plot closely together apart from *Aetosauroides* and *Stagonolepis. Coahomasuchus* and *Longosuchus* plot distantly from each other (though both at the positive end of PC1). There is more constraint amongst the Norian aetosaurs (*Calyptosuchus, Desmatosuchus, Neoaetosauroides, Paratypothorax,* and *Stenomyti*), with *Calyptosuchus, Desmatosuchus, Neoaetosauroides,* and *Stenomyti* plotting nearby in the main cluster of aetosaurs, but *Paratypothorax* still plots more distantly. There does not seem to be a pattern of where the aetosaurs plot based on age. The two recurved aetosaur teeth (*Aetosauroides* and *Coahomasuchus*) are both Carnian in age (though it is possible that the Otis Chalk assemblage is earliest Norian in age), but plot on opposite sides of the morphospace in the 3DGM (Fig. 19). The more bulbous teeth of *Stagonolepis* and *Neoaetosauroides* do plot together, despite being separated by a lot of time. However, they are likely more affected by phylogeny as they are both within Stagonolepidoidea and this is a greater driving force of similarity than age is.

In the NMDS analysis, though more points, particularly from individuals, overlap, there is generally greater separation among taxa. This suggests that, in combination with the 3DGM, this technique could prove useful in teasing apart clustered taxa, enabling finer taxonomic assignments. All aetosaurs fall in the negative of coordinate 1 apart from one tooth each from *Aetosauroides* and *Stenomyti*. This is reflected in where the isolated aetosaur teeth fall (Fig. 24) in that all plot in the negative of coordinate one save for one tooth, which is fairly different compared to the other teeth analysed.

**Differences in jaw element and tooth position**

In the 3DGM, amongst the outgroup taxa, there does seem to be separation among jaw elements in *Euparkeria*, and arguably in *Riojasuchus*. *Euparkeria* forms two distinct lines of teeth with the maxilla plotting relatively more positively along PC2 than the dentary teeth of similar positions along the tooth row. In *Riojasuchus* there does seem to be some separation between tooth types, which is visible when including PC3 as well. Along PC1 maxillary teeth plot around the centre, the premaxillary tooth is more negative and the dentary tooth is more positive. It is impossible to say with only one representative of premaxillary and dentary teeth whether this pattern would be upheld with more teeth.

In the three aetosaurs with teeth representing different jaw elements (*Aetosauroides*, *Coahomasuchus* and *Stenomyti*), there are potentially some distinctions among tooth type. In *Coahomasuchus*, the maxillary teeth plot much more closely together than the dentary tooth. In *Stenomyti*, we see a similar clustering of maxillary teeth, however, dentary teeth are intermingled with this and so it would be difficult to disentangle this with unknown teeth. The premaxillary teeth of *Stenomyti* are not especially distinct from the maxilla and dentary teeth either, plotting lower on PC2 than the majority of other teeth, but not particularly close to each other in any of the first three PCs. However, if teeth do plot lower, it may be a sign that they could be premaxillary. In *Aetosauroides*, the premaxillary tooth used does plot away from the dentary teeth, but it is also clear that the dentary teeth form two sub-clusters, which are around the same distance from each other as the premaxillary tooth is from any dentary tooth and so it is difficult to argue for clean separation.

A limitation of this study is that I do not have tooth representatives from all regions of the mouth (where teeth are present as *Desmatosuchus* and *Longosuchus* have edentulous premaxillae) for all aetosaurs, making the question of differentiation among regions of the mouth

a difficult one to test over a range of taxa. In the future, more specimens with different tooth types could be added to further elucidate whether there is truly separation among elements of the jaw. When looking at both outgroup taxa and aetosaurs, it seems that having differently shaped teeth within elements may be more of a plesiomorphic condition that aetosaurs have lost as they moved to a more morphologically homogeneous and simple dentition. If aetosaurs did move away from a more faunivorous diet towards herbivory, this would contrast with the pattern generally seen in other vertebrates where teeth of herbivores are generally more complex than carnivores, with some exceptions (Melstrom 2017, Melstrom et al. 2021).

In terms of trends along the tooth row of individual elements, this again looks more apparent in the outgroup taxa and particularly *Euparkeria*. Within both the maxillary and dentary teeth, there is a trend (with one exception of the third right maxillary tooth) of posterior to anterior teeth moving towards the main cluster of taxa. This pattern is the same but flipped in *Revueltosaurus*, with anterior to posterior teeth moving away from the cluster. Trends are not possible to observe in *Riojasuchus* and *Ornithosuchus* - in *Riojasuchus* as there are only two teeth from the same element, and in *Ornithosuchus* because it is unclear where the majority of teeth came from along the tooth row. Despite this, the trends seen in *Euparkeria* and *Revueltosaurus* may suggest that teeth gradually changing along the tooth row, indicating mild heterodonty, is an ancestral trait.

Within Aetosauria, however, no patterns of change along the tooth row are discernible in those with multiple teeth from the same element and they are randomly distributed within their taxon clusters. The only exception is potentially *Coahomasuchus*, where we see a line of anterior to posterior teeth moving into the negative of PC2. Along with the trend in *Euparkeria*, this could potentially suggest that carnivory leads to gradual change along the tooth row. Although

with the same pattern observed in *Revueltosaurus*, this may be more likely to be a plesiomorphic trait lost in the earlier diverging *Aetosauroides*.

**Tooth shape changes across phylogeny**

The majority of the outgroups retain the plesiomorphic condition of laterally compressed, recurved, and serrated teeth. This is also seen in the earliest diverging aetosaur: *Aetosauroides*. However, the same is not true for the closest outgroup taxon to the aetosaurs: *Revueltosaurus*. Given the simplicity of other aetosaur teeth, that have lost the recurvedness, some lateral compression, and, in the majority, denticles, it is likely that *Revueltosaurus* diverged evolutionarily from the branch to aetosaurs, developing its own unique dentition, suitable to herbivory (Heckert 2002). This tooth shape did not lead to the ancestral aetosaur tooth shape, which is more likely closer to that seen in *Aetosauroides*. Whereas it is possible that some aetosaurs in this study, namely *Desmatosuchus*, *Coahomasuchus*, and, to an extent, *Paratypothorax*, retained denticles that were lost in other aetosaurs, given that the majority of aetosaurs lack these structures, it is also possible that they re-evolved in these taxa. However, as aetosaur teeth are rarely well preserved and have previously been overprepared, along with the very small size of denticles to begin with (Paes Neto et al. 2021), these denticles may have simply been lost to wear, taphonomy, or preparation.

The Stagonolepidoidea all feature relatively peg-like teeth, with varying degrees of expansion from the cervix creating more “bulbous” teeth. This group may feature taxa with similar diets or may be constrained by phylogeny to produce similarly shaped teeth.

Given the peg-like tooth of *Stenomyti*, sister to *Coahomasuchus* and *Paratypothorax*, it seems most probable that *Coahomasuchus* reverted to a more plesiomorphic condition and "carnivorous" dentition from the more peg-like teeth seen in many other aetosaurs. As teeth have a great deal of functional pressure that determines shape (for example, the teeth of mammals converging on similar shapes from diet rather than phylogeny or size (Evans et al. 2007)), these changes likely reflect shifting diets within Aetosauria.

The ANOVA results suggest a significant phylogenetic signal, for both genus and clade (Tables 2, 5) in that this is important in the placement of teeth within morphospace. Whereas Stagonolepidoidea form a cluster (excluding *Longosuchus*) with the early-diverging aetosaur *Aetosauroides*, Aetosaurinae are much more dispersed across morphospace. So it could be argued that some more closely related aetosaurs have more constrained tooth morphotypes; however, this is not the case for all aetosaurs. This is unsurprising when looking at *Coahomasuchus*, which has a derived tooth shape, clearly being carnivorous, but it is unclear why *Paratypothorax* does not cluster with the majority of other aetosaur teeth.

**Isolated Teeth**

Different aetosaur tooth morphotypes have been noted as rarely being distinctive (Heckert 2004) and may be confused with the teeth of other Archosauriformes when found isolated. Although aetosaur osteoderms are relatively common finds in some deposits, for example throughout the Chinle Formation (Parker & Martz 2011), their teeth are not as common as would be expected based on the frequency with which their osteoderms are found (Long & Ballew 1985, Heckert 2004). It is possible that this pattern is the result of aetosaurs generally having fewer teeth than other archosaurs (Heckert 2004), slow tooth replacement, or potentially

that aetosaur teeth are not being recognised as such in deposits or that osteoderms are "over represented".

Given there is a large clustering of aetosaur teeth in the 3DGM and also in the NMDS to a slightly lesser extent, it is most likely that if an isolated tooth plots within those clusters, especially within both, it is from an aetosaur. Whereas arguments can be made for identification to genus level by isolated teeth plotting with known genera, these assignments would not be confident as many taxa overlap in morphospace, or there are only a couple of data points. This more general identification is still useful and could be used to fill in gaps in the fossil record that are currently seemingly devoid of aetosaur teeth, better constraining the aetosaur record. As these plots encompass aetosaurs from across time and space, it would be relatively simple in most cases to use knowledge of aetosaurs that have already been found in microvertebrate localities or deposits in general to assign a more taxonomically restrictive affinity than simply that it is the tooth of an aetosaur.

The isolated teeth placed into the 3DGM analysis (Fig. 23) plot close to the stagonolepids *Desmatosuchus*, *Neoaetosauroides*, and *Stagonolepis*, along with the earlier diverging *Aetosauroides*. This is not unexpected, given their similar shape, particularly to *Desmatosuchus*, and the presence of *Desmatosuchus* and *Tecovasuchus* in the Tecovas Formation (Small 1985, Martz & Small 2005, Parker 2005), where the isolated teeth are also from.

One tooth (TTU-P24191) is a little further from this cluster and could possibly represent a silesaurid rather than an aetosaur. Instead, it plots within the *Stenomyti* cluster at the edge of where the carnivorous outgroup taxa plot. This shows that we need to include animals that do not only possess the hypothesised ancestral condition for archosaur teeth and close relatives of

aetosaurs, but also teeth that are, at least, superficially similar to aetosaur teeth if we are to use this method for identification.

In the NMDS analysis, again, the majority of teeth plot around *Desmatosuchus* and *Stagonolepis* adding weight to the hypothesis that they are from stagonolepids (Fig. 24). Similarly to the 3DGM, TTU-P 24191 plots near *Stenomyti*, but is closer to the stagonolepids. The smallest tooth by far plots furthest away from *Desmatosuchus* and most other isolated teeth. This tooth could potentially be from a juvenile and does not have the full characteristics of an adult tooth, something that is seen today in extant reptiles (Estes & Williams 1984, Gignac & Erikson 2014, D'Amore 2015).

Given the area in which the majority of teeth plot in both analyses and the fauna of the Tecovas Formation from where they hail, it is most likely that the teeth belong to either *Desmatosuchus* or *Tecovasuchus* (Small 1985, Martz & Small 2005, Parker 2005), both of which are stagonolepids. However, as *Tecovasuchus* is not included in the analysis, it would be wise to add known teeth from this genus into the analysis to get a better understanding of which taxon or taxa the teeth belong to.

**Further testing and Concerns**

One concern is that varying resolutions of scans could affect how each tooth plots in morphospace in the 3DGM, though this likely wouldn't impact the first few PCs. Scans here come in varying degrees of resolution from different sources such as some being from CT scans and others from surface scans, with teeth like *Riojasuchus* being some of the lowest resolution, and teeth like *Desmatosuchus* being far smoother with a greater number of polygons. As the net of semi-landmarks is dense, this could be picking up variation from scan quality rather than

actual tooth morphology. However, when reducing one of the higher quality meshes to match the number of faces of the lowest (*Riojasuchus*), virtually no difference was observed between where it usually plots in the PCA, meaning even with large variations in scan quality this method is promising.

Low sampling of teeth from each taxon is another concern. As some are only represented by one or two teeth, I cannot document variation within the species as I can for other aetosaurs and the outgroup taxa. This means that outliers are impossible to spot, and it is harder to see the overall spread of results. If isolated teeth are added in, they may plot within what would be the space of *Longosuchus*, for example, but with only one point I cannot say this for certain, only that it plots near it.

A similar problem arises from only having representatives from one individual per genus in that we cannot see intrageneric differences and ranges of taxa, and assumptions must be made that these individuals are representative of their genus/species, which cannot be tested here. The solution is, of course, to add more specimens, both of more individuals and of more teeth overall, which I hope will be possible in the future, but currently with a dearth of suitable aetosaur specimens and scans, this cannot be done.

## CONCLUSIONS

This analysis provides more information using quantitative and qualitative methods on the dentition of aetosaurs and how it changes across time and phylogeny. We can identify aetosaurs using the matrices and it is possible that in combination with prior knowledge of fauna in formations that aetosaur teeth discovered here could be identified to genus/species. This will

allow us to fill in gaps in ecosystems recorded in microvertebrate localities and increase our understanding and knowledge of the taxa that were living and interacting together. These methods can be replicated with tooth fossils from other clades and time periods, making them useful for other researchers, and the dataset can be used and built upon to further study the teeth of archosaurs in the Mesozoic.

**ACKNOWLEDGMENTS**

Thank you to Matthew Colbert for scanning *Coahomasuchus*, Joseph Bevitt and Adam Fitch for providing scans of *Stenomyti*, Dr.Valentine Fischer for providing R code and discussion. Thanks are given to Dr. Davide Foffa for providing scans of *Stagonolepis* and *Ornithosuchus,* discussion, and assistance with R coding, Dr. Nicolas Campione for assistance with R coding, Isaac Pugh for creating scans of *Desmatosuchus*, Abigail Chernaut for assistance and training in surface scanning, Jeremías Taborda for providing the scan of PULR 108, Dr. Ben Kligman for assistance with µCT scanning, Dr. Tom G. Davies and Dr. Elizabeth Martin-Silverstone for the scanning of *Stagonolepis.* and Dr. Nick Hebdon for discussion on PCAs.

**REFERENCES**

1. Adams, D., Collyer, M., Kaliontzopoulou, A. & Baken, E. 2025. “Geomorph: Software for geometric morphometric analyses. R package version 4.0.10.” https://cran.r-project.org/package=geomorph.
2. Agassiz, L. 1844. Monographie des Poissons Fossiles du Vieux Grès Rouge ou Système Dévonien (Old Red Sandstone) des Isles Britanniques et de Russie. Soleure, Neuchâtel.

3. Adams, D.C., Rohlf, J.F. & Slice, D.E. 2013. A field comes of age: geometric morphometrics in the 21st century. *Hystrix, The Italian Journal of Mammalogy* **24(1)**: 7-14
4. Argast, S., Farlow, J.O., Gabet, R.M. & Brinkman, D.L. 1987. Transport induced abrasion of fossil reptilian teeth: Implications for the existence of Tertiary dinosaurs in the Hell Creek Formation, Montana. *Geology* **15(10)**: 927-930
5. Baken, E., Collyer, M., Kaliontzopoulou, A. & Adams, D. 2021. "geomorph v4.0 and gmShiny: enhanced analytics and a new graphical interface for a comprehensive morphometric experience." *Methods in Ecology and Evolution* **12**: 2355-2363.
6. Barrett, P.M. & Rayfield, E.J. 2006. Ecological and evolutionary implications of dinosaur feeding behaviour. *Trends in Ecology & Evolution* **21(4):** 217-224
7. Barrett PM, Butler RJ, Nesbitt SJ. 2011. The roles of herbivory and omnivory in early dinosaur evolution. *Earth and Environmental Science Transactions of the Royal Society of Edinburgh* **101(3-4)**: 383-396
8. Barrett, P.M. 2014 Paleobiology of herbivorous dinosaurs. *Annual Review of Earth and Planetary Sciences* **42**: 207-230
9. Benton, M.J. 1990. The species of *Rhynchosaurus*, a rhynchosaur (Reptilia, Diapsida) from the Middle Triassic of England. *Philosophical Transactions of the Royal Society B* **328(1247)**: 213-306
10. Benton, M.J., Dunhill, A.M., Lloyd, G.T. & Marx, F.G. 2011. Assessing the quality of the fossil record: insights from vertebrates. *Geological Society, London, Special Publications* **358**: 63-94

11. Benyoucef, M., Läng, Cavin, L., Mebarki, K., Adaci, M. & Bensalah. 2015. Overabundance of piscivorous dinosaurs (Theropoda: Spinosauridae) in the mid-Cretaceous of North Africa: The Algerian dilemma. *Cretaceous Research* **55**: 44-55
12. Bhat, M.S. 2017. Techniques for systematic collection and processing of vertebrate microfossils from their host mudrocks: a case study from the Upper Triassic Tiki Formation of India. *Journal Geological Society of India* **89:** 369-374
13. Bonaparte JF. 1967. Dos nuevas 'faunas' de reptiles triásicos de Argentina. Gondwana Stratigraphy, 1 Gondwana Symposium, Mar del Plata, 283–325
14. Brocklehurst, N. & Benson, R.J. 2021. Multiple paths to morphological diversification during the origin of amniotes. *Nature Ecology & Evolution* **5:** 1243-1249
15. Broom R. 1913. Note on *Mesosuchus browni*, Watson, and on a new South African Triassic pseudosuchian (*Euparkeria capensis*). *Records of the Albany Museum* **2(5)**: 394-396
16. Brusatte, S.L., Norell, M.A., Carr, T.D., Erikson, G.M., Hutchinson, J.R., Balanoff, A.M., Bever, G.S., Choiniere, J.H., Makovicky, P.J. & Xu, X. 2010. Tyrannosaur paleobiology: new research on ancient exemplar organisms. *Science* **329(5998)**: 1481-1485
17. Buckley, L.G., Larson, D.W., Reichel, M., Samman, T. 2010. Tooth and consequences: quantifying variation of teeth within a single population of *Albertosaurus* sarcophagus (Theropoda: Tyrannosauridae) from the Horseshoe Canyon Formation (Upper Cretaceous: lower Maastrichtian) and implications for identifying isolated tyrannosaurid teeth in Maastrichtian-aged deposits. *Canadian Journal of Earth Sciences* **49**: 1227–1251.

18. Calede, J.J. & Glusman J.W. 2017. Geometric morphometric analyses of worn cheek teeth help identify extant and extinct gophers (Rodentia, Geomyidae). *Paleontology* **60(2)**: 281-307

19. Casamiquela, R.M. 1960. Noticia preliminar sobre dos nuevos estagonolepoideos Argentinos. *Ameghiniana* **2**: 3-9.

20. Currie, P.J., Rigby Jr., J.K. and Sloan, R.E. 1990 Theropod teeth from the Judith River Formation of southern Alberta, Canada. In: Carpenter, K., Currie, P.J. (Eds.) *Dinosaur Systematics: Approaches and Perspectives.* Cambridge University Press, Cambridge, pp. 107-125

21. D'Amore, D.C. 2015. Illustrating ontogenetic change in the dentition of the Nile monitor lizard *Varanus niloticus*: a case study in the application of geometric morphometric methods for the quantification of shape-size heterodonty. *Journal of Anatomy* **226(5):** 403-419.

22. Desojo, J.B., Heckert, A.B., Martz, J.W., Parker,W.G., Schoch, R.R., Small, B.J. and Sulej, T. 2013. Aetosauria: a clade of armoured pseudosuchian archosaurs from the Upper Triassic continental beds. *Geological Society, London, Special Publications* **379**: 203–239.

23. Desojo, J.B., Fiorelli, L.E., Ezcurra, M.D., Martinelli, A.G., Ramezani, J., Da Rosa, A.A. S., von Baczko, M.B., Trotteyn, M.J., Montefeltro, F.C., Ezpeleta, M., Langer, M.C. 2020. The Late Triassic Ischigualasto Formation at Cerro Las Lajas (La Rioja, Argentina): fossil tetrapods, high-resolution chronostratigraphy, and faunal correlations. *Scientific Reports* **10(1)**:1-34.

24. Eberth, D.A., Shannon, M., Noland, B.G. 2007. A bonebeds database: classification, biases and patterns of occurrence. In: Rogers, R.R., Eberth, D.A., Fiorillo, A.R. (Eds.), *Bonebeds: genesis, analysis and paleobiological significance*. The University of Chicago Press, Chicago and London, pp. 103–220.

25. Estes, R. & Williams, E.E. 1984. Ontogenetic variation in the molariform teeth of lizards. *Journal of Vertebrate Paleontology* **4(1):** 96-107.

26. Evans, A.R., Wilson, G.P., Fortelius, M. & Jernvall, J. 2007. High-level similarity of dentitions in carnivorans and rodents. *Nature* **445**: 78-81.

27. Fischer, V., Bennion, R.F., Foffa, D., MacLaren, J.A., McCurry, M.R., Melstrom, K.M. & Bardet, N. 2022. Ecological signal in the size and shape of marine amniote teeth. *Proceedings of the Royal Society B* **289**: 20221214.

28. Gignac, P.M. & Erickson, G.M. 2014. Ontogenetic changes in dental form and pressures facilitate developmental niche shifts in American alligators. *Journal of Zoology* **295(2)**: 132-142.

29. Gower, D.J. and Walker, A.D. 2002. New data on the braincase of the aetosaurian archosaur (Reptilia: Diapsida) *Stagonolepis robertsoni* Agassiz. *Zoological Journal of the Linnean Society* **136**: 7-23.

30. Gower, J.C. 1971. A general coefficient of similarity and some of its properties. *Biometrics* **27**: 857-874.

31. Hammer, Ø., Harper, D. & Ryan P. 2001. PAST-Palaeontological statistics. *Palaeontologia Electronica* **25**: 2009.

32. Heckert, A.B. 2002. A revision of the Upper Triassic ornithischian dinosaur *Revueltosaurus*, with a description of a new species. In Heckert, A.B. & Lucas, S.G., eds.

Upper Triassic Stratigraphy and Paleontology: New Mexico Museum of Natural History and Science Bulletin no. 21. Albuquerque: New Mexico Museum of Natural History and Science, 253-268.

33. Heckert, A.B. 2004. Late Triassic microvertebrates from the lower Chinle Group (Otischalkian – Adamanian: Carnian), southwestern USA. *New Mexico Museum of Natural History & Science Bulletin* **27**: 1-170.
34. Heckert AB, Lucas SG. 1999. A new aetosaur (Reptilia: Archosauria) from the Upper Triassic of Texas and the phylogeny of aetosaurs. *Journal of Vertebrate Paleontology* **19(1)**: 50–68.
35. Heckert, A.B. and Lucas, S.G. 2000. Taxonomy, phylogeny, biostratigraphy, biochronology, paleobiogeography and evolution of the Late Triassic Aetosauria (Archosauria: Crurotarsi) *Zentralblatt für Geologie und Paläontologie* **1(11-12)**: 1539-1587.
36. Hendrickx, C., Mateus, O, and Araújo, R. 2015. A proposed terminology of theropod teeth (Dinosauria, Saurichia). *Journal of Vertebrate Paleontology* **35(5)**: 1-18
37. Hoffman, D.K., Edwards, H.R., Barrett, P.M. & Nesbitt, S.J. 2019. Reconstructing the archosaur radiation using a Middle Triassic archosauriform tooth assemblage from Tanzania. *PeerJ* **7:** e7970.
38. Huene, F.V. 1939. Ein kleiner Pseudosuchier und ein Saurischier aus den ostafrikanischen Mandaschichten. *Neues Jahrbuch für Geologie und Paläeontologie, Beilage-Bände Abteilung B* **81**: 61–9.
39. Hunt AP. 1989. A new ?ornithischian dinosaur from the Bull Canyon Formation (Upper Triassic) of east-central New Mexico. In: Lucas SG, Hunt AP, eds. Dawn of the Age of

Dinosaurs in the American Southwest. Albuquerque: New Mexico Museum of Natural History, 355–358.

40. Hunt, A.P. and Lucas, S.G., 1994. Ornithischian dinosaurs from the Upper Triassic of the United States, in Fraser, N.C., and Sues, H.-D., eds. In the Shadow of the Dinosaurs: Early Mesozoic Tetrapods: 227-241.
41. Kellner, A.W.A. & Mader, B.J. 1997. Archosaur teeth from the Cretaceous of Morocco. *Journal of Paleontology* **71(3)**: 525-527.
42. Langer, M.C., Ramezani, L., and Da Rosa, A.A.S. 2018. U-Pb age constraints on dinosaur rise from south Brazil. *Gondwana Research* **57**:133-140.
43. Larson, D.W. & Currie, P.J. 2013. Multivariate analyses of small theropod dinosaur teeth and implications for paleoecological turnover through time. *PLoS ONE* **8(1)**: e54329.
44. Lawing, A.M. & Polly, P.D. 2009. Geometric morphometrics: recent applications to the study of evolution and development. *Journal of Zoology* **280:** 1-7.
45. Long RA, Ballew KL. 1985. Aetosaur dermal armor from the Late Triassic of southwestern North America, with special reference to material from the Chinle Formation of Petrified Forest National Park. In: Colbert EH, Johnson RR, eds. *The Petrified Forest Through the Ages, 75th Anniversary Symposium* November 7, 1981*, Museum of Northern Arizona Bulletin*. **54**. Flagstaff: Museum of Northern Arizona Press, 45–68.
46. Long, R.A. & Murry, P.A. 1995. Late Triassic (Carnian and Norian) tetrapods from the Southwestern United States. *New Mexico Museum of Natural History and Science Bulletin* **4**: 1-254.

47. Ma, W., Pittman, M., Butler, R.J. & Lautenschlager, S. 2022. Macroevolutionary trends in theropod feeding mechanics. *Current Biology* **32(3)**: 677-686.

48. Marsh, A.D., Smith, M.E., Parker, W.G., Irmis, R.B. & Kligman, B.T. 2020. Skeletal anatomy of *Acaenasuchus geoffreyi* Long and Murry, 1995 (Archosauria: Pseudosuchia) and its implications for the origin of the aetosaurian carapace. *Journal of Vertebrate Paleontology* **40(4):**

49. Martinez, R.N., Apaldetti, C., Alcober, O.A., Colombi, C.E., Sereno, P.C., Fernandez, E., Malnis, P.S., Correa, G.A., and Abelin, D. 2012. Vertebrate succession in the Ischigualasto Formation. *Journal of Vertebrate Paleontology* **32**:10-30.

50. Martz, J.W., Mueller, B. Nesbitt, S.J., Stocker, M.R., Parker, W.G., Atanasov, M., Fraser, N., Weinbaum, J. & Lehane, J.R. 2012. A taxonomic and biostratigraphic re-evaluation of the Post Quarry vertebrate assemblage from the Cooper Canyon Formation (Dockum Group, Upper Triassic) of southern Garza County, western Texas. *Earth and Environmental Science Transactions of the Royal Society of Edinburgh* **103(3-4)**: 339-364.

51. Melstrom, K.M. 2017. The relationship between diet and tooth complexity in living dentigerous saurians. *Journal of Morphology* **278**: 500-522

52. Melstrom, K.M., Chiappe, L.M. & Smith, N.D. 2021. Exceptionally simple, rapidly replaced teeth in sauropod dinosaurs demonstrate a novel evolutionary strategy for herbivory in Late Jurassic ecosystems. *BMC Ecology and Evolution* **21(202).**

53. Murry, P.A. & Long R.A. 1996. A diminutive carnivorous aetosaur from the Upper Triassic of Howard County, Texas [Abstract]. *Journal of Vertebrate Paleontology* **16** (supplement 3): 55A.

54. Nesbitt, S.J. 2011. The early evolution of archosaurs: relationships and the origin of major clades. *Bulletin of the American Museum of Natural History* **352:** 1-292.

55. Nesbitt, S.J. & Butler, R.J. 2013. Redescription of the archosaur *Parringtonia gracilis* from the Middle Triassic Manda beds of Tanzania, and the antiquity of Erpetosuchidae. *Geology Magazine* **150(2)**: 225-238.

56. Nesbitt, S.J., Flynn, J.J., Pritchard, A.C., Parrish, M.J., Ranivoharimanana, L. & Wyss, A.R. 2015. Postcranial osteology of *Azendohsaurus madagaskarensis* (?Middle to Upper Triassic, Isalo Group, Madagascar) and its systematic position among stem archosaur reptiles. *Bulletin of the American Museum of Natural History* **398**:1-126.

57. Nesbitt, S.J., Stocker, M.R., Parker, W.G., Wood, T.A., Sidor, C.A. & Angielczyk, K.D. 2017. The braincase and endocast of *Parringtonia gracilis*, a Middle Triassic suchian (Archosauria: Pseudosuchia). *Journal of Vertebrate Paleontology* **37(6)**: 122-141.

58. Newton, E.T. 1894. XIII. Reptiles from the Elgin sandstone. – description of two new genera. *Proceedings of the Royal Society B* **185**: 573-607.

59. Paes Neto, V.D., Desojo, J.B., Brust, A.C.B, Ribeiro, A.M., Schultz, C.M., and Soares, M.B. 2021. Skull osteology of *Aetosauroides scagliai* Casamiquela, 1960 (Archosauria: Aetosauria) from the Late Triassic of Brazil: new insights into the paleobiology of aetosaurs. *Palaeontologica Electronica* **24(3)**: 1-51

60. Parker, W.G. 2005. A new species of the Late Triassic aetosaur *Desmatosuchus* (Archosauria: Pseudosuchia). *Competes Rendus Palevol* **4**: 327-340.

61. Parker, W.G. 2016. Revised phylogenetic analysis of the Aetosauria (Archosauria: Pseudosuchia) assessing the effects of incongruent morphological character sets. *PeerJ* **4**: e1583.

62. Parker WG. 2018. Redescription of *Calyptosuchus* (*Stagonolepis*) *wellesi* (Archosauria: Pseudosuchia: Aetosauria) from the Late Triassic of the Southwestern United States with a discussion of genera in vertebrate paleontology. *PeerJ* **6**: e429.

63. Parker, W.G., Irmis, R.B., Nesbitt, S.J., Martz, J.W. & Browne, L.S. 2005. The Late Triassic pseudosuchian *Revueltosaurus callenderi* and its implications for the diversity of early ornithischian dinosaurs. *Proceedings of the Royal Society B* **272(1566)**: 963-969.

64. Parker, W.G. & Martz, J.W. 2011. The Late Triassic (Norian) Adamanian – Reveultian tetrapod faunal transition in the Chinle Formation of Petrified Forest National Park, Arizona. Earth and Environmental Science Transactions of the Royal Society of Edinburgh **101**: 231-260.

65. Parker, W.G., Nesbitt, S.J., Irmis, R.B., Martz, J.W., Marsh, A.D., Brown, M.A., Stocker, M.A. and Werning, S. 2021. Osteology and relationships of *Revueltosaurus callenderi* (Archosauria: Suchia) from the Upper Triassic (Norian) Chinle Formation of Petrified Forest National Park, Arizona, United States, *The Anatomical Record* **305(10)**: 2353-2414.

66. Parker, W.G., Stocker, M.R., Reyes, W.A, Werning, S. 2025. Anatomy and ontogeny of the "carnivorous aetosaur": New information on *Coahomasuchus kahleorum* (Archosauria: Pseudosuchia) from the Upper Triassic Dockum Group of Texas. *The Anatomical Record* **308(2)**: 671-735.

67. Parrish, J.M. 1994. Cranial osteology of *Longosuchus meadei* and the phylogeny and distribution of the Aetosauria. *Journal of Vertebrate Paleontology* **14**(2): 196-209.

68. Qvarnström, M., Ahlberg, P.E. & Niedźwiesdzki, G. 2019. Tyrannosaurid-like osteophagy by a Triassic archosaur. *Scientific Reports* **9**: 1-9

69. Raup, D.M. 1972. Taxonomic diversity during the Phanerozoic: the increase in the number of species since the Paleozoic may be more apparent than real. *Science* **177**: 1065-1071.

70. Reyes, W. A., Parker, W. G., & Marsh, A.D. (2020). Cranial anatomy and dentition of the aetosaur *Typothorax coccinarum* (Archosauria: Pseudosuchia) from the Upper Triassic (Revueltian–mid Norian) Chinle Formation of Arizona. *Journal of Vertebrate Paleontology* **40**: e1876080.

71. Reyes, W.A, Martz, J.W. & Small, B.J. 2024a. *Garzapelta muelleri* gen. et sp. nov., a new aetosaur (Archosauria: Pseudosuchia) from the Late Triassic (middle Norian) middle Cooper Canyon Formation, Dockum Group, Texas, USA, and its implications on our understanding of the morphological disparity of the aetosaurian dorsal carapace. *The Anatomical Record* **307(4)**: 1271-1299.

72. Reyes, W.A., Parker, W.G., Marsh, A.D. & Kligman, B.T. 2024b. Cranial anatomy, intraspecific variation, and positional variation within *Calyptosuchus wellesi* (Pseudosuchia: Aetosauria) based on new specimens from the Upper Triassic Chinle Formation (Adamanian, early middle Norian) of Petrified Forest National Park, Arizona, USA. *Journal of Paleontology,* **99(97)** 1-39.

73. Sawin, H. J. 1947. The pseudosuchian reptile *Typothorax meadei*. *Journal of Paleontology* **21**: 201-238.

74. Schoch, R.R. & Desojo, J.B. 2016. Cranial anatomy of the aetosaur *Paratypothorax andressorum* Long & Ballew, 1985, from the Upper Triassic of Germany and its bearing on aetosaur phylogeny. *Neues Jahrbuch für Geologie und Paläeontology Abhandlungen* **279**: 73-95.

75. Senter, P. 2003. New information on cranial and dental features of the Triassic archosauriform reptile *Euparkeria capensis. Palaeontology* **46(3)**: 613-621.

76. Sethapanichsakul, T., Coram, R.A. & Benton, M.J. 2023. Unique dentition of rhynchosaurs and their two-phase success as herbivores in the Triassic. *Palaeontology* **66(3)**: e12654.

77. Small, B.J. 1985. The Triassic thecodontian reptile *Desmatosuchus*: osteology and relationships, M. Sci. thesis, Texas Tech University, Lubbock, USA. 1-83.

78. Small, B.J. 2002. Cranial anatomy of *Desmatosuchus haplocerus* (Reptilia: Archosauria: Stagonolepididae. *Zoological Journal of the Linnean Society* **136(1)**: 97-111.

79. Small, B.J. & Martz J.W. 2013. A new aetosaur from the Upper Triassic Chinle Formation of the Eagle Basin, Colorado, USA. *Geological Society, London, Special Publications* **379**: 393-412.

80. Sookias, R.B. 2016, The relationships of the Euparkeriidae and the rise of Archosauria. *Royal Society Open Science* **3(3)**: 150674.

81. Sookias, R.B. & Butler, R.J. 2013. Euparkeriudae. *Geological Society of London Special Publications* **379**: 35-48.

82. Sookias, R.B., Dilkes, D., Sobral, G., Smith, R.M.H., Wolvaart, F.P., Arucci, A.B., Bhullar, B-A.S. & Werneburg, I. 2020 The craniomandibular anatomy of the early archosauriform *Euparkeria capensis* and the dawn of the archosaur skull. *Royal Society Open Science* **2**: 200116.

83. Srikant, N., Junaid, A., Shravan, S., Nidhin, J.P., Sharada, C. & Kavery, C. 2019. Unveiling the third dimension of tooth shape: 2D versus 3D geometric morphometry of

human post-canine dentition. *Journal of Oral and Maxillofacial Pathology* **24(4)**: 716-724.

84. Taborda, J.R.A, Desojo, J.B. & Dvorkin, E.B. 2021. Biomechanical skull study of the aetosaur *Neoaetosauroides engaeus* using Finite Element Analysis. *Ameghiniana* **58(5):** 401–415.
85. Van Valkenburgh, B. 1989. Carnivore Dental Adaptations and Diet: A Study of Trophic Diversity within Guilds. In Gittleman, J.L., ed. *Carnivore Behavior, Ecology, and Evolution*. Springer, Boston, MA. 410-436.
86. von Baczko, M.B. & Desojo, J.B. 2016. Cranial anatomy and palaeoneurology of the archosaur *Riojasuchus tenuisceps* from the Los Colorados Formation, La Rioja, Argentina. *PLoS ONE* **11(2):** e0148575.
87. . von Baczko, M.B., Taborda, J.R.A. & Desojo, J.B. 2018. Paleoneuroanatomy of the aetosaur *Neoaetosauroides engaeus* (Archosauria: Pseudosuchia) and its paleobiological implications among archosauriforms. *PeerJ* **6:** e5456.
88. Walker. A.D. 1961. Triassic reptiles from the Elgin area: *Stagonolepis, Dasygnathus*, and their allies. Philosophical Transactions of the Royal Society of London **244**: 103-204.
89. Walker, A.D. 1964. Triassic reptiles from the Elgin area: *Ornithosuchus* and the origin of carnosaurs. *Philosophical Transactions of the Royal Society B* **248(744)**: 53-134.
90. Weishampel, D.B. & Norman, D.B. 1989. Vertebrate herbivory in the Mesozoic; jaws, plants, and evolutionary metrics. *Geological Society, London, Special Publications* **238**: 87-100.

91. Wiley, D.F., Amenta, N., Alcantara D.A., Ghosh D., Kil Y.J., Delson E., Harcourt-Smith W., Rohlf F.J., St John K. & Hamann B. 2005. Evolutionary morphing. Minneapolis: VIS 05 IEEE Visualization.

92. Wills, S., Underwood, C.J. & Barrett, P.M. 2021. Learning to see the wood for the trees: machine learning, decision trees, and the classification of isolated theropod teeth. *Palaeontology* **64(1)**: 75-99.

93. Wills, S., Underwood, C.J. & Barrett, P.M. 2023. Machine learning confirms new records of maniraptoran theropods in Middle Jurassic UK microvertebrate faunas. *Papers in Palaeontology* **9(2)**: e1487.

94. Wynd, B., Abdala, F. & Nesbitt, S.J. 2022. Ontogenetic growth in the crania of *Exaretodon argentinus* (Synapsida: Cynodontia) captures a dietary shift. *PeerJ* **10: e14196.**

95. Xing. L., Persons, E.S., Bell, P.R. Xu, X., Zhang, J. Miyashita, T., Wang, F. & Currie, P.J. 2013. Piscivory in the feathered dinosaur *Microraptor. Evolution* **67(8)**: 2441-2445.

**CHAPTER 2 – Assessing deviation from the plesiomorphic archosaur tooth: examining shape diversification amongst carnivorous Late Triassic archosaurs**

## ABSTRACT

The Late Triassic is an ideal time to study diversification of life after a mass extinction. By focusing on microvertebrate sites, we record greater diversity than with macrofossils alone, allowing us to produce a more complete picture of Triassic vertebrate diversity. Teeth are the most common fossils in these deposits due to their relative hardness, but are often isolated, leading to difficulty in identifying their clades. Identifying taxa from these isolated teeth is crucial to understanding the radiations of successful groups such as Archosauria. The hypothesised plesiomorphic tooth shape of archosaurs is recurved, serrated, and laterally compressed, indicating carnivory. Despite forays into other morphotypes (e.g. herbivory in some aetosaurs, omnivory in silesaurids), a great number of archosaurs (e.g., dinosaurs, loricatans, crocodylomorphs) have this ancestral state. The similarity of 'carnivorous' teeth complicates identifying isolated archosaur teeth, hampering studies of faunal composition, diversification, and ecology. To address this problem, I compared teeth within the jaws of carnivorous species across archosaurian clades. I separated premaxillary, maxillary, and dentary teeth when possible to test whether tooth shape differs in these regions and identify trends within jaws. I compared the teeth using both quantitative and qualitative approaches. I placed five homologous fixed landmarks and draped a disk of semi-landmarks over the model for three-dimensional geometric morphometrics (3DGM) to describe overall shape. To complement this quantitative approach, non-metric multidimensional scaling (NMDS) was used to provide further separation between

taxa and tooth type using discrete characters of the teeth. Results from both analyses show that many distantly related taxa plot closely together, with teeth from each individual tending to plot in clusters. I did not record any repeated pattern between how the different regions of the mouth plot in any taxon within this sample; however, some taxa show the more anterior teeth plotting across morphospace in order (i.e. tooth one is followed by tooth 2 is followed by tooth 3) towards the more posterior teeth. *Euparkeria* in both analyses plots fairly centrally in the main clusters of taxa – as hypothesised for the ancestral tooth shape. The aetosaur *Coahomasuchus* and early diverging crocodylomorph *Redondavenator* plot away from the main clusters in the quantitative analysis, suggesting these may be the most distinct teeth in the sample. Dinosaur and pseudosuchian teeth occupy distinct areas of morphospace, indicating that my methods distinguish between these major clades of archosaurs despite not being able to separate individual taxa from each other within the dense clusters.

## INTRODUCTION

In the wake of the Permian-Triassic extinction, the Middle and Late Triassic saw an extensive adaptive radiation of archosaurs (Benson et al. 2014). Whereas Archosauria explored a great range of dietary niches in the Late Triassic (Nesbitt 2011, Ezcurra 2016, Ezcurra & Butler 2018), most groups remained carnivorous (e.g., theropod dinosaurs, crocodylomorphs, rauisuchids, many other pseudosuchians). Archosaurs are hypothesised to have descended from a small carnivorous ancestor, similar to animals like *Euparkeria* (Sookias 2016), and many retained the likely plesiomorphic tooth shape, which is laterally compressed, serrated, and recurved. Despite these shared aspects, a variety of carnivores within Archosauria and their close

relatives use this dentition in a wide range of niches, such as semiaquatic carnivores, large-bodied apex predators, and early dinosaurs (Ezcurra 2016). However, this tooth disparity of carnivorous archosaurs is low, and teeth are similar and hard to tell apart when they are the only elements available for study, as is often the case in microvertebrate assemblages.

Microvertebrate localities are defined as sites where most fossils found are <50 mm across (Eberth et al. 2007), and they are excellent for investigating ecological structure of a community and faunal diversity through time. This is due to the preservation of both small organisms and smaller parts (such as teeth and osteoderms) of larger animals. Teeth preserve well because of their resistance to physical and chemical weathering, and so are the most common finds in microvertebrate localities (Buckley & Currie 2014, Bhat 2017). In addition, many animals, including archosaurs, are polyphyodont and exhibit continuous tooth replacement throughout their lifetimes (Tucker & Fraser 2014), leading to an overabundance of teeth compared with other skeletal fossils. The difficulty comes in identifying which taxon each tooth belongs to in the absence of other information.

Whereas much work has been done on the isolated teeth of dinosaurs in the Jurassic and Cretaceous periods (Currie et al. 1990, Hendrickx & Mateus 2014, Wills et al. 2021, Wills et al. 2023, Meso et al. 2024), little work has focussed more broadly on early archosaurs and their close relatives during the Triassic Period. In addition, previous studies focused on identifying teeth use two dimensional measurements and methods (e.g. Calede & Glusman 2017, Wyatt et al. 2021) and, consequently, will lose aspects of tooth shape that are only possible to use when working with teeth in three dimensions. Here, I aimed to create a framework for the identification of unknown teeth by carefully characterising known archosaur (and close relatives) teeth using three-dimensional geometric morphometrics (3DGM) and non-metric

multidimensional scaling (NMDS), and following the methods used in chapter 1, I aimed to potentially better aid in identification to more exclusive clades. Through this characterization of known teeth, I was also able to investigate the morphology and variation in archosaur teeth, both among taxa, within the regions of the mouth (maxillary, premaxillary, dentary), and along the tooth row. Ultimately, I used this framework to investigate the diversification of tooth forms in archosaurs and their relatives of the Middle and Late Triassic of what appears to be the plesiomorphic tooth shape to test how much divergence there is from this shape, if any. I found that there was very little deviation from the ancestral tooth condition in gross morphology or discrete characters. Some teeth from some taxa show slight variation along the tooth row, causing these teeth to plot subsequently one after the other.

**INSTITUTIONAL ABBREVIATIONS**

**AMNH** – American Museum of Natural History, New York, NY, USA; **CM** – Carnegie Museum of Natural History, Pittsburgh, PA, USA; **GR** – Ruth Hall Museum of Paleontology at Ghost Ranch, NM, USA; **IVPP** – Institute of Vertebrate Paleontology and Paleoanthropology, Chinese Academy of Sciences, Beijing, China; **MCZ** - Museum of Comparative Zoology, Harvard University, Cambridge, MA, USA; **NHMUK** – The Natural History Museum, London, UK; **NMMNH** – New Mexico Museum of Natural History and Science, Albuquerque, NM, USA; **NMT -** National Museum of Tanzania, Dar es Salaam, Tanzania; **PEFO** – Petrified Forest National Park, AZ, USA; PVL - Paleontología de Vertebrados, Tucuman, Argentina; **SAM** - South African Museum, Cape Town, South Africa; **SMNS** - Staatliches Museum für Naturkunde, Stuttgart, Germany; **TMM** - Vertebrate Paleontology Laboratory, Texas Natural Science Center, Austin, Texas, USA; **TTUP** - Museum of Texas Tech University, Lubbock, TX;

**USNM** - National Museum of Natural History, Smithsonian Institution, Washington DC, USA; **ZMNH** - Zhejiang Museum of Natural History, Hangzhou, China.

## MATERIALS AND METHODS

The three-dimensional geometric morphometric (3DGM) and non-metric multidimensional scaling (NMDS) methods used in this study are comparable to those outlined in Chapter 1. They are briefly described here.

### 3D Geometric Morphometrics

All teeth in the study were made into 3D models (i.e., meshes) from computed tomography (CT) scans or surface scans (i.e., reflected light or photogrammetry methods). CT files were segmented in Mimics 22 (https://www.materialise.com/en/healthcare/mimics), using the threshold tool, auto-separation where possible, and then by cleaning or defining individual slices. Teeth were fully segmented out of the jaws focusing on the crowns necessary for analysis.

Other teeth were surface scanned using reflected light scanning with an Artec Spider. Models were refined in the accompanying software. Exposed tooth crowns were digitally cut out of the jaws using the freeware program Meshlab 2021.07.

Finally, some models were created by photogrammetry in the Abound (formerly Metascan) application for iPhone. Exposed tooth crowns were digitally cut out of the jaws using Meshlab 2021.07.

In Meshlab, some CT scanned teeth were Laplacian smoothed to prevent the analysis from focusing on jagged edges as a result of the scan slices rather than the actual morphology of the tooth. This also brought them closer in line with the resolution of the surface scanned teeth.

The resulting models were placed into morphospace using the method described in Fischer et al. (2022) and described in brief here. All teeth were oriented to face the same direction, that of the teeth in the left maxilla. Those that were in the opposite orientation were flipped using the Transform: Flip and/or Swap Axis function in Meshlab. A .ply file of each tooth in ASCII format had five fixed landmarks applied using the single point function in IDAV Landmark on the apex, the mesial edge, the distal edge, the labial side, and the lingual side, following that order each time. The latter four points were placed as close as could be distinguished to the cervix where the crown meets the root. In isolated teeth, it was simple to compare with in situ teeth and to look at the angle of recurvedness, i.e. how the apex pointed distally, and morphology of the tooth to determine orientation. This method works well where 3D data is of varying quality as landmarks are easy to consistently place on the centre of each side and dense semilandmarks are objectively draped over based on the five fixed landmarks, rather than needing to be hand placed. The .ply and .pts files were loaded into the code provided by Fischer et al. (2022) and had semi landmarks draped over them by a template disk. Teeth were normalised as part of a Procrustes analysis in R. They were plotted as a principal component analysis (PCA). Thin plate splines were created for the minimum and maximum ends of the first three PCs using the R package geomorph.

**Non-Metric Multi-Dimensional Scaling**

A non-metric multidimensional scaling analysis was used to capture qualitative data using discrete shape details, such as those utilised in a phylogenetic analysis, to complement the morphometric analysis. A total of 14 characters were used to score teeth. The majority of these characters were taken from Hoffman et al. (2019), and the remainder were modified from characters in Brocklehurst & Benson (2021) to be more applicable to isolated teeth and to make some characters binary. Taxa were further subdivided by tooth type where this was applicable as there can be significant variation in tooth characters among the premaxilla, maxilla, and dentary of an individual. For the characters that could only be scored in teeth with denticles, teeth without these were scored with a "?". Characters were scored in Mesquite before being copied to palaeontological statistics (PAST) (Hammer et al. 2001) to conduct the analysis. In PAST, the NMDS analysis was conducted using a Gower similarity index as this copes well with missing information that is typical of fossil data (Gower 1971).

| | |
|---|---|
| 1 | Tooth apex, location, relative to the distal margin of the tooth base: tip mesial to or in the same vertical plane as the distal edge (0) or tip is located more distal than the distal edge (1)<br><br>From Hoffman et al. 2019 |

| | |
|---|---|
| 2 | Tooth lingual/labial, surfaces: texture is smooth (lack of crenulations, ridges, etc.) (0) or surface texture possess a series of parallel ridges from tooth apex to base (= fluted) (1).<br><br>From Hoffman et al. 2019 |
| 3 | Tooth labial/lingual, shape: crown curvature unequal (one side expanded relative to other) (0) or equal labial and lingual curvature (1).<br><br>From Hoffman et al. 2019 |
| 4 | Mesial tooth margin, shape: curvature angles change gradually (0) or angle changes abruptly at a single discrete point along mesial edge (1).<br><br>From Hoffman et al. 2019 |
| 5 | Tooth crown, size: labiolingual widths dorsal to the tooth crown base are all less than the crown base width (0) or a crown labiolingual width dorsal to the tooth crown base is greater than the crown base width (1).<br><br>From Hoffman et al. 2019 |
| 6 | Denticles, mesial edge: absent (0) or present (1)<br><br>Modified from Brocklehurst and Benson 2021 |
| 7 | Denticles, distal edge: absent (0) or present (1)<br><br>Modified from Brocklehurst and Benson 2021 |
| 8 | Mesial/distal crown margins, surfaces: denticle caudae (= grooves on crown surface from between individual denticles) are absent (0) or present (1)<br><br>From Hoffman et al. 2019, originally from Abler, 1992 |

| | |
|---|---|
| 9 | Mesial margin, length: mesial denticle row ends at a point sub-equal with distal denticle row (0) or mesial denticle row ends significantly further apically on crown than distal row (1). Can only be scored for teeth with both mesial and distal denticle series.<br><br>From Hoffman et al. 2019 |
| 10 | Mesial/distal margins, denticle density: number of mesial and distal denticles is <3 per mm (0), or >3 per mm (1). Measurements are taken near the middle of the carina.<br><br>From Hoffman et al. 2019 |
| 11 | Mesial margin, location: vertical axis of the mesial carina is in line with the mesial-distal long axis (0) or laterally offset from the mesial distal long axis (1).<br><br>From Hoffman et al. 2019 |
| 12 | Mesial/distal margins, size: average size of mesial and distal denticles are the same (0) or the average size of the mesial and distal denticles is different (1)<br><br>From Hoffman et al. 2019 |
| 13 | Mesial/distal margins, shape: lateral profile shape of mesial and distal denticles remains constant (0) or denticles lateral profile changes shape (e.g., rounded to square) (1).<br><br>From Hoffman et al. 2019 |
| 14 | Lingual side: heel (=cingulum) on teeth: absent (0); present (1)<br><br>Modified from Brocklehurst and Benson 2021 |

**Statistical Tests**

An analysis of variance test (ANOVA) was used to test how different the taxa were from each other. This was further examined using a pairwise test. Both were conducted in R package geomorph (Baken et el. 2021, Adams et al. 2025).

**Archosauromorph Teeth**

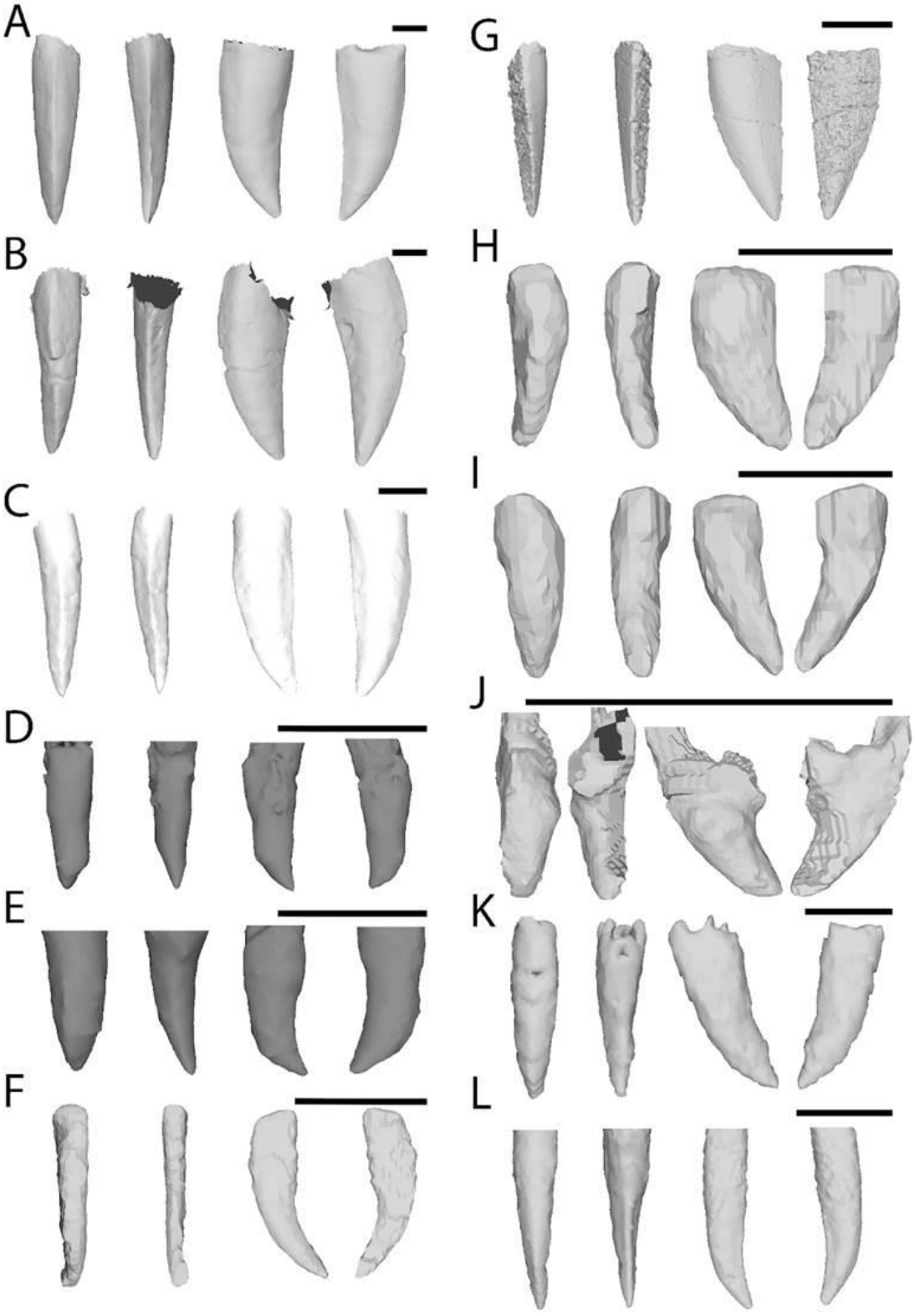
A
B
C
D
E
F
G
H
I
J
K
L

**Figure 1**. Illustration of the first part of tooth types from each taxon. A: *Batrachotomus kurpferzellensis* left dentary tooth in position three (SMNS 80260), B: *Batrachotomus kurpferzellensis* (SMNS 80260) right maxilla tooth in position two, C: *Batrachotomus kurpferzellensis* (SMNS 80260) left premaxilla in position four, D: *Coahomasuchus kahleorum* (TMM 31100-437) right dentary tooth in position one, E: *Coahomasuchus kahleorum* (TMM 31100-437) left maxilla tooth in position three, F: *Coelophysis bauri* (AMNH 7241) right maxilla tooth in position five, G: unnamed crocodylomorph (CM 87670) left maxilla tooth in position five, H: *Diandongosuchus fuyuanensis* (ZMNH M8770) left maxilla tooth in position five, I: *Diandongosuchus fuyuanensis* (ZMNH M8770) left premaxilla tooth in position six, J: *Erpetosuchus granti* (AMNH 29300) right maxilla tooth in position four, K: *Euparkeria capensis* (SAM PK 5867) left dentary tooth in position 11, L: *Euparkeria capensis* (SAM PK 5867) right maxilla tooth in position 12. Scale bars are 1 cm.

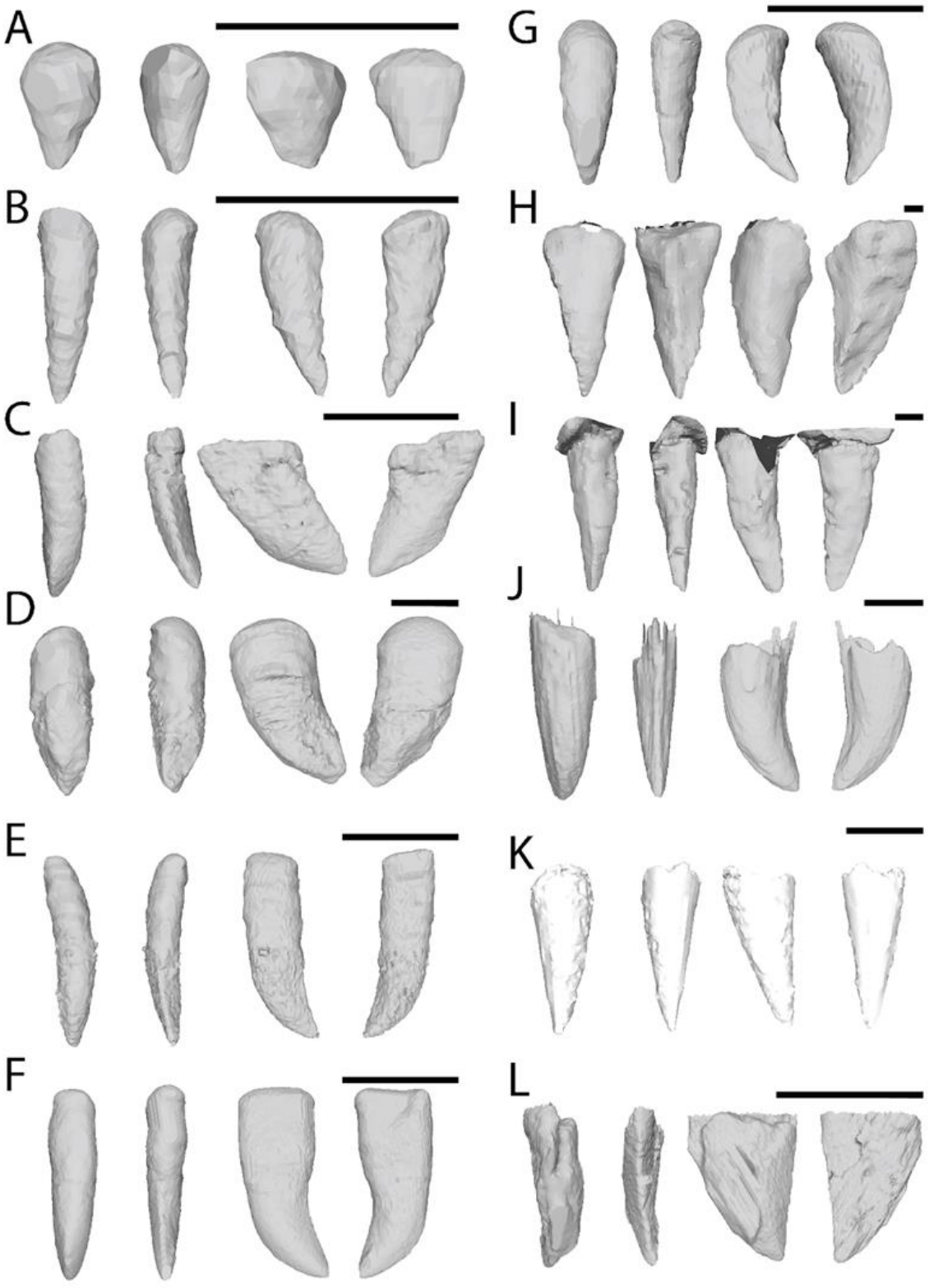
A
B
C
D
E
F
G
H
I
J
K
L

**Figure 2.** Illustration of the second part of all tooth types from each taxon. A: *Gracilisuchus stipanicicorum (*MCZ 4117) left premaxilla tooth in position two, B: *Gracilisuchus stipanicicorum (*MCZ 4117) right maxilla tooth in position four, C: *Hesperosuchus agilis* (AMNH 6758) right dentary tooth in position eight, D: *Hesperosuchus agilis* (AMNH 6758) left maxilla tooth in position four, E: *Junggarsuchus sloani* (IVPP V14010) right dentary tooth in position six, F: *Junggarsuchus sloani* (IVPP V14010) left maxilla tooth in position eight, G: *Junggarsuchus sloani* (IVPP V14010) right premaxilla tooth in position four, H: *Mambawakale ruhuhu* (NHMUK R 36620) right maxilla tooth in position four, I: *Mambawakale ruhuhu* (NHMUK R 36620) left premaxilla tooth in position three, J: *Ornithosuchus woodwardia* (NHMUK R 3143) left dentary tooth, K: *Parringtonia gracilis* (NMT RB 426) premaxilla tooth, L: *Tawa*-like dinosaur (CM 31368) dentary tooth. Scale bars are 1 cm.

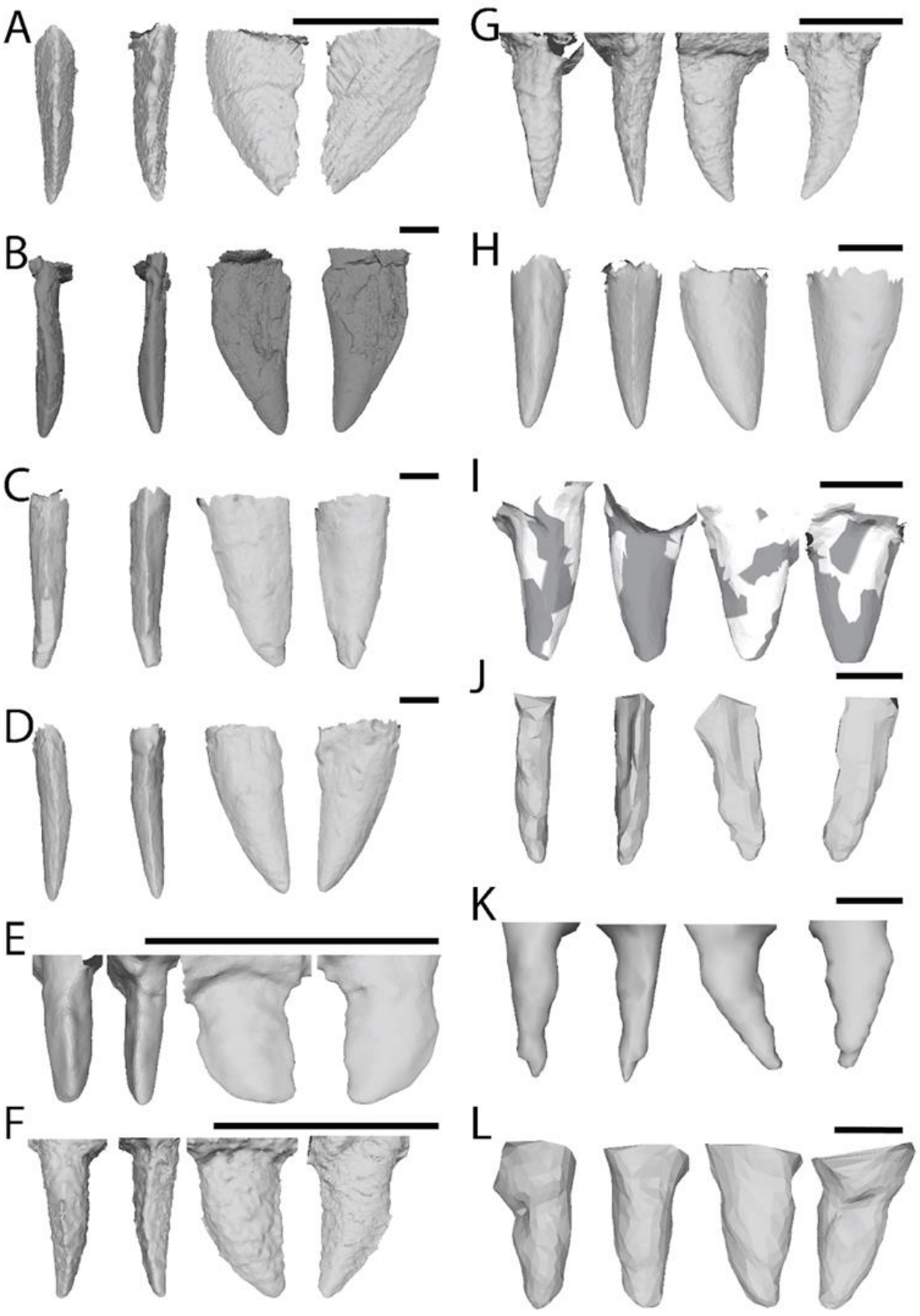
A
B
C
D
E
F
G
H
I
J
K
L

**Figure 3.** Illustration of the third part of all tooth types from each taxon. A: *Tawa*-like dinosaur (CM 31368) maxilla tooth, B: *Poposaurus gracilis* (PEFO 34865) left maxilla tooth in position three, C: *Postosuchus kirkpatricki* (TTU-P 9000) left dentary tooth in position two, D: *Postosuchus kirkpatricki* (TTU-P 9000) right maxilla tooth in position two, E: *Puercosuchus travereorum* (PEFO 38606) right dentary tooth in position seven, F: *Puercosuchus travereorum* (PEFO 43914) right maxilla tooth in position four, G: *Puercosuchus travereorum* (PEFO 43914) right premaxilla tooth in position four, H: *Redondavenator quayensis* (NMMNH 25615) right maxilla tooth in position one, I: *Redondavenator quayensis* (NMMNH 25615) right premaxilla tooth in position two, J: *Riojasuchus tenuiceps* (PVL 3827) right dentary tooth in position one, K: *Riojasuchus tenuiceps* (PVL 3827) right maxilla tooth in position one, L: *Riojasuchus tenuiceps* (PVL 3827) left premaxilla tooth in position two. Scale bars are 1 cm.

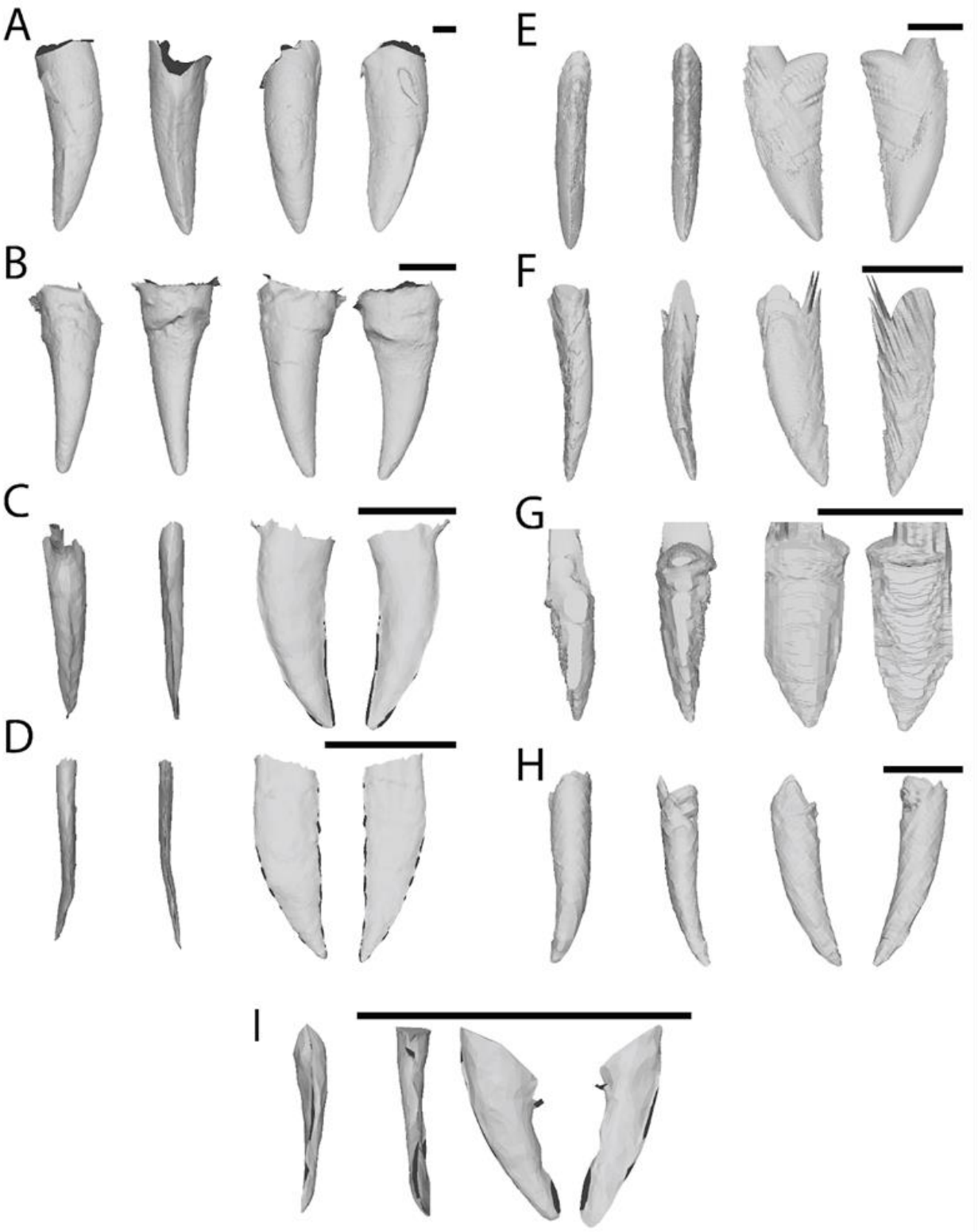
A
B
C
D
E
F
G
H
I

**Figure 4.** Illustration of the fourth part of all tooth types from each taxon. A: *Smilosuchus gregorii* (USNM 18313) left dentary tooth in position two, B: *Smilosuchus gregorii* (USNM 18313) right premaxilla tooth in position one, C: *Tawa hallae* (GR 241) left dentary tooth in position three, D: *Tawa* (GR 241) right maxilla tooth in position four, E: *Tawa hallae* (GR 241) right premaxilla tooth in position two, F: *Teratosaurus suevicus* (NHMUK OR 38646) right maxilla tooth in position four, G: *Vancleavea campi* (GR 138) right dentary tooth in position two, H: *Vancleavea campi* (GR 138) left maxilla in position tooth 10, I: *Vancleavea campi* (GR 138) right premaxilla tooth in position one. Scale bars are 1 cm.

***Puercosuchus travereorum*** (Marsh et al. 2022)

**Specimen:** PEFO 38605: left premaxilla, PEFO 38606: right dentary, PEFO 43914 (holotype): right premaxilla and maxilla, PEFO 43915: right maxilla.

**Locality and Age:** Upper part of the Blue Mesa Member of the Chinle Formation in Petrified Forest National Park, Arizona, USA; early Norian ((218-220 Ma), Late Triassic (Marsh et al. 2024).

**Scan:** Reflected light surface scans created with an Artec Spider scanner onsite at Petrified Forest National Park.

**Description:** There are four teeth in the premaxilla of *Puercosuchus*, around 19 in the maxilla, and 19 in the dentary giving a total count of 84 for the entire mouth (Marsh et al. 2022). All teeth are ankylothecodont when fully erupted.

The teeth of the premaxilla are far rounder at the base than those of the maxilla or dentary, although they become more laterally compressed toward the apex. All teeth are serrated,

save the most anterior tooth, although it is noted that in larger tooth specimens, the denticles seem worn and are not present (Marsh et al. 2022). The serrations are fine and vary in density along the tooth row, becoming less dense posteriorly along the jaw. The anterior teeth have approximately nine-10 denticles per mm, whereas the posterior teeth have six-seven per mm and are broader in shape (Marsh et al. 2022).

The teeth of the dentary and maxilla are similar and show a similar pattern of heterodonty wherein the anterior teeth are dramatically different compared to the posterior teeth. The anterior teeth of the maxilla and dentary are laterally compressed, serrated on both mesial and distal carinae, and are recurved at their tips. The posterior teeth of both maxilla and dentary are shorter and leaf-shaped in lateral view with a distally orientated apex. Teeth are also preserved on the palatine and pterygoid (Marsh et al. 2022), but these are not used in this study.

The teeth used here are as follows: PEFO 38605, premaxillary teeth one and two; PEFO 38606, dentary teeth two, four (Fig. 5C), seven, nine, 11, 12, 13; PEFO 43914, premaxillary teeth one, two, three (Fig. 5A), maxillary teeth four (Fig. 5B), 12, 13; PEFO 43915, maxillary teeth four, seven, eight. As these were taken from surface scans, some teeth were unavailable to be used due to being obscured by other teeth. This is the highest number of specimens and variety of teeth of any taxon described here.

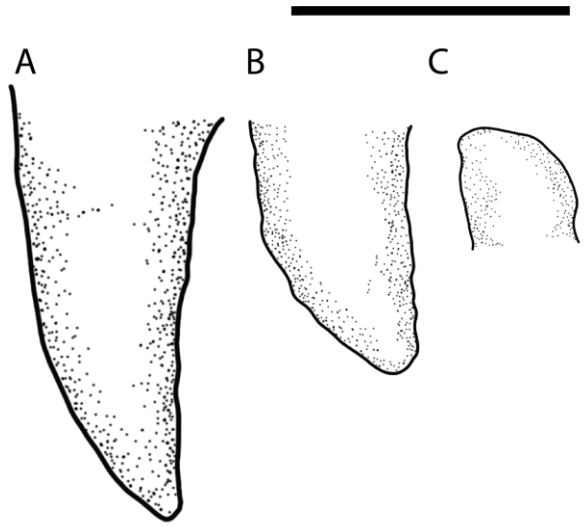


**Figure 5.** Selected teeth of *Puercosuchus travereorum* in lateral view: A right premaxillary tooth in position three (PEFO 43914); B right maxillary tooth in position 4 (PEFO 43914); C right dentary tooth in position four (PEFO 38606). Scale bar is 1 cm.

***Vancleavea campi*** (Long & Murray 1995)

**Specimen:** GR 138

**Locality and Age:** *Coelophysis* Quarry at Ghost Ranch, 'siltstone member', Chinle Formation, Chama Basin, New Mexico, USA; late Norian-Rhaetian, Late Triassic.

**Scan:** Scanned on an NSI scanner at The University of Texas High-Resolution X-ray Computed Tomography Facility in Austin at 150kV, 0.15mA with an aluminium filter.

**Description:** *Vancleavea* is described as having five premaxillary teeth, 13 maxillary teeth (Nesbitt et al. 2008). These teeth are disparate in form and range from the large caniniform teeth found in all elements of the jaw, which are labiolingually compressed, recurved at its tip and

have serrations on both mesial and distal edges, save the caniniform tooth on the dentary, which lacks serrations on the mesial carina (Nesbitt et al. 2008). These caniniform teeth are surrounded by smaller teeth, which in the anterior portion of the jaw are generally round in cross section and unserrated. Posterior to the caniniform teeth, some smaller teeth are minimally bulbous, with the crown slightly extending out from the cervix (Nesbitt et al. 2008). The posteriormost dentary teeth are rounded and unrecurved, with serrations that do not extend to the apex of the tooth (Nesbitt et al. 2008).

The teeth used in this study are as follows: left premaxilla – positions one, two, three; right premaxilla – position one (Fig. 6A); left maxilla – positions three, 10 (Fig. 6B), 11; right maxilla – position two; left dentary – positions one, two; and right dentary – positions one, two, three. These were the best preserved teeth and the most suitable to conduct 3DGM on.

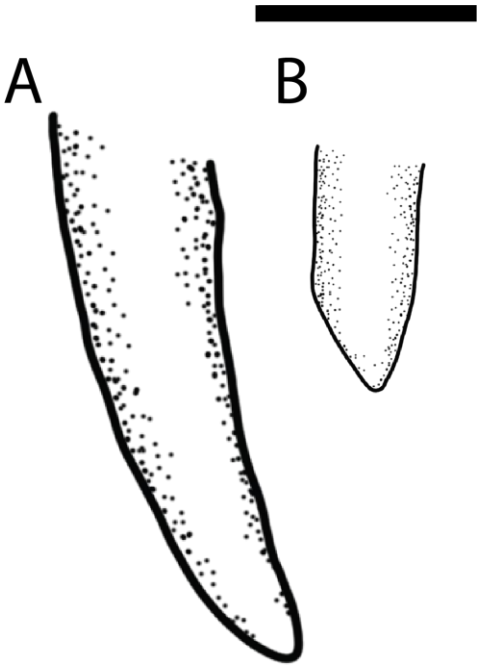

**Figure 6.** Selected teeth of *Vancleavea campi* in lateral view: A right premaxillary tooth in position one; B left maxillary tooth in position 10 (GR 138). Scale bar is 1 cm.

***Euparkeria capensis*** (Broome 1913)

**Specimen:** SAM PK 5867 (holotype) consists of an articulated and almost complete skull and partial skeleton. The postcranial material includes much of the axial skeleton except the caudal series, girdles, and limb material (Sookias & Butler 2013).

**Locality and Age:** Middle Triassic (Olenekian – Anisian) *Cynognathus* Zone of the Karoo of South Africa (Senter 2003, Sookias & Butler 2013).

**Scan:** CT scanned at the Evolutionary studies Institute at the University of the Witwatersrand, Johannesburg, South Africa using a Nikon X Tek HMX ST 225 machine with a tungsten target and 70Kv, 140 μA, 1000 ms, 57.50 μm voxel size with a 1.8 mm aluminium filter (Sookias et al 2020).

**Description:** The premaxilla contains four alveoli; the maxilla and dentary both contain 13 alveoli (Sookias et al. 2020), giving a total tooth count of 60 in the entire mouth. Whereas it could be an alternating pattern of replacement teeth, it seems that there is a pattern of smaller teeth replaced by larger teeth across the jaws. The teeth themselves reflect those of the hypothesised plesiomorphic tooth condition in archosaurs. The teeth of *Euparkeria* are laterally compressed and recurved at its tips, with those of the maxilla and dentary having serrations on both the mesial and distal edges with fine serrations, around eight denticles per mm (Senter

2003). The teeth of the dentary are generally smaller than those of the maxilla but otherwise reflect their appearance (Sookias et al. 2020).

The premaxillary teeth are not as labiolingually compressed as those in the maxilla or dentary and have a more rounded cross section. The most posterior premaxillary tooth is the only one that seems to be serrated in SAM PK 5867, though it is possible that matrix is obscuring this feature (Sookias et al. 2020). It does not seem like any teeth have ridges etc. on their surfaces.

The teeth of the right maxilla and left dentary are the best preserved in SAM PK 5867. From the right maxilla, teeth one, three, five, seven, nine, and 12 (Fig. 7A) were used, and from the dentary teeth three, four, six, eight, 10, and 11 (Fig. 7B) were used. The teeth of the premaxilla were not well enough preserved to be used in this study. The small teeth of the pterygoid, palate, and vomer are not included here.

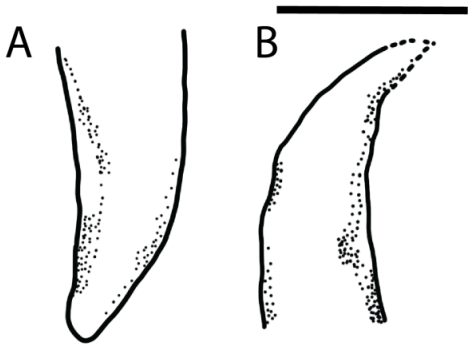


**Figure 7.** Selected teeth of *Euparkeria capensis* in lateral view: A right maxillary tooth in position 12; B left dentary tooth in position 11. (SAM PK 5867). Scale bar is 1 cm.

***Diandongosuchus fuyuanensis*** (Li et al. 2012)

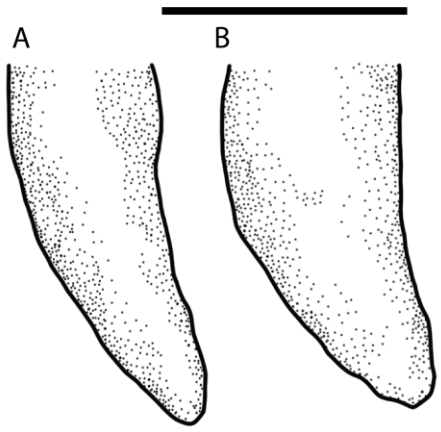


**Figure 8.** Selected teeth of *Diandongosuchus fuyuanensis* in lateral view: A left premaxillary tooth in position six; B left maxillary tooth five **(**ZMNH M8770). Scale bar is 1 cm.

**Specimen:** ZMNH M8770 (holotype) skull prepared on both sides and most post-crania apart from the tail, which is only known to the 8$^{th}$ caudal.

**Locality and Age:** Southeast of Fuyan County, Yunnan Province from the Ladinian Zhuganpo Member of the Falang Formation (Li et al. 2012); late Middle Triassic (Li et al. 2012, Chen, 1985).

**Scan:** Scanned on a Mi-CT 225 kV micro-computerised tomography scanner at the Key Laboratory of Vertebrate Evolution and Human Origins, IVPP.

**Description:** There are nine premaxillary teeth and 15 maxillary teeth (Li et al. 2012). The dentary teeth are completely hidden in the fossil by the maxilla and premaxilla and are not easily distinguishable in the μCT scan, because the skull is flattened, and so their number is unknown. All teeth, except the last tooth of the maxilla, are the same shape – recurved, convex on both labial and lingual sides, with serrations on the mesial and distal edges (Li et al. 2012). These serrations extend the length of the distal carinae but begin significantly further apically on the

mesial edge (Li et al. 2012). The final maxillary tooth is spade shaped and smaller than others (Stocker et al. 2017).

*Diandongosuchus* is hypothesized to represent the ancestral condition in phytosaurs (Stocker et al. 2017). A total of 12 teeth are used in this study from the right premaxilla: tooth one, from the left premaxilla: tooth six (Fig. 8A), from the left maxilla: teeth one, five (Fig. 8B), eight, 10, 13, 14, from the right maxilla: teeth four, eight, 10, 16**.**

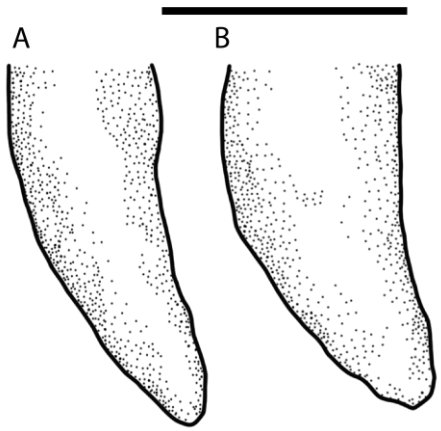


**Figure 8.** Selected teeth of *Diandongosuchus fuyuanensis* in lateral view: A left premaxillary tooth in position six; B left maxillary tooth five **(**ZMNH M8770). Scale bar is 1 cm.

***Smilosuchus gregorii*** (Camp 1930 *sensu* Long & Murry 1995)

**Specimen:** USNM 18313, a large skull and much of the postcrania.

**Locality and Age:** Blue Mesa Member, Chinle Formation near St. Johns, Arizona, USA (Heckert et al. 2021); Early-middle Norian, Late Triassic.

**Scan:** Photogrammetry via the Abound (formerly Metascan) application for iPhone. Scanned at USNM.

**Description:** The premaxilla contains 21 teeth, the maxilla 21, and the dentary 34 (Camp 1930) giving a total tooth count for the entire mouth of 152. *Smilosuchus* exhibits "extreme heterodonty" (Long & Murry 1995) with "fang" teeth at the anteriormost part of the snout. The regions of phytosaur heterodonty can be divided into the "tip of snout set", the "premaxilla set" and the "maxilla set" as defined in Hungerbühler (2000). The anterior teeth have ridges and are round in cross section (Camp 1930) whereas the more posterior teeth are closer to leaf-shaped in lateral view and are laterally compressed. All teeth are serrated on the mesial and distal edges (Camp 1930).

The teeth used in this study are from the right premaxilla: tooth one (Fig. 9A); from the left dentary: positions two (Fig. 9B), 27, 29, and 30; and from the right dentary: teeth five, ten, and 11.

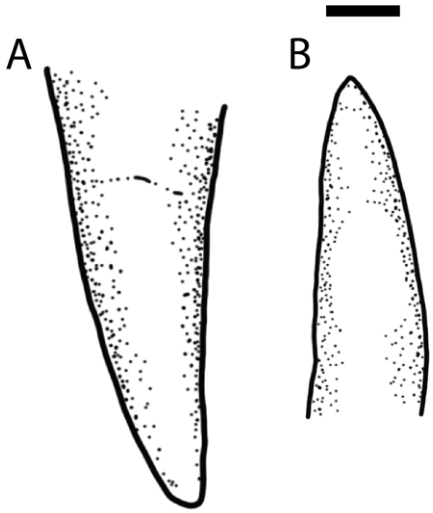

**Figure 9.** Selected teeth of *Smilosuchus gregorii* in lateral view: A right premaxillary tooth in position one; B left dentary tooth in position two. **(**USNM 18313). Scale bar is 1 cm.

***Ornithosuchus woodwardia*** (Newton 1894)

**Specimen:** NHMUK R 3143, (holotype) comprises the anteriormost portion of the skull, including premaxilla, maxilla, and dentary.

**Locality and Age:** Lossimouth Sandstone from Elgin, Scotland, UK. Carnian-early Norian, Late Triassic.

**Scan:** μCT scanned on a Nikon HMX ST 225 at the Natural History Museum, London.

**Description:** *Ornithosuchus* had three teeth in the premaxilla, nine in the maxilla, and around ten in the dentary (Walker 1964) giving a total tooth count of 44.

The teeth of *Ornithosuchus* are recurved at their tips, save for one of the premaxillary teeth. The teeth lack features such as fluting, crenulations, or ridges on the labial and lingual sides and are instead smooth. Most teeth exhibit unequal curvature on the labial and lingual sides, but some teeth of the maxilla are symmetrical in lateral view. All teeth of the maxilla and dentary observed have serrations. The denticles on the distal edge of the tooth extend further down than on the mesial edge. Whereas they may have been lost during preparation or taphonomy, denticles are only found on one side each of the premaxillary teeth, though it is likely both sides would have had them in life.

The teeth, all from the dentary used here include one replacement tooth and the others that are known are found in positions one and two. There are also five from unknown positions (Fig. 10).

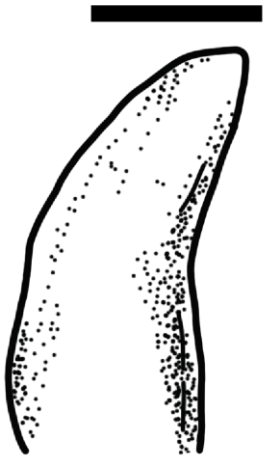

**Figure 10.** Selected tooth of *Ornithosuchus woodwardia* in lateral view: left dentary tooth from unknown position **(**NHMUK R 3143). Scale bar is 1 cm.

***Riojasuchus tenuiceps*** (Bonaparte 1967)

**Specimen**: PVL 3827, (holotype) a complete skull and virtually complete postcranium.

**Locality and Age:** Los Colorados Formation, La Rioja, Argentina (Bonaparte 1967); Norian, Late Triassic (Baczko & Desojo 2016).

**Scan:** Scanned on a medical 64 channel axial tomography multi-slicer at the Clínica la Sagrada Familia in Buenos Aires at 120 kV and 279 mA.

**Description:** There are three teeth in the premaxilla, seven in the maxilla, and nine in the dentary (Baczko & Desojo 2016) giving a tooth count of 38. The maxillary teeth are highly recurved at their tips, which contrasts with dentary tooth one, which is conical in lateral view. The shape of the premaxillary teeth fall between these two extremes, being more weakly recurved than the maxillary teeth. No denticles are found on the premaxillary teeth, though this may be a result of overpreparation rather than how they would have been in life (von Baczko & Desojo 2016) the lack of surface features on the teeth may also be due to this. Denticles on the mesial and distal edges are, however, found in the maxillary and dentary teeth.

Two teeth from the left maxilla (positions one and four), one from the left maxilla in position six (Fig. 11B), one from the left premaxilla in position two (Fig. 11A), and one right dentary tooth in position one (Fig. 11C) were used here.

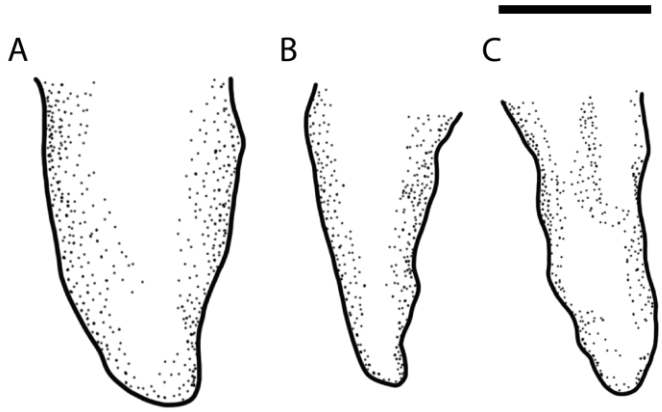


**Figure 11.** Selected teeth of *Riojasuchus tenuiceps* (PVL 3827) in lateral view: A left premaxillary tooth in position two; B right maxillary tooth in position six; C right dentary tooth in position one (PVL 3827). Scale bar is 1 cm.

***Parringtonia gracilis*** (Huene 1939)

**Specimen:** NMT RB426 is the most complete specimen of *Parringtonia* comprising a nearly complete skeleton with most of the skull intact (Nesbitt et al. 2017).

**Locality and Age:** Lifua Member of the Manda Beds in the Ruhuhu Valley of southwestern Tanzania; Middle Triassic (Nesbitt & Butler 2013).

**Scan:** μCT scan created at the University of Texas CT Facility on an Xradia with scan parameters of 90 kV, 0.7 x objective, 1344 slices, and voxel size of 44.80 microns (Nesbitt et al. 2017).

**Description:** The maxilla is not complete, but the teeth seem to be constrained to the anterior portion, which contains five alveoli (Nesbitt & Butler 2013). Only one maxillary tooth is known from NHMUK R8646, and none are used in this study, but it is described as being similar to the teeth of *Erpetosuchus* in that it is round in cross section, without serrations, and is slightly recurved at its tip (Nesbitt & Butler 2013). The premaxillary teeth, of which two are used here from unknown positions (Fig. 12), are also round in cross section, are gently recurved and are wider at the base on the labiolingual axis than they are mesiodistally. They do not have any ridges or fluting on the labial or lingual surface.

**Figure 12.** Selected tooth of *Parringtonia gracilis* in lateral view: premaxillary tooth, unknown position (NMT RB426). Scale bar is 1 cm.

***Erpetosuchus granti*** (Newton 1894)

**Specimen:** AMNH FR 29300, partial right side of the skull with partial mandible in occlusion, associated with several vertebrae and bone fragments (Olsen 2000).

**Locality and Age:** New Haven Formation of the Hartford Basin in Cheshire, Connecticut, USA; Norian, Late Triassic (Olsen et al. 2000).

**Scan:** μCT at the Microscopy and Imaging Facility at the American Museum of Natural History with a voxel size of 0.0678 (Foffa et al. 2020).

**Description:** Little original material is preserved of the jaws of *Erpetosuchus*, but from what is preserved, the maxilla has only seven to eight teeth (Foffa et al. 2020), confined to the anterior

portion of the bone (Olsen 2000). In Newton's original description (1894) he described the premaxilla, a mould as is common in animals from the Elgin Sandstones, as having three-four teeth. The teeth of the maxilla are described as being larger than those in the premaxilla. Though difficult to expose the moulds of the lower jaw, around 11 teeth are present. Taking the upper estimates of each bone, a total of around 46 teeth were likely present in the mouth.

Out of the three maxillary teeth preserved in AMNH 29300, the second, fourth (Fig. 13), and fifth tooth positions are used in this study. The teeth are oval in cross section, are recurved at their tips and look similar along the tooth row in shape and size. Tooth surfaces are smooth and featureless without serrations. Although a fragment of the premaxilla, and the posterior part of the dentary are preserved (Olsen 2000), neither of these elements have alveoli or teeth present.

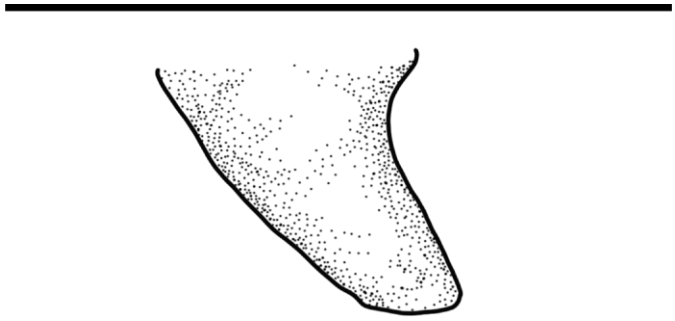

**Figure 13.** Selected tooth of *Erpetosuchus* in lateral view: right maxillary tooth in position four (AMNH FR 29300). Scale bar is 1 cm.

***Coahomasuchus kahleorum*** (Heckert & Lucas 1999)

**Specimen:** TMM 31100-437 is a partial skeleton consisting of the incomplete skull and postcranial elements including trunk vertebrae, many paramedian, lateral, ventral, and appendicular osteoderms, and limb elements. (Parker 2016, Parker et al. 2024).

**Locality and Age:** Otis Chalk Quarry 3, Colorado City Formation from the Dockum Group of western Texas, USA Dockum Group, Late Triassic of Texas, USA (Sawin 1947, Parrish 1994); Otischalkian, Late Triassic (Stocker et al. 2016).

**Scan:** MicroCT scanned at the University of Texas High Resolution X-ray CT Facility with source voltage of 120 kV and a current of 0.18 mA.

**Description:** The premaxilla of TMM 31100-437 is not present and so a tooth count cannot be made. The maxilla has seven alveoli (Parker et al. 2024). Neither dentary is complete in TMM 31100-437 and so a tooth count can only be estimated. However, based on the dentaries of other aetosaurs, this number is not likely to be more than 12 (Parker et al. 2024). Given the incomplete dentaries and the lack of premaxillae, it is difficult to make an estimated tooth count for this taxon.

*Coahomasuchus* has been known as the "carnivorous" aetosaur, owing to the shape of its teeth (Murry & Long 1996, Parker 2016). This might be the only taxon in the study that may have reverted to a more plesiomorphic state from a peg-like tooth typical to aetosaurs. However, it is fully possible that the teeth are plesiomorphic and further study and specimens of close relatives would be needed to confirm or refute this. The teeth are strongly recurved and have denticles on the distal edge (Parker et al. 2024) and they are less laterally compressed than the teeth of other taxa in this study. The teeth are tall with a narrow apex, and show little variation

across the tooth row, as is typical in aetosaurs. The surfaces of the teeth are free from striations, ridges, or crenulations.

The teeth used here are from the maxilla: one, three (Fig. 14A), and four; and from the dentary: tooth one (Fig. 14B). These were the best preserved teeth and most suitable for use in 3D GM. Maxillary teeth three and four have a point where the angle of curvature on the mesial side shifts to a more acute angle. This is not present in the first tooth, which has a more gradual curve.

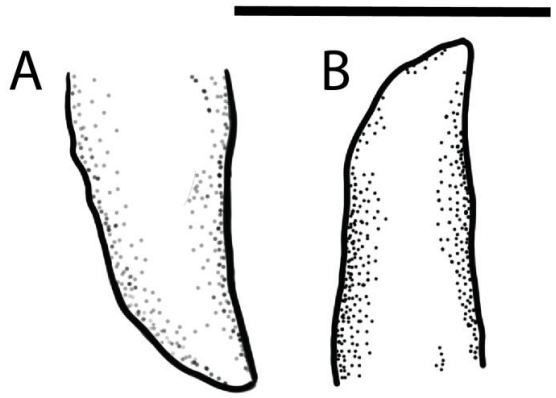


**Figure 14.** Selected teeth of *Coahomasuchus kahleorum* in lateral view: A left maxillary tooth in position three; B right dentary tooth in position one (TMM 31100- 437). Scale bar is 1 cm.

***Gracilisuchus stipanicicorum*** (Romer 1972)

**Specimen:** MCZ 4117, a virtually complete skull

**Locality and Age:** Chañeres Formation from the Ischigulasto-Villa Unión Basin, Argentina (Lecuona 2012); Early Carnian, Late Triassic (Marsicano et al. 2016).

**Scan:** Scanned at the Micro-CT Scan Facility at Laboratory for Integrated Science and Engineering at the Museum of Comparative Zoology, Harvard.

**Description:** The premaxilla has four teeth, there are 14 in the maxilla and around 16 in the dentary (Romer 1972, Lecuona 2013) giving a total tooth count of 66 in the entire mouth. The teeth are laterally compressed, recurved at its tip, and oval in cross section. The teeth do not seem to have any ridges or fluting on the labial or lingual surfaces. In the maxilla, the fourth tooth is the largest – the anterior teeth start small and increase in size moving posteriorly up to this tooth, and posterior to the fourth tooth they decrease in size again. The denticles of the maxillary teeth are fine, with 11 denticles per mm (Lecuona 2013). Denticles are not observable on the few dentary teeth that are exposed; however, this may be due to damage rather than absence (Lecuona 2013). The dentary teeth are relatively smaller than those of the maxilla (Romer 1972) and are more akin to the shape of the posterior maxillary teeth than their corresponding tooth of the maxilla (Lecuona 2013).

The teeth used in this study are from the left premaxilla, tooth two (Fig. 15A); from the right maxilla, teeth 4 (Fig. 15B), and seven; and from the left maxilla, teeth five and seven. The dentary is fully occluded with the skull and the dentary teeth were not possible to extract.

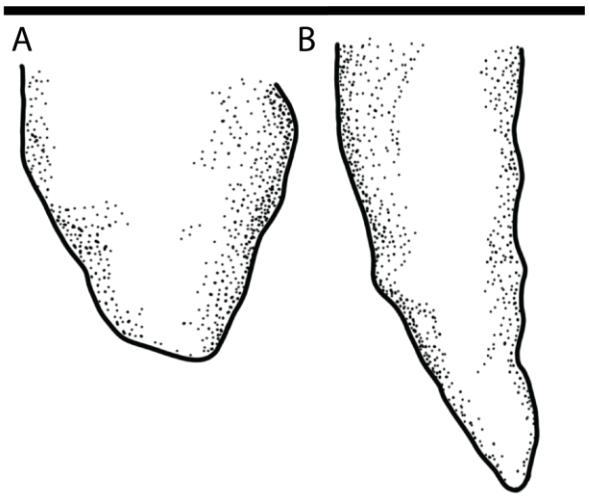


**Figure 15.** Selected teeth of *Gracilisuchus stipanicicorum* in lateral view: A left premaxillary tooth in position two; B right maxillary tooth in position four (MCZ 4117). Scale bar is 1 cm.

***Mambawakale ruhuhu*** (Butler et al. 2022)

**Specimen:** NHMUK R 36620 (holotype) A partial skull, cervical vertebrae, and manus.

**Locality and Age:** Lifua Member of the Manda Beds in the Ruhuhu Valley of southwestern Tanzania; Middle Triassic a (Butler et al. 2022).

**Scan:** Taken on a Nikon HMX ST 225 at the Natural History Museum, London, with a voltage of 225 kV, and current of 600 μA (Butler et al. 2022).

**Description:** There are four alveoli in the premaxilla and 12 in the maxilla (Butler et al. 2022). In the dentaries, there are 15-16 alveoli, though it is hard to tell due to damage to the posterior of the tooth rows (Butler et al. 2022). This gives a maximum total tooth count for the mouth of 64. The premaxillary teeth are transversely compressed and have denticles on both mesial and distal

sides. However, Butler et al. (2022) note that these are not always preserved, which may be the case due to their having been damaged during preservation, weathering, and/or preparation. The denticles that are preserved are relatively fine (around two-three per mm) given the overall large size of the teeth (Butler et al. 2022). The fourth premaxillary tooth is significantly larger than the other three.

The maxillary teeth are all around the same size, though the posteriormost preserved tooth is somewhat smaller. Denticles are once again present on both mesial and distal edges, and are around the same size as those found on the premaxillary teeth, though may be slightly smaller on the distal edge (Butler et al. 2022). The teeth of the dentary are similarly ziphodont (Butler et al. 2022). The teeth used here are left premaxilla, tooth positions one, two, three (Fig. 16A); right maxilla, tooth positions one, two, four (Fig. 16B), six.

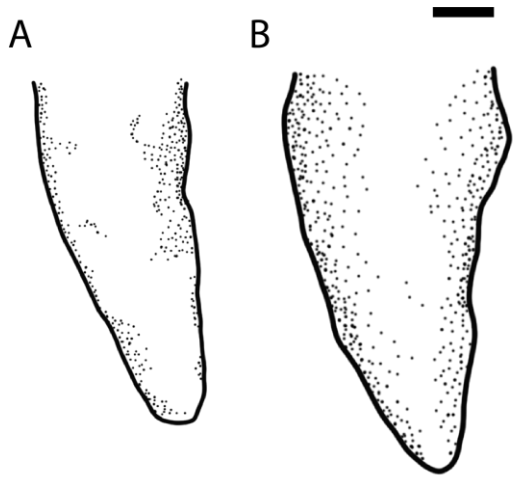


**Figure 16.** Selected teeth of *Mambawakale ruhuhu* in lateral view: A left premaxillary tooth in position three; B right maxillary tooth in position four (NHMUK R 36620). Scale bar is 1 cm.

***Poposaurus gracilis*** (Mehl 1915)

**Specimen:** PEFO 34865 left maxilla, dentary, and partial postcranial remains (Parker & Nesbitt 2013)

**Locality and Age:** Base of the Sonsela Member of the Chinle Formation in Petrified Forest National Park, Arizona, USA (Parker & Nesbitt 2013); middle Norian, Late Triassic.

**Scan:** Surface scans created with an Artec Spider scanner onsite at Petrified Forest National Park.

**Description:** *Poposaurus* has five premaxillary teeth. The only known confirmed maxilla from this taxon, used here, is incomplete and only preserves the three most anterior alveoli making tooth count estimates impossible. The dentary of PEFO 34865 preserves ten alveoli (Parker & Nesbitt 2013) but not complete, unbroken teeth are fully exposed and so are not used in this study. The third tooth of the left maxilla, the only preserved, is used (Fig. 17).

The maxillary tooth (Fig. 17) is finely serrated, with four denticles per mm (Parker & Nesbitt 2013). The carinae extend the full length of the mesial and distal edges, from cervix to apex. The labial and lingual surfaces preserve faint crenulations parallel to the cervix. Of what can be seen of the dentary teeth, the more anterior teeth are more rounded in cross section than the other highly labiolingually compressed teeth. They are serrated on both mesial and distal edges; however, these denticles are slightly larger than those of the maxillary tooth (Parker & Nesbitt 2013).

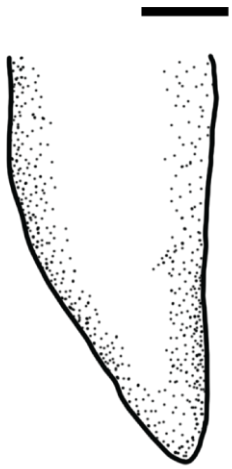

**Figure 17.** Selected tooth of *Poposaurus gracilis* (PEFO 34865) in lateral view: left maxillary tooth in position three. Scale bar is 1 cm.

***Batrachotomus kupferzellensis*** (Gower 1999)

**Specimen:** SMNS 52970 (holotype), a partial disarticulated skull and postcrania including vertebrae, pelvic and pectoral girdle material, and hindlimb elements (Gower & Schoch 2009) and SMNS 80260, a reasonably complete but disarticulated skull (Gower & Schoch 2009).

**Locality and Age:** Erfurt Formation from Baden-Württemburg, southern Germany; Late Ladinian, Middle Triassic (Gower & Schoch 2009).

**Scan:** Photogrammetry via the Abound (formerly Metascan) application for iPhone.

**Description:** The teeth of SMNS 52970 and 80260 are well preserved. The premaxilla contains four teeth, 11 are present in the maxilla and 11 or 12 in the dentary giving a tooth count between 52-54 in the whole mouth. The teeth are laterally compressed, recurved, and serrated on both the mesial and distal edges with pits for replacement teeth. Gower (1999) hypothesised that there

was an alternate pattern of tooth replacement due to observations made of each skull: one tooth fully erupted followed by another partially erupted, repeated.

Some teeth seem to expand mesiodistally outward further than the cervix at the base (Gower 1999). This is the case in the premaxillary teeth, which, while subtle, project mesially. This is most observable in premaxillary tooth four in SMNS 80260. They remain laterally compressed on the labial and lingual sides, however, and cannot be considered bulbous. Unlike the premaxillary teeth, the maxillary and dentary teeth do not exhibit this and all sides remain less than the width/length of the base. Fully erupted maxillary and dentary teeth are generally larger than those in the premaxilla and have a more acute angle of recurvature.

The teeth used in this study are from SMNS 52970: left maxillary tooth in the fifth alveolus; and from SMNS 80260: left premaxillary teeth two and four (Fig. 18A); right premaxillary tooth three; left maxillary teeth three, five, and seven; right maxillary tooth two (Fig. 18B); left maxillary tooth five; and left dentary tooth three (Fig. 18C).

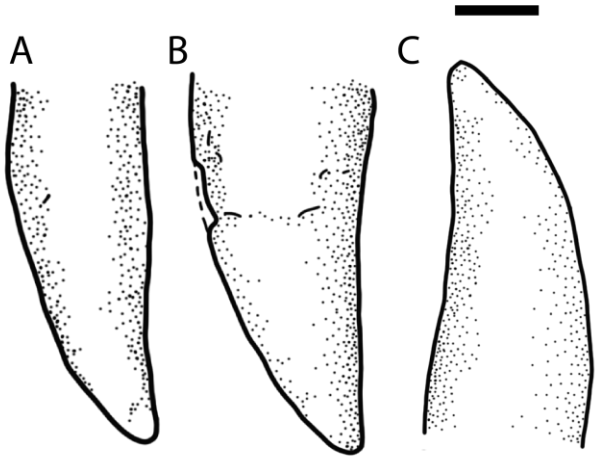

**Figure 18.** Selected teeth of *Batrachotomus kupferzellensis* in lateral view: A left premaxillary tooth in position four; B right maxillary tooth in position two; C left dentary tooth in position three (SMNS 52970). Scale bar is 1 cm.

***Teratosaurus suevicus*** (Meyer 1861)

**Specimen:** NHMUK R 38646 (holotype), a right maxilla.

**Locality and Age:** Heslach, near Stuttgart, Germany (Benton 1986); Mid-Norian.

**Scan:** μCT scanned at The Natural History Museum, London on a Nikon HMX ST 225.

**Description:** *Teratosaurus suevicus* is known from a single right maxilla, NHMUK 38646 (Brusatte et al 2009). Despite other material having been previously assigned to the species, none of these teeth or bones overlap with the holotype and so can only be assigned to "archosaur indet." (Brusatte et al. 2009). Due to the lack of other material, nothing can be said about the other elements of the jaw.

Thirteen alveoli are preserved in the maxilla (Benton 1986) and out of eight teeth and partial teeth (Brusatte et al 2009), three were complete enough to be used here from positions two, and four (Fig. 19). These teeth are not fully erupted and so were likely more protected. Whereas the sixth tooth is also unerupted, it was too damaged to be used here. The teeth have fine denticles on both the mesial and distal edges, though the exact count per mm is not known from the literature, which extend the full length of the crown, as seen on the broken but fully erupted teeth, and over the apex. The labial and lingual surfaces are smooth, lacking ridges etc.

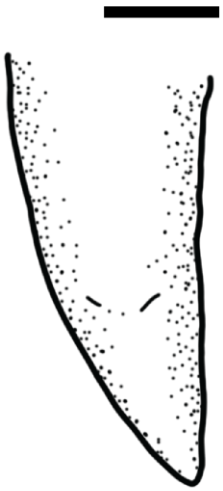

**Figure 19.** Selected tooth of the rauisuchid *Teratosaurus suevicus* in lateral view: right maxillary tooth in position four (NHMUK R 38646). Scale bar is 1 cm.

***Postosuchus kirkpatricki*** (Chatterjee 1985)

**Specimen:** TTU-P 9000 (holotype), nearly complete skull and partial postcranium.

**Locality and Age:** Post Quarry, Early Norian Cooper Canyon Formation (Dockum Group) from Post Quarry in Garza County, Texas, USA (Chatterjee 1985, Martz et al. 2012; Weinbaum 2011). Early-middle Norian, Late Triassic.

**Scan:** Surface scanned at Texas Tech museum using the Abound (previously Metascan) photogrammetry application for iPhone.

**Description:** *Postosuchus kirkpatricki* has four alveoli present in the premaxilla, 13 in the maxilla, and 15 in the dentary (Chatterjee 1985) giving a total tooth count of 64 for the entire mouth.

The teeth exhibit different shapes along the tooth row. Those of the premaxilla are predominantly round in cross section and are more conical and less recurved than those in the maxilla and dentary (Weinbaum 2011). The first maxillary tooth is noted by Weinbaum (2011) to have the same form as the premaxillary teeth and the second dentary tooth is "indistinguishable from those of the premaxillary teeth of some phytosaurs". The anterior portion of the maxilla (excluding tooth one) and dentary teeth are similar, being large, laterally compressed and recurved at their tips. The posterior teeth are less blade-like and are more of a short leaf-shape, with curved mesial and straight distal edge in lateral view. They are slightly bulbous with the base of the crown expanding out from the cervix. All teeth are serrated on both the mesial and distal margins, save for some premaxillary teeth, which are only serrated on the distal edge. These serrations are fine, between two - three per mm.

The teeth used in this study are: from the left dentary, two (Fig. 20B), seven, 11; from the left maxilla, three, four, 10; from the right maxilla two (Fig. 20A), four. In addition to these, four isolated teeth are used and, based on appearance, two of these are from the anterior portion of the tooth row, and two are from the posterior of the jaw.

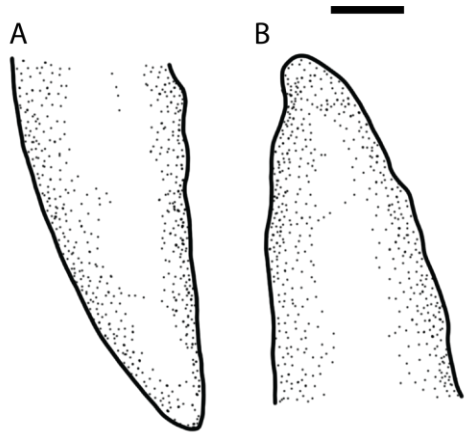

**Figure 20.** Selected teeth of the rauisuchid *Postosuchus kirkpatricki* (TTU-P 9000) in lateral view: A right maxillary tooth in position two; B left dentary tooth in position two (TTU-P 9000). Scale bar is 1 cm.

***Redondavenator quayensis*** (Nesbitt et al. 2005)

**Specimen:** NMMNH 25615 (holotype), anterior portion of a skull.

**Locality and Age:** Uppermost part of the Redonda Formation of Quay County, northwestern New Mexico (Nesbitt et al. 2005); Apachean, late Norian to Rhaetian.

**Scan:** Photogrammetry via the Abound (formerly Metascan) application for iPhone. Scanned at the New Mexico Museum of Natural History.

**Description:** The premaxilla of *Redondavenator* contains five alveoli. The maxillae are incomplete and only the first four alveoli in the right maxilla, and six in the left are present (Nesbitt et al. 2005), though there were likely more in life posterior to these. No dentary is preserved and so conclusions about total tooth number cannot be drawn.

The teeth of the premaxilla have an almost D-shaped cross section and would have been the same size, based on alveoli size if fully preserved (Nesbitt et al. 2005). The maxillary teeth are labiolingually compressed, a pinched oval in cross section, and somewhat recurved at their tips. The serrations are fine, having 4 per mm (Nesbitt et al. 2005). Based on alveoli size, the teeth would have been different sizes along the maxilla. Out of those preserved, the anteriormost teeth are smaller with the posterior preserved teeth being much larger. Most teeth that are

preserved are broken, and only two were complete enough to be used in this study. Those are the right premaxillary tooth two (Fig. 21A), and the first right maxillary tooth (Fig. 21B).

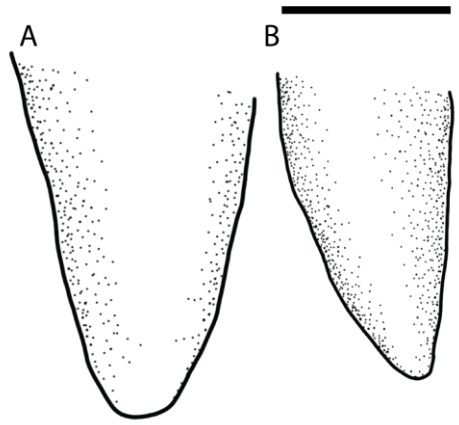


**Figure 21.** Selected teeth of the crocodylomorph *Redondavenator quayensis* in lateral view: A right premaxillary tooth in position two; B right maxillary tooth in position one (NMMNH 25615). Scale bar is 1 cm.

***Hesperosuchus agilis*** (Colbert 1952)

**Specimen:** AMNH FR 6758 (holotype) a partial skeleton with a fragmentary skull (Colbert 1952)

**Locality and Age:** Blue Mesa Member of the Chinle Formation (Late Triassic) from near Cameron, Arizona, USA (Clark et al. 2000); early Norian, Late Triassic.

**Scan:** μCT at the Microscopy and Imaging Facility at the American Museum of Natural History.

**Description:** In specimens of *Hesperosuchus*, the jaws are fragmentary making estimates of tooth count difficult. The maxilla had at least 16 teeth (Colbert 1952) and the dentary at least 18

(Colbert 1952). The premaxilla had four alveoli (Colbert 1952) This means that *Hesperosuchus* would have possessed at least 76 teeth in its entire mouth, and possibly more.

In the premaxilla, the first tooth is small and more conical than the other teeth (Colbert 1952). Posterior to this, the teeth increase in size, with the fourth tooth being the largest (Colbert 1952). The fourth and sixth maxillary teeth are the largest, and teeth quickly decrease in overall size posterior to these. Maxillary teeth have prominent denticles on both mesial and distal edges, but denticle count per mm is not specified (Colbert 1952).

As in the premaxilla and maxilla, the fourth dentary tooth is the largest and is recurved, with teeth after this becoming more leaf shaped (Colbert 1952). No teeth are noted as having ridging or other ornamentation on the crowns.

The teeth used in this study are maxillary teeth one and four (Fig. 22A), and dentary teeth eight (Fig. 22B) and 12.

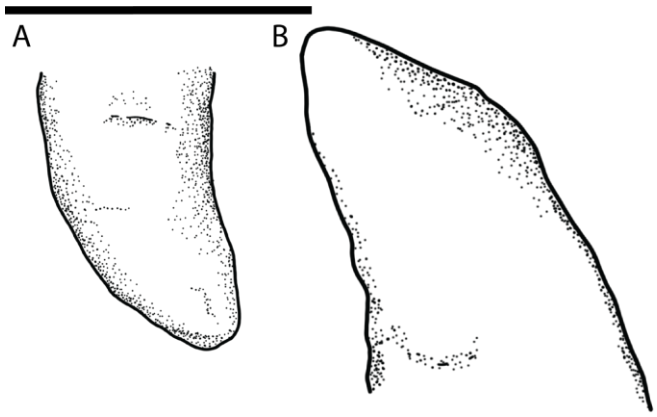


**Figure 22.** Selected teeth of the crocodylomorph *Hesperosuchus agilis* in lateral view: A left maxillary tooth in position four; B right dentary tooth in position eight (AMNH FR 6758). Scale bar is 1 cm.

***Junggarsuchus sloani*** (Clark et al. 2004)

**Specimen:** IVPP V14010 (holotype) consisting of a largely complete skull and the anterior portion of the postcranial skeleton (Clark et al. 2004).

**Locality and Age:** Lower Shishugou Formation in Xinjiang, China; approximately 162.2 Ma, Middle Jurassic (Ruebenstahl et al. 2022).

**Scan:** Scanned on a Mi-CT 225 kV micro-computerised tomography scanner at the Key Laboratory of Vertebrate Evolution and Human Origins, IVPP (Ruebenstahl et al 2022).

**Description:** Although hailing from the Middle Jurassic, *Junggarsuchus* is an excellent example of an early diverging crocodylomorph with a 'sphenosuchian' body form, which are known from the Late Triassic, with a well-preserved dentition, and so is suitable to be included here. The premaxilla contains five alveoli, though the fifth is only preserved on the right side (Ruebenstahl at al. 2022). There are an estimated 14-15 alveoli in the maxilla and 17 in the dentary (Ruebanstahl et al. 2022), giving a total tooth count for the mouth of 72-74.

The teeth of the premaxilla are only slightly recurved at their tips and are round with only slight mediolateral compression. Serrations are noted on the distal edge of the posterior three teeth, though the anterior two are not well enough preserved to determine the presence of serrations (Ruebenstahl et al. 2022). In the maxilla, all teeth, save the posteriormost, are recurved and have denticles on the distal carinae though denticles per mm could not be found in the literature. From the sixth tooth posteriorly, the teeth are also serrated on the apical half of the mesial carinae. The dentary teeth adjacent to the premaxilla and maxilla reflect the shape of the

teeth of these bones, with the anteriormost dentary teeth being more conical, and those adjacent to the maxilla being more mediolaterally compressed and recurved, with a teardrop cross section apically from the base (Ruebenstahl et al. 2022).

There is some degree of tooth shape changes along the tooth row of the maxilla, where the fourth is the largest tooth and is gradually recurved. Moving posteriorly, there is a point at the sixth tooth where this angle becomes sharper approximately halfway down the mesial edge and the teeth become shorter. Towards the back posterior portion, the teeth are no longer recurved and rather U-shaped in lateral view. This pattern is reflected in the dentary (Ruebenstahl et al. 2022). A total of 19 of the best preserved teeth were segmented out of IVPP V14010 from different elements of the jaw as follows: left dentary positions two, 11, 12; right dentary positions two, five, six (Fig. 23C), seven, 13, 14; left maxilla positions two, eight (Fig. 23B), nine; right maxilla positions eight, 10, 11, 12, 13, 14; and right premaxilla position four (Fig. 23A).

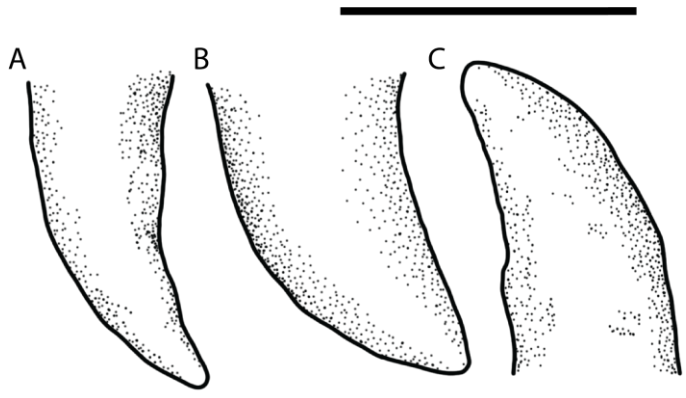


**Figure 23.** Selected teeth of the crocodylomorph *Junggarsuchus sloani* in lateral view: A right premaxillary tooth in position four; B left maxillary tooth in position eight; C right dentary tooth in position six (IVPP V14010). Scale bar is 1 cm.

**Crocodylomorph**

**Specimen:** CM 87670

**Locality and Age:** *Coelophysis* Quarry at Ghost Ranch, 'siltstone member', Chinle Formation, Chama Basin, New Mexico, USA; late Norian-Rhaetian, Late Triassic.

**Scan:** CT-scanned at the Shared Materials Instrumentation Facility at Duke University using a Nikon XTH 225 ST.

**Description:** There are four teeth in the premaxilla, and at least nine in the maxilla. The maxilla is, however, incomplete and so it is likely there were more in life. The dentary is fully occluded and did not show up well on scans, making estimates of tooth count difficult.

The teeth themselves are mediolaterally compressed, finely serrated, and recurved at their tips in the anterior portion of the jaw. Towards the posterior end, the degree of recurvedness lessens with the mesial edge being curved, but the distal edge being virtually straight. There are fine ridges on the labial surfaces of the teeth.

Here I used teeth one, two, three, four, five (Fig. 24), and seven of the left maxilla.

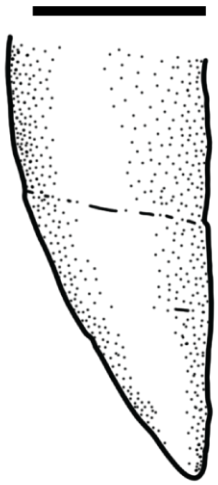

**Figure 24.** Selected tooth of unspecified Crocodylomorpha in lateral view: left maxillary tooth in position five (CM 87670). Scale bar is 1 cm.

***Tawa hallae*** (Nesbitt et al. 2009a)

**Specimen:** GR 241, an almost complete disarticulated associated skeleton.

**Locality and Age:** Hayden Quarry 2 at Ghost Ranch, Petrified Forest Member of the Chinle Formation, New Mexico, USA; dated to about 211.9 ± 0.7 Ma to the late Norian, Late Triassic (Irmis et al. 2007; Irmis et al. 2011).

**Scan:** Photogrammetry via the Abound (formerly Metascan) application for iPhone. Scanned at Virginia Tech.

**Description:** *Tawa* has four premaxillary teeth, at least 12 maxillary teeth, and 16 dentary teeth, giving a total tooth count of 64. The premaxillary teeth are unserrated and vary in shape. The

first tooth of the premaxilla is conical, whereas the posterior premaxillary teeth are heavily ridged and more similar to those of the maxilla and dentary, being very narrow and recurved.

The maxillary and dentary teeth are similar and are extremely laterally compressed – the most out of any teeth in this study. Many have a central groove that trends from apex to base on the labial and lingual sides. The teeth are relatively tall when compared to the teeth of most, if not all other taxa.

The teeth used here are the best preserved fully erupted and uncovered with sediment teeth as they were taken from a surface rather than a CT scan. From the right premaxilla, teeth one and two (Fig. 25A) are used. From the left maxilla, three, five, and seven are used, and from the right two and four (Fig. 25B) are taken. In the left dentary, three (Fig. 25C), seven, and 15 are used.

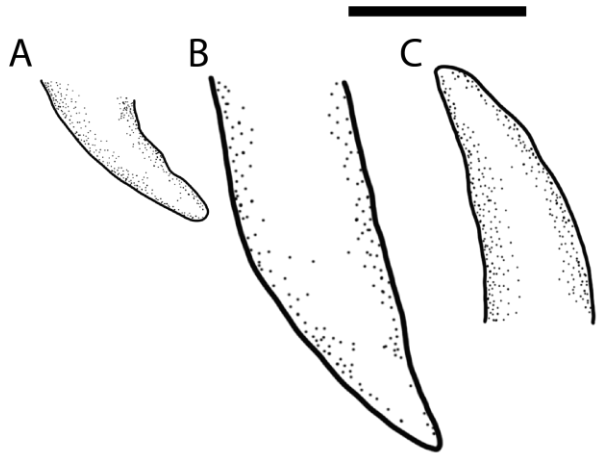


**Figure 25.** Selected teeth of the saurischian *Tawa hallae* (GR 241) in lateral view: A right premaxillary tooth in position two; B right maxillary tooth in position four; C left dentary tooth in position three (GR 241). Scale bar is 1 cm.

***Tawa*-like Dinosaur**

**Specimen:** CM 31368, a partial skull.

**Locality and Age:** *Coelophysis* Quarry at Ghost Ranch, 'siltstone member', Chinle Formation, Chama Basin, New Mexico, USA; late Norian-Rhaetian, Late Triassic.

**Scan:** CT-scanned at the Shared Materials Instrumentation Facility at Duke University using a Nikon XTH 225 ST

**Description:** The teeth are recurved and smooth on the labial and lingual surfaces with denticles present on both mesial and distal edges (Fig. 26). On those teeth where it is possible to see, the mesial denticles end further apically than those on the distal carina; denticles are around the same size on both edges. Denticles are fine (four - five per mm).

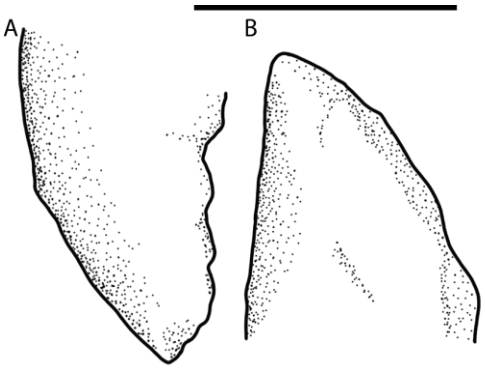


**Figure 26.** Selected teeth of the *Tawa*-like dinosaur in lateral view: A left maxillary tooth in unknown position; B right dentary tooth in unknown position (CM 31368). Scale bar is 1 cm.

***Coelophysis bauri*** (Cope 1887)

**Specimen:** AMNH 7241.

**Locality and Age:** *Coelophysis* Quarry at Ghost Ranch, 'siltstone member', Chinle Formation, Chama Basin, New Mexico, USA; late Norian-Rhaetian, Late Triassic.

**Scan:** μCT at the Microscopy and Imaging Facility at the American Museum of Natural History.

**Description:** *Coelophysis* has four premaxillary teeth, between 13-28 maxillary teeth, and 17-27 dentary teeth (Buckley & Currie 2014) giving a range of 68-118 teeth in the entire mouth. This extreme variation in tooth number was explained by Buckley & Currie (2014) as being a feature that changes during ontogeny as they looked at skulls of many different sizes, with teeth gained as *C. bauri* grew. The teeth are typical of theropods, with most being mediolaterally compressed, and have denticles on both mesial and distal carinae, though count per mm is not specified (Buckley & Currie 2014). Whereas all teeth are generally recurved at their tips, maxillary and dentary teeth are more acutely curved than premaxillary teeth (Buckley & Currie 2014). Few specimens have serrated premaxillary teeth; this is restricted to the posterior two, but all show varyingly serrated maxillary and dentary teeth.

Generally, the teeth are smooth and featureless on the labial and lingual sides, though in some smaller skulls, the premaxillary teeth possess longitudinal ridges, which are also present on some of the anterior maxillary and dentary teeth. This could be indicative of an ontogenetic diet shift (Buckley & Currie) if skull size does reflect age. AMNH 7241 does not possess any ridging on any teeth.

Teeth used here are from the right maxilla in positions one, three, five (Fig. 27), and ten.

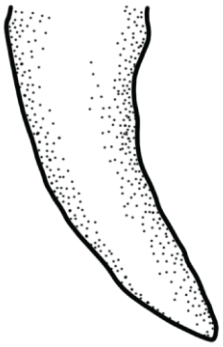

**Figure 27.** Selected tooth of *Coelophysis bauri* in lateral view: right maxillary tooth in position five (AMNH 7241). Scale bar is 1 cm.

**RESULTS**

In the 3DGM, PC1 accounts for 47.23% of the variation (Figs. 28, 29), PC2 accounts for 25.96% of variation (Figs. 28, 30), and PC3 accounts for 6.18% of variation (Figs. 29, 30) together describing a total of 79.37% of variation. From the thin plate splines, PC1 represents an extreme narrowing and flattening of the tooth in all directions at the minimum, and a widening in all directions and slight lowering of apicobasal height at the maximum. PC2 seems to represent greater tooth recurvedness at the positive, and a lessening of this and widening in the xy axis, but a narrowing in the yz axis of the teeth at the negative. PC3 represents a greater recurving of the tooth at the minimum, and a straightening of the tooth at the maximum and is also associated with the orientation of the tooth base. Most teeth in all PCAs plot in or around a large main cluster which sits on 0 of both axes. The main outliers from this cluster in PC1 vs PC2 (Fig. 28)

are *Coahomasuchus*, *Redondavenator*, and the *Tawa*-like dinosaur, the latter of which has one point that forms a sparse cluster with the other two. The dinosaurs all plot outside or on the edge of the main cluster.

However, this is not the case in the other two PCAs (Figs. 29, 30), where dinosaurs generally plot within the main cluster. Though in PC2 vs PC3 (Fig. 29) the dinosaurs are found close to the edge of the main cluster. *Coahomasuchus* and *Redondavenator* remain outside of this cluster in all analyses.

The ANOVA of genus shows that genus is a significant factor in determining where taxa plot (P = 0.001). However, according to the $R^2$ value (0.55607) only 56% of the variation is explained meaning that other factors than genus are likely also important. The pairwise tests show that *Coahomasuchus*, followed by *Puercosuchus* and *Redondavenator* have the most significant differences between themselves and the other taxa.

| | df | Sum Sq | Mean Sq | F-value | P-value | Sig. |
|---|---|---|---|---|---|---|
| Genus | 22 | 4.7242 | 0.214738 | 6.8875 | 0.001 | *** |
| Residuals | 145 | 4.5208 | 0.031178 | | | |

**Table 2**. Table of ANOVA results examining significance of genus where significance cut-offs are "." 0.1>p>0.05, "*" 0.05>p>0.01, "**" 0.01>p>0.001, "***" p<0.001

| | Coa | Coelo | Croc | Dia | Erpet | Eup | Grac | Hesp | Jungg | Mamba | Ornith | Parr | Pop | Post | Puerc | Red | Rio | Smilo | *Tawa* | *Tawa*-like | Terat | Van |
|---|---|---|---|---|---|---|---|---|---|---|---|---|---|---|---|---|---|---|---|---|---|---|
| Bat | 0.001 | 0.31 | 0.999 | 0.21 | 0.324 | 0.525 | 0.038 | 0.287 | 0.091 | 0.203 | 0.447 | 0.663 | 0.636 | 0.353 | 0.001 | 0.004 | 0.21 | 0.298 | 0.309 | 0.049 | 0.867 | 0.588 |
| Coa | | 0.001 | 0.001 | 0 | 0.001 | 0..001 | 0.001 | 0.001 | 0.001 | 0.001 | 0.001 | 0.001 | 0.091 | 0.001 | 0.001 | 0.026 | 0 | 0.001 | 0.002 | 0.014 | 0.004 | 0.001 |
| Coelo | | | 0.285 | 0.03 | 0.079 | 0.173 | 0.007 | 0.036 | 0.018 | 0.029 | 0.265 | 0.362 | 0.396 | 0.024 | 0.001 | 0.004 | 0.04 | 0.038 | 0.226 | 0.02 | 0.278 | 0.439 |
| Croc | | | | 0.32 | 0.389 | 0.658 | 0.09 | 0.362 | 0.146 | 0.316 | 0.453 | 0.756 | 0.618 | 0.483 | 0.001 | 0.004 | 0.26 | 0.521 | 0.283 | 0.057 | 0.948 | 0.627 |
| Dia | | | | | 0.558 | 0.273 | 0.267 | 0.761 | 0.452 | 0.724 | 0.205 | 0.611 | 0.341 | 0.314 | 0.001 | 0.001 | 0.49 | 0.533 | 0.002 | 0.021 | 0.517 | 0.05 |
| Erpet | | | | | | 0.381 | 0.303 | 0.67 | 0.368 | 0.773 | 0.363 | 0.456 | 0.38 | 0.472 | 0.068 | 0.001 | 0.54 | 0.482 | 0.065 | 0.066 | 0.469 | 0.155 |
| Eup | | | | | | | 0.068 | 0.318 | 0.176 | 0.351 | 0.833 | 0.858 | 0.348 | 0.096 | 0.001 | 0.001 | 0.26 | 0.319 | 0.016 | 0.015 | 0.488 | 0.478 |
| Grac | | | | | | | | 0.799 | 0.166 | 0.489 | 0.041 | 0.534 | 0.221 | 0.162 | 0.031 | 0.001 | 0.28 | 0.476 | 0.002 | 0.012 | 0.335 | 0.018 |
| Hesp | | | | | | | | | 0.603 | 0.957 | 0.199 | 0.593 | 0.362 | 0.748 | 0.127 | 0.001 | 0.6 | 0.893 | 0.026 | 0.052 | 0.575 | 0.109 |
| Jungg | | | | | | | | | | 0.357 | 0.124 | 0.499 | 0.24 | 0.103 | 0.001 | 0.001 | 0.16 | 0.283 | 0.001 | 0.021 | 0.436 | 0.014 |
| Mamba | | | | | | | | | | | 0.219 | 0.598 | 0.292 | 0.379 | 0.004 | 0.001 | 0.69 | 0.763 | 0.004 | 0.019 | 0.436 | 0.063 |
| Ornith | | | | | | | | | | | | 0.658 | 0.329 | 0.069 | 0.001 | 0.001 | 0.25 | 0.14 | 0.037 | 0.008 | 0.359 | 0.392 |
| Parr | | | | | | | | | | | | | 0.492 | 0.443 | 0.049 | 0.001 | 0.49 | 0.74 | 0.19 | 0.049 | 0.7 | 0.838 |
| Pop | | | | | | | | | | | | | | 0.499 | 0.108 | 0.063 | 0.31 | 0.371 | 0.686 | 0.361 | 0.8 | 0.393 |
| Post | | | | | | | | | | | | | | | 0.002 | 0.004 | 0.21 | 0.65 | 0.025 | 0.075 | 0.903 | 0.03 |
| Puerc | | | | | | | | | | | | | | | | 0.001 | 0.01 | 0.007 | 0.001 | 0.023 | 0.109 | 0.001 |
| Red | | | | | | | | | | | | | | | | | 0 | 0.004 | 0.006 | 0.114 | 0.101 | 0.002 |
| Rio | | | | | | | | | | | | | | | | | | 0.437 | 0.025 | 0.019 | 0.387 | 0.072 |
| Smilo | | | | | | | | | | | | | | | | | | | 0.016 | 0.037 | 0.759 | 0.093 |
| *Tawa* | | | | | | | | | | | | | | | | | | | | 0.104 | 0.514 | 0.032 |
| *Tawa*-like | | | | | | | | | | | | | | | | | | | | | 0.273 | 0.015 |
| Terat | | | | | | | | | | | | | | | | | | | | | | 0.46 |

**Table 3**. Summary of pairwise comparison results for the ANOVA in Table 2. Bat - *Batrachotomus*, Coa – *Coahomasuchus*, Coelo – *Coelophysis*, Croc – the crocodylomorph, Dia – *Diandongosuchus*, Erpet – *Erpetosuchus*, Eup – *Euparkeria*, Grac – *Gracilisuchus*, Hesp – *Hesperosuchus*, Jungg – *Junggarsuchus*, Mamba – *Mambawakale*, Ornith – *Ornithosuchus*, Parr – *Parringtonia*, Pop – *Poposaurus*, Post – *Postosuchus*, Puerc – *Puercosuchus*, Red – *Redondavenator*, Rio – *Riojasuchus*, Smilo – *Smilosuchus*, *Tawa* – *Tawa*, *Tawa*-like – the *Tawa*-like dinosaur, Terat – *Teratosaurus*, Van – *Vancleavea*

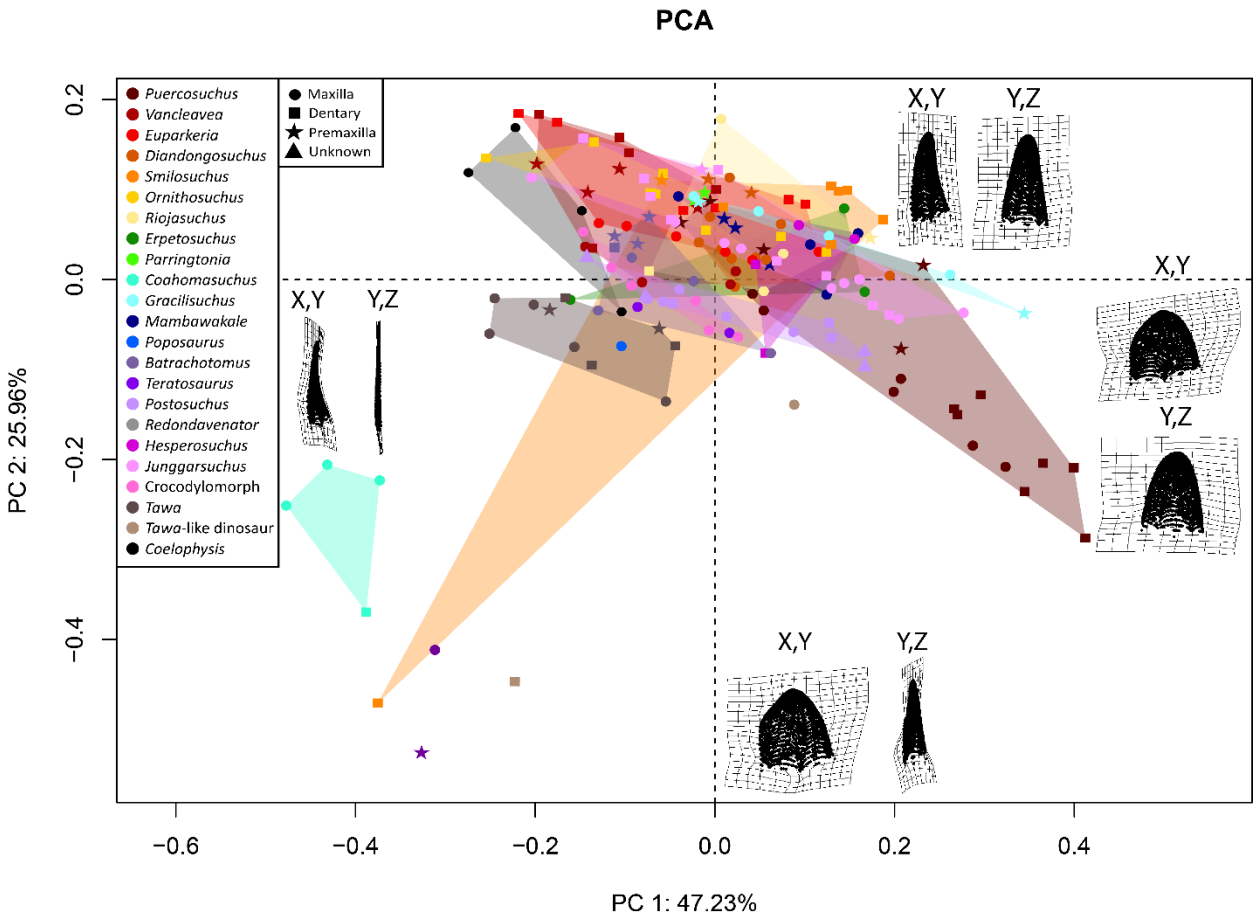


**Figure 28.** PCA of PC1 vs PC2 with all archosaurs and tooth types with thin plate splines superimposed on the extremes of the axis. Points represent individual teeth. Convex hulls show the spread of individual taxa.

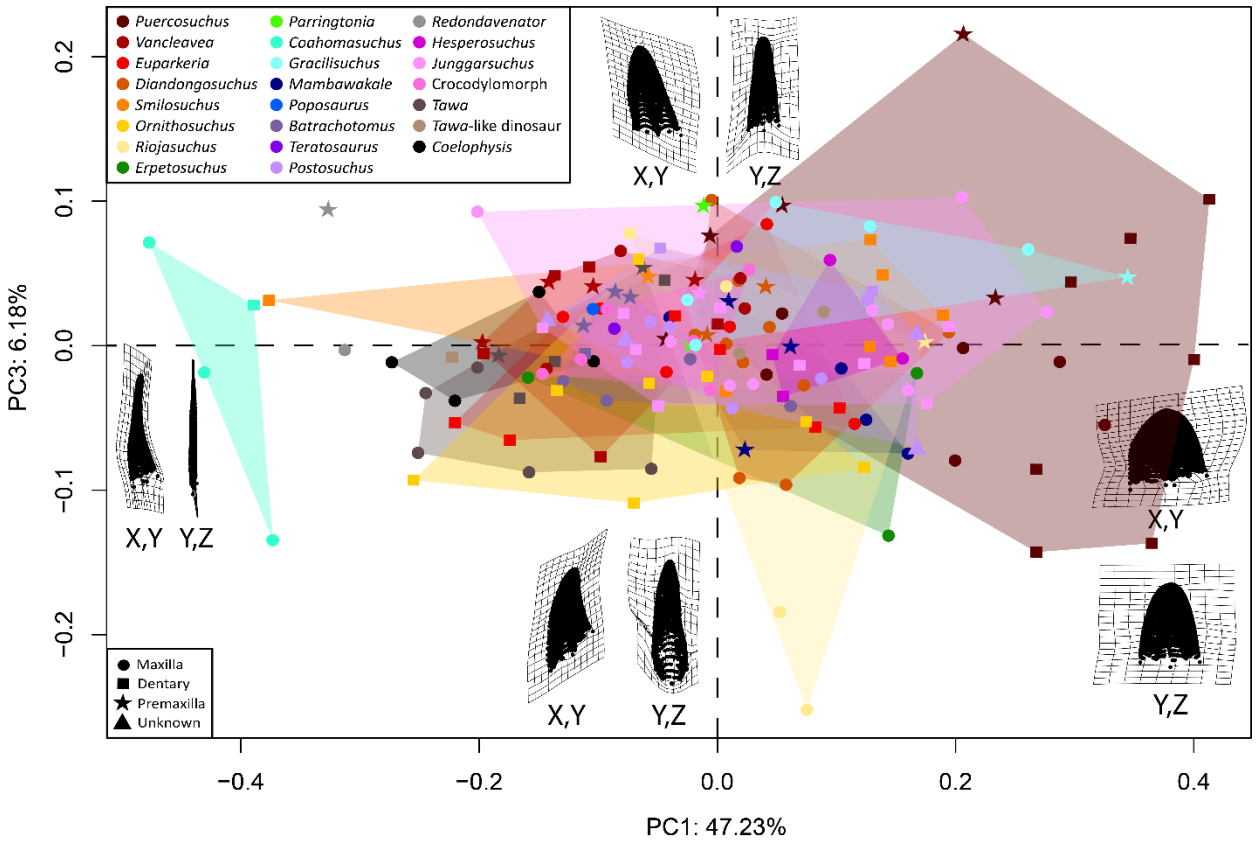


**Figure 29.** PCA of PC1 vs PC3 showing all archosaur and close relative teeth with thin plate splines on the extremes of each axis. Points represent individual teeth. Convex hulls show the spread of individual taxa.

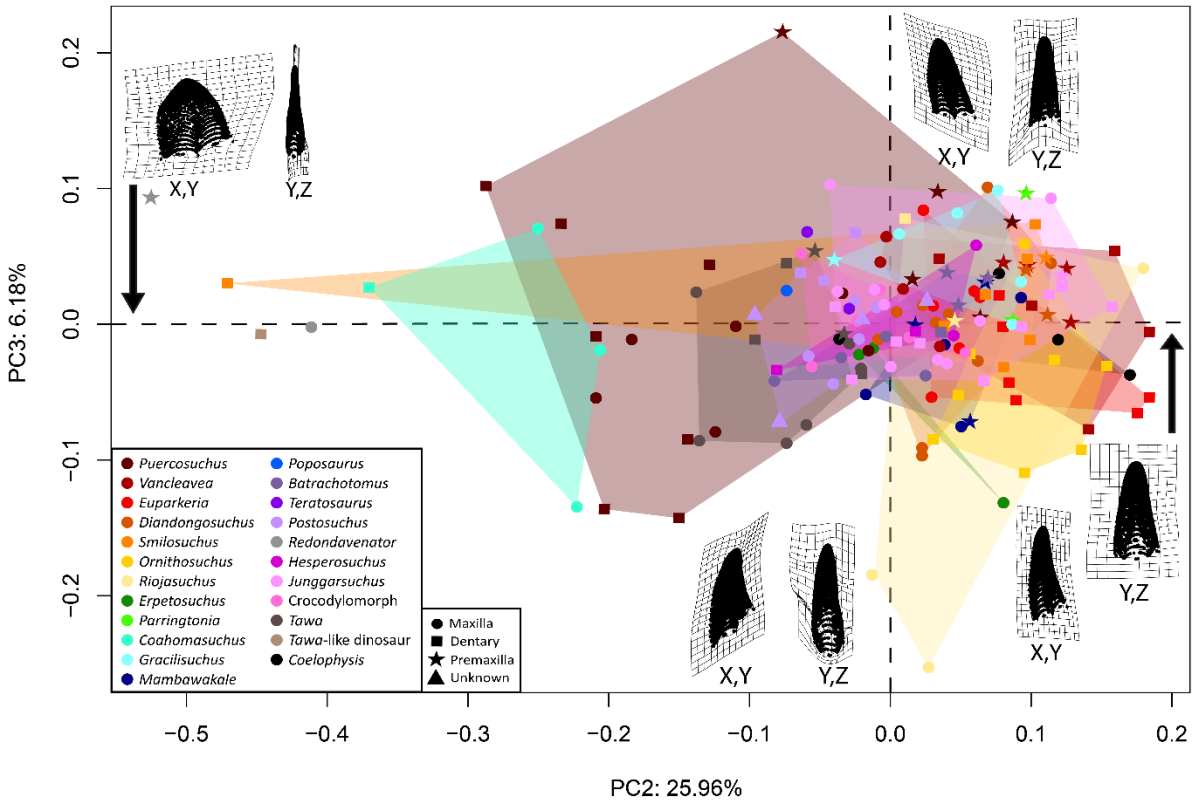


**Figure 30.** PCA of PC2 vs PC3 showing all archosaur and close relative teeth with thin plate splines on the extremes of each axis. Points represent individual teeth. Convex hulls show the spread of individual taxa.

An ANOVA of tooth type (Table 4) does not produce a significant result and the $R^2$ value (0.01496) shows that this hardly explains any variation.

| | df | Sum Sq | Mean Sq | F-value | P-value | Sig. |
|---|---|---|---|---|---|---|
| Tooth Type | 3 | 0.1383 | 0.046112 | 0.8304 | 0.588 | . |
| Residuals | 164 | 9.1067 | 0.55529 | | | |

**Table 4**. Table of ANOVA results where significance cut-offs are "." 0.1>p>0.05, "*" 0.05>p>0.01, "**" 0.01>p>0.001, "***" p<0.001

Running a coarser ANOVA to test if the difference between dinosaurs and pseudosuchians is significant (Table 5) does indeed return a significant result but explains very little of the variation with an $R^2$ of 0.0502.

| | df | Sum Sq | Mean Sq | F-value | P-value | Sig. |
|---|---|---|---|---|---|---|
| Clade | 1 | 0.4641 | 0.46411 | 8.7738 | 0.001 | *** |
| Residuals | 166 | 8.7809 | 0.95290 | | | |

Table 5. Table of ANOVA results of dinosaurs vs pseudosuchians where significance cut-offs are "." 0.1>p>0.05, "*" 0.05>p>0.01, "**" 0.01>p>0.001, "***" p<0.001

The NMDS analysis also shows a large central cluster that virtually all taxa fall within, with a handful of taxa (*Vancleavea, Erpetosuchus,* and *Parringtonia*) more on the edge of this without points falling into the dense central cluster. Again, *Puercosuchus* takes up the largest area on the graph, possibly reflecting the greater number of specimens and individuals of this taxon, and more likely its heterodont dentition across the tooth-bearing bones.

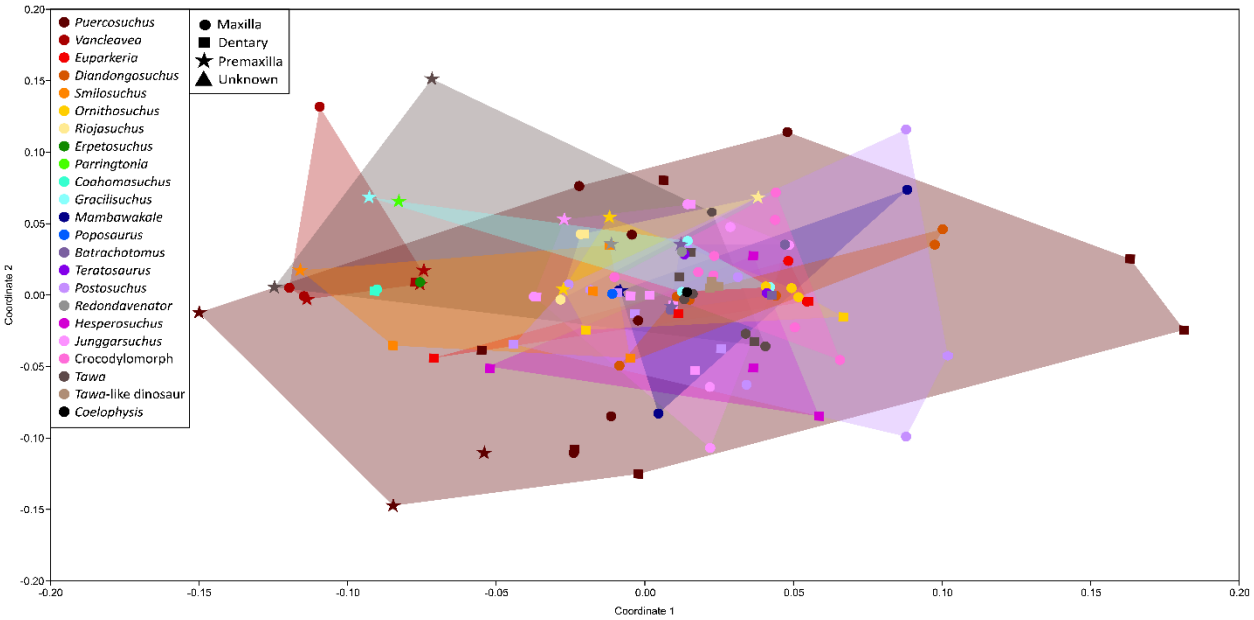


**Figure 31.** Ordination plot of archosaurs and their close relatives. Points represent individual teeth. Convex hulls show the spread of individual taxa.

As there is much overlap among taxa in a central dense area in the 3DGM, this was repeated using only maxillary teeth to test whether there would be greater separation by using only one jaw element (Fig. 32). This does not seem to be the case for the majority of taxa; however, dinosaurs are much more clearly separate from the main cluster the first two PCAs (Fig. 32 and 33), with some pseudosuchian outliers such as *Coahomasuchus*. When comparing PCs one and three, the *Tawa*-like dinosaur is virtually within the main cluster, as is the case for one of the *Coelophysis* points in the comparison of PCs two and three.

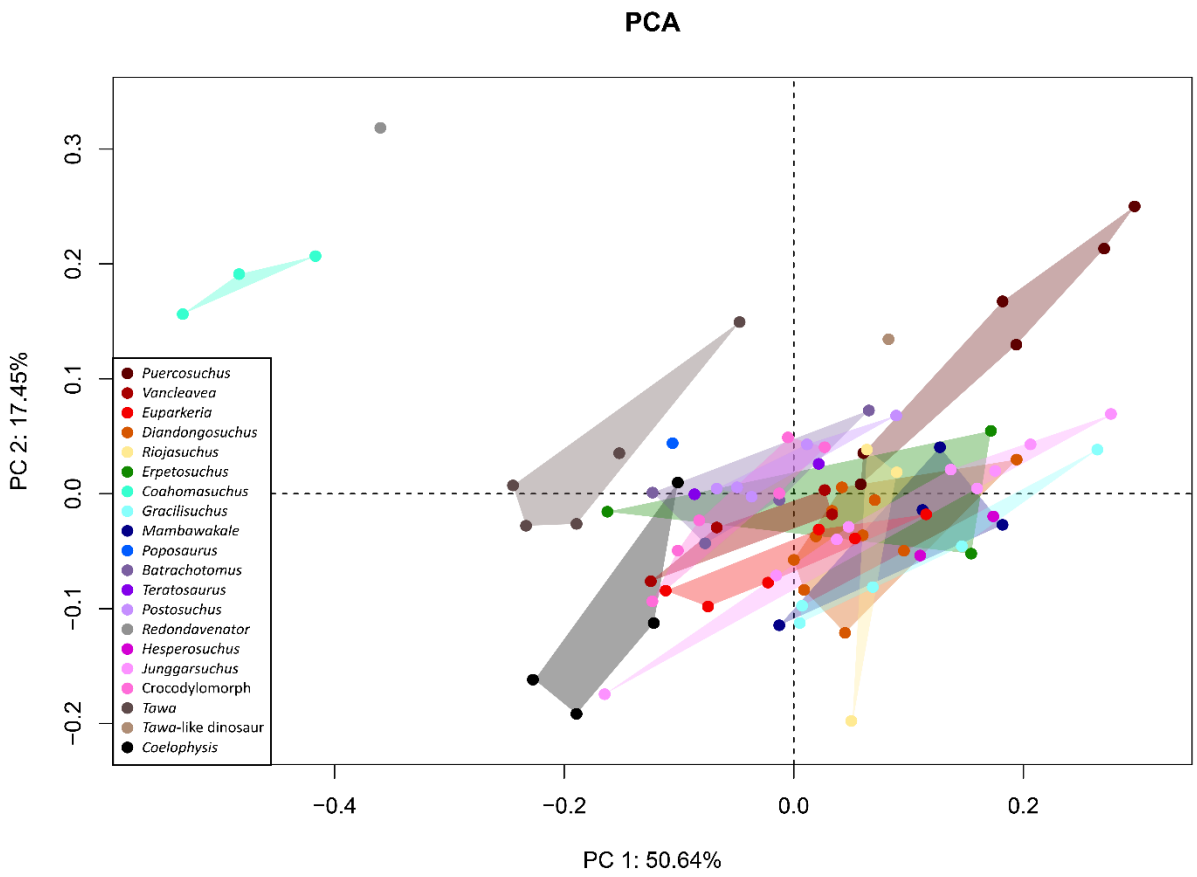


**Figure 32.** 3DGM morphospace plot of PCs one and two showing only teeth from the maxillae of each taxon. Points represent individual teeth. Convex hulls show the spread of each taxon.

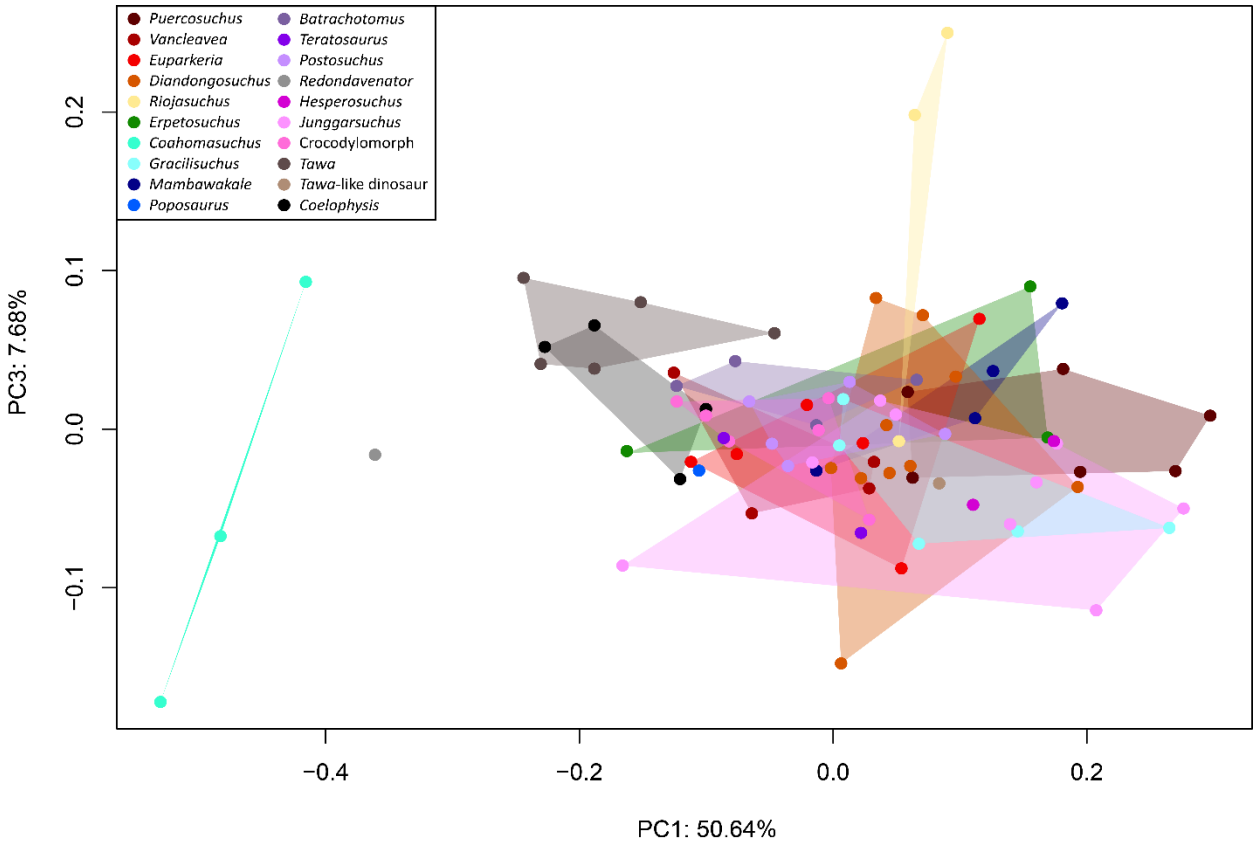


**Figure 33.** 3DGM morphospace plot of PCs one and three showing only teeth from the maxillae of each taxon. Points represent individual teeth. Convex hulls show the spread of each taxon.

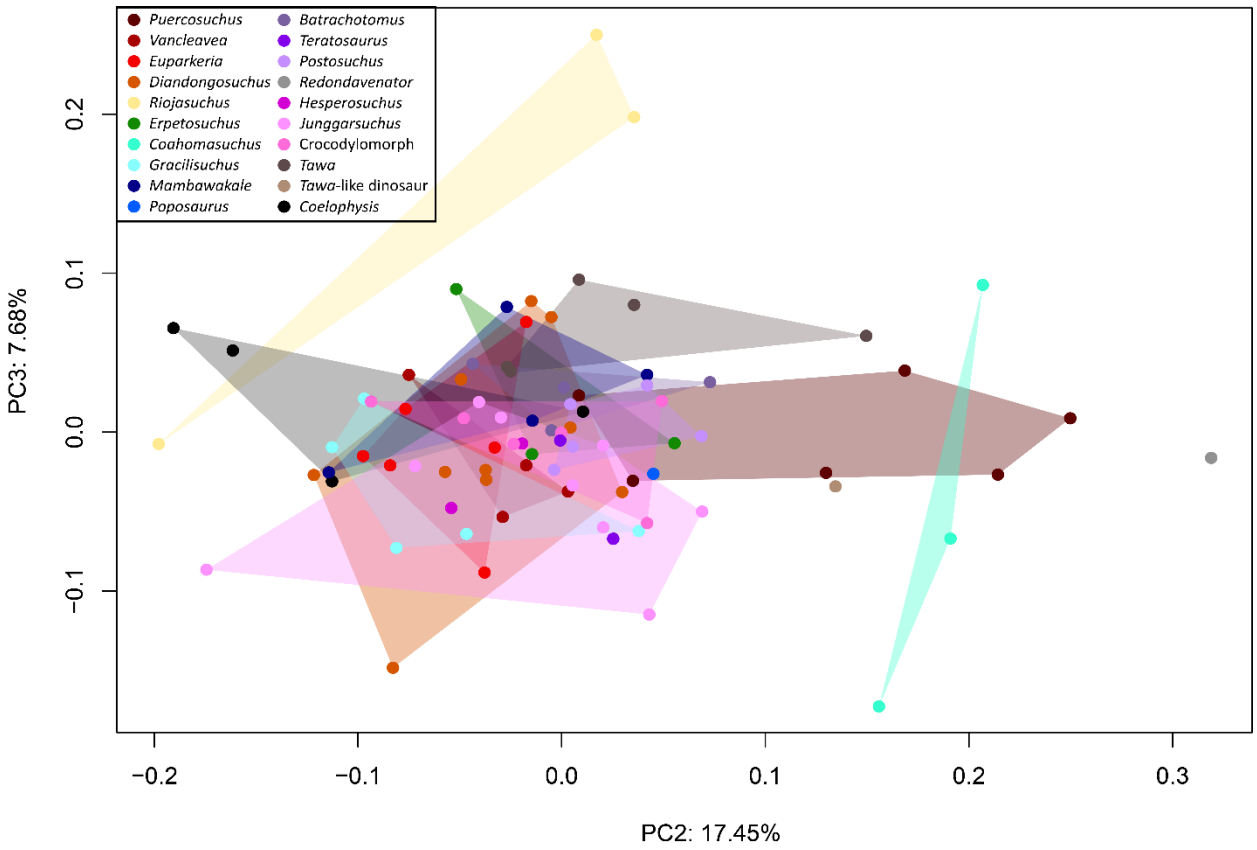


**Figure 34.** 3DGM morphospace plot of PCs two and three showing only teeth from the maxillae of each taxon. Points represent individual teeth. Convex hulls show the spread of each taxon.

## DISCUSSION

Given the large clusters containing most taxa in both analyses (Figs. 28-31), there has been little deviation from the ancestral tooth condition amongst Triassic archosaurs and close relatives. However, all dinosaurs fall either on the edge of the cluster in the 3DGM when looking at PCs one and two (Fig. 28), or away from it entirely, suggesting that there are some shape differences between dinosaur and pseudosuchian teeth. This is not seen in the NMDS analysis (Fig. 31), meaning these differences are attributable to overall shape rather than discrete features. In the case of *Tawa*, in particular, this may be due to how much more labiolingually compressed the teeth are compared to other taxa. The dinosaurs, however, do not all plot together in the 3DGM (Fig. 28, Supplemental Fig. 1), complicating the ability to differentiate between dinosaur

and pseudosuchian, and generally plot much more closely to the majority of pseudosuchians when looking beyond the first two axes (Supplemental Figs 2, 3). However, the ANOVA finds significant differences between dinosaurs and pseudosuchians indicating that the 3DGM method could be used to differentiate these two major clades.

The early diverging archosauromorph *Puercosuchus* takes up the largest area in both analyses (Figs. 28-31), which is to be expected given that it is the only taxon where teeth are sourced from multiple individuals and has the greatest number of teeth representing it in the study. This may also be predominantly due to the strongly heterodont dentition of *Puercosuchus* wherein the anterior teeth are taller, with a sharper apex and rounder cross section than those at the posterior of the mouth, which have a rounded apex, are more laterally compressed and are far shorter (Marsh et al. 2022). This is likely at least partially due to differences in varying pressures on teeth across the tooth row, as seen in crocodylians today, where the rear teeth are subject to greater pressures than the anterior teeth and teeth with less height are more suited to the greater pressures closer to the fulcrum of the jaws (Erickson et al. 2012). The lower height of the posterior teeth also prevents impediment of jaw closure (D'Amore et al. 2019). Heterodont dentitions likely allowed *Puercosuchus* and others to process food differently throughout the mouth as is seen in crocodyliforms (Ösi 2013). This evidence of heterodonty can be seen to an extent in both the 3DGM and NMDS (Figs. 28-31), where in the latter of which we see that the premaxillary teeth plot relatively close together at one end of the spread for this taxon, compared to most maxillary and dentary teeth, which sit in the middle and at the opposite end. When looking just at the teeth of the maxilla (Figs. 32-34), the area of points is much more in line with the area of other taxa. Interestingly, this wide spread of points is not seen in either the 3DGM or NMDS in two other heterodont taxa, *Smilosuchus* and *Vancleavea* (Figs. 28 and 31), but as

mentioned, this may just be an artefact of not having teeth from multiple individuals. However, in the 3DGM (Fig. 28), the teeth of *Vancleavea* plot in distinct rows based on region of the mouth, with one errant dentary tooth, with dentary teeth at the top of the spread, premaxillary teeth in the middle, and maxillary teeth at the bottom.

In the 3DGM of the first two axes (Fig. 28) the teeth of *Puercosuchus* follow a pattern of more anterior teeth plotting closer to 0 on both axes, and, in order, the more posterior teeth gradually plot further away. This pattern (Fig. 35) is more clearly seen in *Euparkeria* and *Junggarsuchus*, with one exception in *Euparkeria* (right maxilla tooth 3) and one in *Junggarsuchus* (right dentary tooth 6), where the anterior teeth of both the dentary and maxilla lead into the posterior teeth in order along a line. This is also observed in the maxilla, the only part tested, of the crocodylomorph and *Coelophysis*. *Tawa* exhibits a similar pattern in both maxilla and dentary. Interestingly, all anterior teeth plot towards the left of the PCA and lead into more posterior teeth the further right they are (Fig. 35) showing that the teeth are gradually changing in shape along the tooth row. This loosely reflects findings in mammals in the inhibitory cascade model (Kavanagh et al. 2007) where teeth closer together share more similarities than teeth that are further apart from one another. However, while this model has been examined in fossils (e.g. Halliday & Goswami, Schroer & Wood 2015, Wilson et al. 2012) it has been restricted to mammalian molars as a way to predict their size and so may not be applicable to this gradual heterodonty.

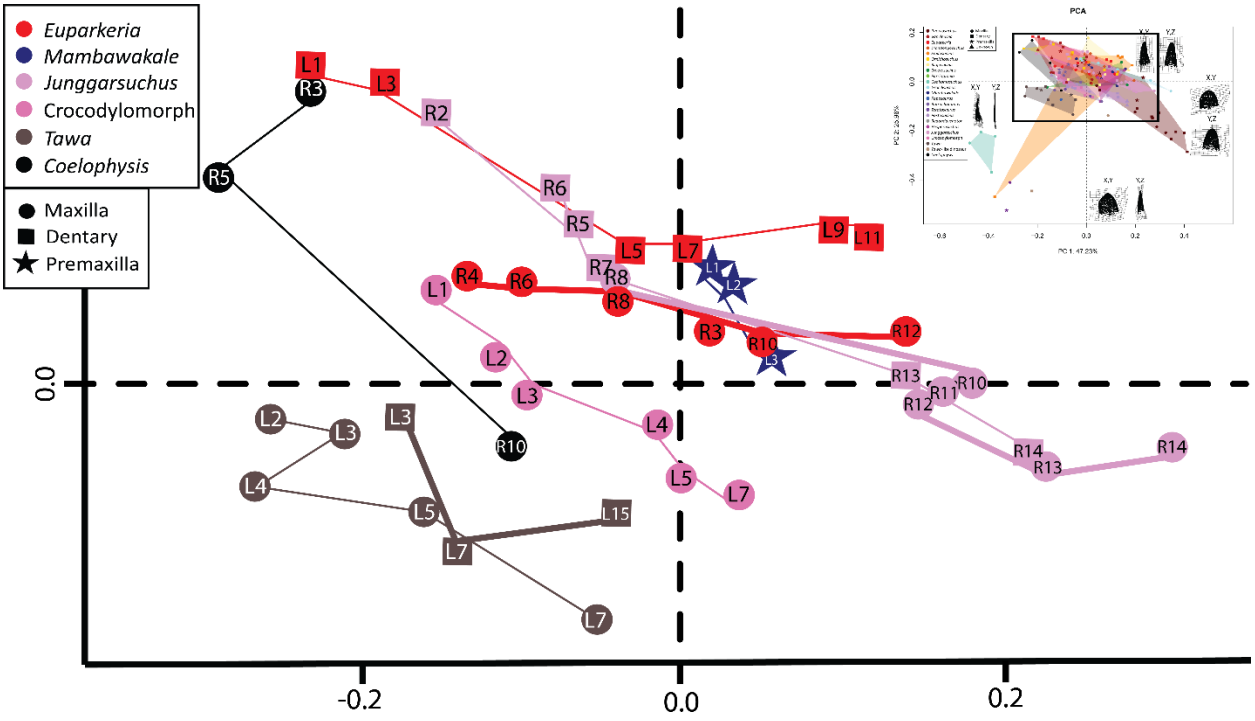


**Figure 35.** Selected taxa from the 3DGM PCA that exhibit teeth plotting in the order seen in the mouth. The highlighted section is from the rectangle within the full PCA (Fig. 28) in the corner. Teeth are represented by the circles (maxilla), squares (dentary), and stars (premaxilla). Lines between them show the anterior to posterior tooth row. Lines from taxa with two different tooth rows (e.g. left dentary and right maxilla) are shown in two different thicknesses. Letters in the points describe what side the tooth has come from (L = left, R = right) and numbers reflect the position of the tooth along the tooth row.

In the 3DGM (Fig. 28), *Coahomasuchus* sits distantly from the main cluster. However, in the NMDS (Fig.31), it sits within the cluster of taxa, though not in the densest part. This suggests that despite the teeth being functionally similar to the teeth of other taxa in this study, they are distinct in shape, which may stem from having deviated from, then returning to a more plesiomorphic shape within Aetosauria. This shape is, however, more hook-like than other taxa

(Fig. 14), perhaps resulting in its position in the 3DGM. It is unclear why *Redondavenator* (Fig. 21) and one *Smilosuchus* tooth (Fig. 9) also plot in this area rather than with the more "typical" archosaur teeth despite appearing similar.

The teeth of *Teratosaurus* have been described as "indistinguishable from those of typical rauisuchids" (Benton 1986) and this is seen in the results of the 3DGM across all axes (Figs. 28-30), where *Teratosaurus* plots directly close to *Postosuchus*, and in the NMDS analysis (Fig. 31), where it plots within the range of *Postosuchus* quantitively confirming this.

When looking at the maxilla only plot (Fig. 32), there appears to be trends in where the teeth of most individuals plot in PCA space. Some of these do reflect what is seen in Figure 35, where teeth plot subsequently after one another from anterior to posterior (e.g. in *Junggarsuchus* and the crocodylomorph), but the majority do not seem to follow any such pattern, making it curious that there seems to be such strong trends.

It does not seem that prey type affects where the teeth plot in morphospace, given that the large *Mambawakale* was probably eating relatively large prey as an apex predator, whereas the small *Gracilisuchus* was likely eating much smaller prey, yet they plot closely together. This suggests that body size does not reflect in the shape or features of the teeth (once size is removed as a confounding factor through the generalised Procrustes analysis for the 3DGM), and that, despite large discrepancies in body size, teeth are generally very similar across archosaurs, and particularly within pseudosuchians.

**Further testing and Concerns**

From both 3DGM and NMDS plots, it is clear that these methods struggle to isolate most taxa with carnivorous dentition, and they may be unsuitable for identifying isolated teeth when the teeth are so similar in form. When adding more disparate teeth from other clades (e.g. from temnospondyls), it would be interesting to see if the archosaur cluster plots separately, thus allowing us to identify archosaurs with reasonable confidence in places like microvertebrate localities, though this would be future research not covered in this dissertation.

Based on the extended spread of the best sampled taxon, *Puercosuchus*, it seems that adding in additional specimens from each taxon would significantly expand the area in which they plot. The lack of any other multispecimen taxa is a concern as it means that we are not capturing potential intraspecific variation of the teeth. The only way to rectify this is to find more specimens that are suitable for scanning and include them in the analyses. However, *Puercosuchus* does exhibit some strong heterodonty between the anterior and posterior teeth, which may be increasing the spread of points to a greater degree and that without this, the teeth may plot more closely together. Furthermore, some taxa are only represented by one or two teeth, meaning that I cannot document variation within these taxa. This also means that outliers are harder to identify, and I cannot see what would have been the full spread of results.

Though there are differences in scan quality between and even within the different methods used to obtain models, this is not likely to affect results much. I tested whether this is a problem in chapter 1 by reducing a mesh down to the same number of faces as the lowest quality scan (*Riojasuchus*) and found virtually no difference in where it plotted in the 3DGM morphospace, suggesting that the different scan qualities do not matter in this analysis as long as they capture gross shape.

## CONCLUSIONS

We cannot clearly identify individual carnivorous archosauriforms from the Triassic using these analyses due to the great overlap among taxa in both the NMDS and 3DGM, as the majority of taxa have hardly deviated from the implied ancestral tooth shape, even when using only teeth from one area of the mouth. However, it seems that dinosaurs plot on the periphery or away from the main cluster of pseudosuchians in the 3DGM. This suggests that we may be able to use this method to differentiate between these two major clades of archosaurs in the Triassic Period. Some taxa (e.g. *Euparkeria, Tawa*) also show teeth plotting subsequently along the tooth row across the 3DGM morphospace, suggesting that as the teeth become more posterior in position, they change subtly and in series in these taxa.

## ACKNOWLEDGEMENTS

Thank you to Adam Marsh and Matthew Smith for scan provision and assistance at PEFO. To Matthew Colbert for scanning *Coahomasuchus.* Val Fischer for coding help and provision. Davide Foffa for providing scans of *Ornithosuchus,* discussion, and assistance with R coding; Isaac Pugh for photogrammetry of specimens and provision of scans.

## REFERENCES

1. Adams D, Collyer M, Kaliontzopoulou A, Baken E (2025). "Geomorph: Software for geometric morphometric analyses. R package version 4.0.10." https://cran.r-project.org/package=geomorph.

2. Baczko, M.B. & Desojo, J.B. 2016. Cranial anatomy and palaeoneurology of the archosaur *Riojasuchus tenuisceps* from the Los Colorados Formation, La Rioja, Argentina. *PLoS ONE* **11(2):** e0148575.
3. Baken E, Collyer M, Kaliontzopoulou A, Adams D (2021). "geomorph v4.0 and gmShiny: enhanced analytics and a new graphical interface for a comprehensive morphometric experience." *Methods in Ecology and Evolution* **12**: 2355-2363.
4. Benson, R.B.J., Campione, N.E., Carrano, M.T., Mannion, P.D., Sullivan, C., Upchurch, P. & Evans, D.C. 2014. Raters of dinosaur body mass evolution indicate 170 million years of sustained ecological innovation on the avian stem lineage. PLOS Biology **12(5)**: e1001853
5. Benton, M.J. 1986. The Late Triassic reptile *Teratosaurus* – a rauisuchian, not a dinosaur. *Palaeontology* **29(2)**: 293-301.
6. Bhat, M.S. 2017. Techniques for systematic collection and processing of vertebrate microfossils from their host mudrocks: a case study from the Upper Triassic Tiki Formation of India. *Journal Geological Society of India* **89:** 369-374.
7. Bonaparte JF. 1967. Dos nuevas 'faunas' de reptiles triásicos de Argentina. Gondwana Stratigraphy, 1 Gondwana Symposium, Mar del Plata, 283–325.
8. Broom R. 1913. Note on *Mesosuchus browni*, Watson, and on a new South African Triassic pseudosuchian (*Euparkeria capensis*). *Records of the Albany Museum* **2(5)**: 394-396.
9. Brusatte, S.L., Butler, R.J., Sulej, T. & Niedźwiedzki, G. 2009. The taxonomy and anatomy of rauisuchian archosaurs from the Late Triassic of Germany and Poland. *Acta Palaeontologica Polonica* **54(2)**: 221-230.

10. Buckley, L.G. & Currie, P.J. 2014. Analysis of intraspecific and ontogenetic variation in the dentition of *Coelophysis bauri* (Late Triassic), and implications for the systematics of isolated teeth. *New Mexico Museum of Natural History and Science Bulletin* **63**: 1-73.
11. Butler, R.J., Vincent, F., Nesbitt, S.J., Leiti J.V. & Gower, D.J. 2022. A new pseudosuchian archosaur, *Mambawakale ruhuhu* gen. et sp. nov., from the Middle Triassic Manda Beds of Tanzania. *Royal Society Open Science*. 9211622.
12. Calede, J.J.M. & Glusman, J.W. 2017, Geometric morphometric analyses of worn cheek teeth help identify extant and extinct gophers (Rodentia, Geomyidae). *Palaeontology* **60**: 281-307.
13. Camp. C.L. 1930. A study of the phytosaurs with a description of new material from western North America. *Memoirs of the University of California* **10**: 1-161.
14. Chatterjee, S. 1985. *Postosuchus*, a new thecodontian reptile from the Triassic of Texas and the origin of tyrannosaurs. *Philosophical Transactions of the Royal Society of London, Series B* **309**: 395-460.
15. Chen , Z. 1985 . [Stratigraphical position of *Keichousaurus hui* Young from the Middle Triassic of southwestern Guizhou and its significance] . *Guizhou Geology* **5**: 289 – 290 . [Chinese]
16. Clark, J., Xu, X., Forster, C. & Wang, Y. 2004 A Middle Jurassic 'sphenosuchian' from China and the origin of the crocodylian skull. *Nature* **430**: 1021–1024.
17. Clark, J.M., Sues, H.D.& Berman, D.S. 2000. A new specimen of *Hesperosuchus agilis* from the Upper Triassic of New Mexico and the interrelationships of basal crocodylomorph archosaurs. *Journal of Vertebrate Paleontology* **20(4)**: 683-704.

18. Colbert, E.H. 1952. A pseudosuchian reptile from Arizona. *Bulletin of the American Museum of Natural History* **99**: 561-592.

19. Cope E.D. 1887. The dinosaurian genus *Coelurus*. *The American Naturalist* **21**: 367-369

20. Currie, P.J., Rigby, J.K. Jr. & Sloan, R.E. (1990) Theropod teeth from the Judith River Formation of southern Alberta, Canada. In: Carpenter, K. & Currie, P.J. (Eds.), Dinosaur Systematics: Approaches and Perspectives. Cambridge, Cambridge University Press, pp. 107–125.

21. D'Amore, D.C., Harmon, M., Drumheller, S.K. & Testin, J.J. 2019. Quantitative heterodonty in Crocodylia: assessing size and shape across modern and extinct taxa. *PeerJ* **7**:e6485

22. Eberth, D.A., Rogers, R.R. & Fiorillo, A.R. 2007. A practical approach to the study of bonebeds. In *Bonebeds: Genesis, Analysis, and Paleobiological Significance*; Rogers, R.R., Eberth, D.A., Fiorillo, A.R., Eds.; University of Chicago Press: Chicago, IL, USA; pp. 103–220

23. Erickson, G.M., Gignac, P.M., Steppan, S.J., Lappin, A.K., Vliet, K.A., Brueggen, J.D., Inouye, B.D., Kledzik, D. & Webb, G.J. 2012. Insights into the Ecology and Evolutionary Success of Crocodilians Revealed through Bite-Force and Tooth-Pressure Experimentation. *PLoS ONE* **7(3)**: e31781.

24. Ezcurra, M.D. 2016. The phylogenetic relationships of basal archosauromorphs, with an emphasis on the systematics of proterosuchian archosauriforms. *PeerJ* **4**: e1778.

25. Ezcurra, M.D. & Butler, R.J. 2018. The rise of the ruling reptiles and ecosystem recovery from the Permo-Triassic mass extinction Proceeding of the Royal Society B **285**: 20180361.

26. Foffa, D., Butler, R.J., Nesbitt, S.J., Walsh, S., Barrett, P.M., Brussatte, S.L. & Fraser, N.C. 2020. Revision of *Erpetosuchus* (Archosauria: Pseudosuchia) and new erpetosuchid material from the Late Triassic 'Elgin Reptile' fauna based on μCT scanning techniques. *Earth and Environmental Science Transactions of the Royal Society of Edinburgh* **111(4)**: 209-233.

27. Gower, J.C. 1971. A general coefficient of similarity and some of its properties. *Biometrics* **27**: 857-874.

28. Gower, D.J. 1999. The cranial and mandibular anatomy of a new rauisuchian archosaur from the Middle Triassic of southern Germany. *Stuttgarter Beiträge zur Naturkunde B* **280**: 1–9.

29. Gower, D.J. & Schoch R.R. 2009. Postcranial anatomy of the rauisuchian archosaur *Batrachotomus kupferzellensis*. *Journal of Vertebrate Paleontology* **29(1)**: 103-122

30. Halliday, T.J. & Goswami, A. 2013. Testing the inhibitory cascade model in Mesozoic and Cenozoic mammaliaforms. *BMC Evolutionary Biology* **13:** 79.

31. Hammer Ø, Harper D, Ryan P. 2001. PAST-Palaeontological statistics. *Palaeontologia Electronica* **25**: 2009.

32. Heckert, A.B., Lucas, S.G. 1999. A new aetosaur (Reptilia: Archosauria) from the Upper Triassic of Texas and the phylogeny of aetosaurs. *Journal of Vertebrate Paleontology* **19(1)**: 50–68.

33. Heckert, A.B., Viner, T.C. & Carrano, M.T. 2021. A large pathological skeleton of *Smilosuchus gregorii* (Archosauriformes: Phytosauria) from the Upper Triassic of Arizona, U.S.A., with discussion of the paleobiological implications of paleopathology in fossil archosauromorphs. *Palaeontologica Electronica* **24(2)**: a21.

34. Hendrickx, C., & Mateus O. 2014. Abelisauridae (Dinosauria: Theropoda) from the Late Jurassic of Portugal and dentition-based phylogeny as a contribution for the identification of isolated theropod teeth. *Zootaxa* **3759**: 1-74.

35. Huene, F. V. 1939. Ein kleiner Pseudosuchier und ein Saurischier aus den ostafrikanischen Mandaschichten. *Neues Jahrbuch für Geologie und Paläeontologie, Beilage-Bände Abteilung B* **81**: 61–9.

36. Hungerbühler, A. 2000. Heterodonty in the European phytosaur *Nicrosaurus kapffi* and its implications for the taxonomic utility and functional morphology of phytosaur dentition. *Journal of Vertebrate Paleontology* **20(1)**: 31-48

37. Irmis, R.B., Nesbitt, S.J., Padian, K., Smith, N.D., Turner, A.H., Woody, D. & Downs, A. 2007. A Late Triassic dinosauromorph assemblage from New Mexico and the rise of dinosaurs. *Science* **317(5836)**: 358-361.

38. Irmis, R.B., Mundil, R., Martz, J.W. & Parker, W.G. 2011. High resolution U-Pb ages from the Upper Triassic Chinle Formation (New Mexico, USA) support a diachronous rise of dinosaurs. *Earth and Planetary Science Letters* **309(3-4)**: 258-267.

39. Kavanagh, K.D., Evans, A.R. & Jernvall J. 2007. Predicting evolutionary patterns of mammalian teeth from development. *Nature* **449**, 427–432.

40. Lecuona, A. 2013. *Anatomía y relaciones filogenéticas de Gracilisuchus stipanicicorum y sus implicancias en el origen de Crocodylomorpha*, PhD thesis. Universidad de Buenos Aires: Facultad de Ciencias Exactas y Naturales. 1-145.

41. Lecuona, A. Desojo, J.B. 2012. Hind limb osteology of *Gracilisuchus stipanicicorum* (Archosauria: Pseudosuchia). *Earth and Environmental Science Transactions of the Royal Society of Edinburgh* **102(2)** :105-128.

42. Li, C., Wu, X-C., Zhao, L-J., Sato, T. & Wang, L-T. 2012. A new archosaur (Diapsida: Archosauriformes) from the marine Triassic of China. *Journal of Vertebrate Paleontology* **32(5)**: 1064-1081.

43. Long, R.A. & Murry, P.A. 1995. Late Triassic (Carnian and Norian) tetrapods from the southwestern United States. *New Mexico Museum of Natural History and Science Bulletin* **4**: 1-254.

44. Marsh, A.D., Parker, W.G., Nesbitt, S.J., Kligman, B.T. & Stocker, M.R. 2022. *Puercosuchus travereorum* n. gen. n. sp.: a new malerisaurine azandohsaurid (Archosauromorpha: Allokotosauria) from two monodominant bonebeds in the Chinle Formation (Upper Triassic, Norian) of Arizona. *Journal of Paleontology* **96(90)**: 1-39

45. Marsicano, C.A., Irmis, R.B., Mancuso, A.C., Mundil, R. & Chemale, F. 2016 The precise temporal calibration of dinosaur origins. *Proceedings of the National Academy of Science* **113(3)**: 509-513.

46. Martz, J.W., Mueller, B., Nesbitt, S.J., Stocker, M.R., Parker, W.G., Atanassov, M., Fraser, N., Weinbaum, J. & Lehane, J.R. 2012. A taxonomic and biostratigraphic re-evaluation of the Post Quarry vertebrate assemblage from the Cooper Canyon Formation (Dockum Group, Upper Triassic) of southern Garza County, western Texas. *Earth and Environmental Transactions of the Royal Society of Edinburgh* **103(3-4)**: 339-364.

47. Mehl, M.G. 1915. *Poposaurus gracilis,* a new reptile from the Triassic of Wyoming. *Journal of Geology* **23**: 516-522.

48. Meso, J.G., Gianechini, F., Gomez, K.L., Muci, L., Baiano, M.A., Kaluza, J., Garrido, A. & Pittman, M. 2014. Shed teeth from Portezuelo Formation at Sierra del Portezuelo

reveal a higher diversity of predator theropods during Turonian-Coniacian times in northern Patagonia. *BMC Ecology and Evolution* **24(59)**: 1-20.

49. Murry, P.A. & Long R.A. 1996. A diminutive carnivorous aetosaur from the Upper Triassic of Howard County, Texas [Abstract]. *Journal of Vertebrate Paleontology* **16** (supplement 3): 55A.
50. Nesbitt, S.J. 2011. The early evolution of archosaurs: relationships and the origin of major clades. *Bulletin of the American Museum of Natural History* **352:** 1-292.
51. Nesbitt, S.J. & Butler, R.J. 2013. Redescription of the archosaur *Parringtonia gracilis* from the Middle Triassic Manda beds of Tanzania, and the antiquity of Erpetosuchidae. *Geology Magazine* **150(2)**: 225-238.
52. Nesbitt, S.J., Irmis, R.B. & Hunt, A.P. 2005. A giant crocodylomorph from the Upper Triassic of New Mexico. *Paläontologische Zeitscrift* **79(4)**: 471-478.
53. Nesbitt, S.J., Smith, N.D., Irmis, R.B., Turner, A.H., Downs, A. & Norell, M.A. 2009. A complete skeleton of a Late Triassic saurischian and the early evolution of dinosaurs. *Science* **326(5959)**: 1530-1533.
54. Nesbitt, S.J., Stocker, M.R., Parker, W.G., Wood, T.A., Sidor, C.A. & Angielczyk, K.D. 2017. The braincase and endocast of *Parringtonia gracilis*, a Middle Triassic suchian (Archosaria: Pseudosuchia). *Journal of Vertebrate Paleontology* **37(6)**: 122-141.
55. Nesbitt, S.J., Stocker, M.R., Small, B.J. & Downs, A. 2008. The osteology and relationships of *Vancleavea campi* (Reptilia: Archosauriformes). *Zoological Journal of the Linnean Society* **157**: 814-864.
56. Newton, E.T. 1894. XIII. Reptiles from the Elgin sandstone. – description of two new genera. *Proceedings of the Royal Society B* **185**: 573-607.

57. Olsen, P.E., Sues, H-D. & Norell, M.A. 2000. First record of *Erpetosuchus* (Reptilia: Archosauria) from the Late Triassic of North America. *Journal of Vertebrate Paleontology* **20(4)**: 633-636.

58. Ösi, A. 2013. The evolution of jaw mechanism and dental function in heterodont crocodyliforms. *Historical Biology* **26(3)**: 279-414.

59. Parker, W.G. 2016. Revised phylogenetic analysis of the Aetosauria (Archosauria: Pseudosuchia) assessing the effects of incongruent morphological character sets. *PeerJ* **4**: e1583.

60. Parker, W.G. & Nesbitt, S.J. 2013. Cranial remains of *Poposaurus gracilis* (Pseudosuchia: Poposauroidea) from the Upper Triassic, the distribution of the taxon, and its implications for poposauroid evolution. *Geological society, London, Special Publications* **379**: 503-523.

61. Parker, W.G., Stocker, M.R., Reyes, W.A, Werning, S. 2024. Anatomy and ontogeny of the "carnivorous aetosaur": New information on *Coahomasuchus kahleorum* (Archosauria: Pseudosuchia) from the Upper Triassic Dockum Group of Texas. *The Anatomical Record* **308(2)**: 671-735.

62. Ruebenstahl, A.A., Klein, M.D., Yi, H., Xu, X. & Clark, J.M. 2022. Anatomy and the relationships of the early diverging Crocodylomorphs *Junggarsuchus sloani* and *Dibothrosuchus elaphros. The Anatomical Record* **305**: 2463-2556.

63. Schroer, K. & Wood, B. 2015. Modelling the dental development of fossil hominins through the inhibitory cascade. *Journal of Anatomy* **226**: 150-162.

64. Senter, P. 2003. New information on cranial and dental features of the Triassic archosauriform reptile *Euparkeria capensis. Palaeontology* **46(3)**: 613-621

65. Sookias, R.B. 2016, The relationships of the Euparkeriidae and the rise of Archosauria. *Royal Society Open Science* **3(3)**: 150674.

66. Sookias, R.B. & Butler, R.J. 2013. Euparkeriudae. *Geological Society of London Special Publications* **379**: 35-48.

67. Sookias, R.B., Dilkes, D., Sobral, G., Smith, R.M.H., Wolvaart, F.P., Arucci, A.B., Bhullar, B-A.S. & Werneburg, I. 2020 The craniomandibular anatomy of the early archosauriform *Euparkeria capensis* and the dawn of the archosaur skull. *Royal Society Open Science* **2**: 200116.

68. Stocker, M.R., Zhao, L-J., Nesbitt, S.J., Wu, X-C. & Li, C. 2017. A short-snouted, Middle Triassic phytosaur and its implications for the morphological evolution and biogeography of Phytosauria. *Scientific Reports* **7**: 46028.

69. Tucker, A.S. & Fraser G.J. 2014. Evolution and developmental diversity of tooth regeneration. *Seminars in Cell & Developmental Biology* **26-26**: 71-80.

70. Weinbaum, J.C. 2011. The skull of *Postosuchus kirkpatricki* (Archosauria: Paracrocodyliformes) from the Upper Triassic of the United States. *PaleoBios* **30(1)**: 18-44.

71. Wills, S., Underwood, C.J. & Barrett, P.M. 2021. Learning to see the wood for the trees: machine learning, decision trees, and the classification of isolated theropod teeth. *Palaeontology* **64(1)**: 75-99.

72. Wills, S., Underwood, C.J. & Barrett, P.M. 2023. Machine learning confirms new records of maniraptoran theropods in Middle Jurassic UK microvertebrate faunas. *Papers in Palaeontology* **9(2)**: e1487.

73. Wilson, L.A.B., Madden, R.H., Kay, R.F. & Sánchez-Villagra, M.R. 2012. Testing a developmental model in the fossil record: molar proportions in South American ungulates. *Paleobiology* **38(2)**: 308-321.

74. Wyatt, M.R., Hopkins, S.B. & Davis, E.B. 2021. Using 2D dental geometric morphometrics to identify modern *Perognathus* and *Chaetodipus* specimens (Rodentia, Heteromyidae). *Journal of Mammalogy* **104(4)**: 1087-1100.

## CHAPTER 3 – A New Taxon of Hybodontiform (Chondrichthyes, Hybodontiformes) from the Late Triassic of Arizona, USA and its Biostratigraphic Importance within the Chinle Formation

### ABSTRACT

Chondrichthyans make excellent candidates for biostratigraphy, with distinctive dentitions and wide distributions over a long period of time. However, the high variation in tooth

shapes present within a single species of some chondrichthyans (e.g., hybodontiforms) makes disentangling species variation from higher levels of taxonomy (e.g., genus) difficult. Here, I described a sample of over 200 isolated tooth crowns of a new taxon of hybodontiform shark from a highly productive microvertebrate site from the Sonsela Member of the Chinle Formation of Arizona,USA. This large sample is assigned to a new species of the genus *Lonchidion* Estes 1964, a genus-level taxon known globally and from the Upper Triassic Chinle Formation and Dockum Group of the southwestern US. The new taxon *Lonchidion minimorsus* sp. nov. possesses teeth that are mesiodistally twice as long as they are labiolingually wide, show no or small (up to 25% height of principal cusp) lateral cusps, have a weak to moderately defined labial peg consistent with other members of *Lonchidion*, and lack ornamentation apart from the common occurrence of two or three lingually oriented cristae on the lingual side. I observed variation among teeth, mainly relating to the presence and/or size of the cusplets and labial peg, cristae on the lingual side, and the angle of the distal edge of the principal cusp (=center) relative to the base, which ranges from approximately 70-90°. *Lonchidion minimorsus* sp. nov. increases the diversity of the genus *Lonchidion* from the early Norian and fills a stratigraphic gap in the previously recognized distribution of chondrichthyans from the Upper Triassic of the western US. Together, the stratigraphic sequence of *Lonchidion* appears useful for biostratigraphic correlation of localities within the Chinle Formation and across the Chinle Formation and Dockum Group of the southwestern US.

**INSTITUTIONAL ABBREVIATIONS**

**DMNH**, Perot Museum of Nature and Science, Texas, U.S.A.; **NMMNH**, New Mexico Museum of Natural History and Science, New Mexico, U.S.A.; **PEFO**, Petrified Forest National Park, Arizona, U.S.A.

## INTRODUCTION

Chondrichthyan teeth are useful index fossils and allow correlation among different stratigraphic units (e.g., formations, members, beds) (Murry & Kirby 2002, Williamson et al. 2016, He et al. 2017, Ginter 2022). Among chondrichthyans, hybodontiforms were a globally ecological disparate and long-lived group, with a stratigraphic range from the Late Devonian through to the end of the Cretaceous Period (Fischer 2008). They were highly abundant during the Triassic Period (Bhat et al. 2018) and are known from deposits worldwide, indicating a distribution across Pangea (e.g. Bhat et al. 2018, Bhat et al. 2017, Manzanares et al. 2016, Koot et al. 2013, Błażejowski 2004) predominantly from freshwater to brackish environments (Everhart 2011). However, tolerance of marine environments must have been present originally to allow for this wide geographic range (Johns et al. 2014). They have been used for biostratigraphy in correlating Cretaceous beds in Malaysia and Thailand (He et al. 2017), and in the southwestern United States (Murry & Kirby 2002), thanks to their abundance and wide distribution. Despite this abundance in the Triassic Period, as is the case for chondrichthyans, skeletal material is scarce, and most hybodontiform taxa are described based on isolated teeth (Rees and Underwood 2002).

Freshwater hybodontiforms have been recognised from the Upper Triassic Chinle Formation and Dockum Group before (e.g., Fischer et al. 2010, Heckert 2004). The two common

taxa include *Reticulodus synergus* (Murry & Kirby 2002; Voris & Heckert 2017), and *Lonchidion humblei* (Murry 1981), with the rarer *Diplolonchidion murryi* known only from the Dockum Group, and along with a possible singular instance of *Acrodus* sp. from the *Placerias* Quarry (Kaye & Padian 1994, but see Heckert 2004 where doubt is cast on the assignment to *Acrodus*). *Lonchidion humblei* was reported to be widespread geographically and temporally across the Upper Triassic deposits of the western United States (Murry 1981; Murry & Long 1989; Huber et al. 1993; Heckert 2004; Heckert et al. 2007; Heckert & Lucas 2006). The holotype was described from the Tecovas Formation of the Dockum Group (Murry 1981; Heckert 2004) and referred specimens were reported from the Sloan Canyon Formation of the Dockum Group (Heckert et al. 2006; 2007), the *Placerias* Quarry (Jacobs & Murry 1980 as *Lonchidion* sp; Murry & Long 1989 as *Lissodus humblei*), and the 'Dying Grounds' and 'Crocodile Hill' localities (Murry & Long 1989 as *Lissodus humblei*) within Petrified Forest National Park in the Chinle Formation of Arizona. Furthermore, the species was reported from the Ojo Huelos Member of the San Pedro Arroyo Formation of New Mexico (Heckert 2004). Given the wide distribution, the species was used to correlate sediments across the Upper Triassic in Arizona, New Mexico, and Texas (Murry & Kirby 2002) suggesting that the species had a pre-Revueltian distribution with the possibility of a single late occurrence in the Sloan Canyon Formation (see Discussion).

A major challenge in confirming that all these occurrences are *Lonchidion humblei* is the large degree of variation, which complicates the identification of referred specimens of Upper Triassic hybodontiforms from the western US because the holotype of *Lonchidion humblei* (Murry 1981) is an isolated tooth. As is seen in other hybodontiforms, there is significant variation among teeth from different areas of the mouth within a single species (Murry 1981,

Heckert et al. 2007, e.g., *Asteracanthus,* Rees & Underwood 2008, Stumpf et al. 2021). It is clear that there is variation in the type series of *Lonchidion humblei* (Murry 1981, plate 1), but the variation is not explicitly discussed or quantified. Compounding the problem further, without a way to identify variation within a single species, the biostratgraphic use of that taxon is questionable given the wide distribution of previously referred specimens across vast geography and stratigraphy.

To clarify the taxonomic diversity and biostratigraphic use of hybodontiforms from the Upper Triassic sediments of the western United States, this study focuses on a large sample of hybodontiform teeth from a single locality within the Chinle Formation. My sample consists of over 200 isolated tooth crowns collected from bulk sorting of sediment from the microvertebrate site known as the 'Green Layer Locality' (Stocker et al. 2019, Kligman et al 2020), southeast of Petrified Forest National Park in Arizona, USA. I deduce that this large sample of teeth come from a single taxon named here and provide much needed insights on the variation of hybodontiform teeth within the Chinle Formation. Partial crowns from a similarly aged locality confirm that this taxon was found in multiple locations at the time and that we can detect variation across *Lonchidion* from the southwestern United States. This suggests a greater diversity than previously known of hybodontiforms within the Chinle Formation and Dockum Group.

**Taxonomic note: *Lissodus* vs *Lonchidion***

The histories of the genera *Lonchidion* and *Lissodus* are intertwined and complex. Looking at *Lonchidion humblei* alone, the species was initially described as *Lonchidion* (Murry

1981), but was then placed into *Lissodus* by Duffin (1985) when he synonymised the two genera, considering *Lonchidion* a junior synonym, particularly based on the presence of a labial protuberance, which was echoed in Case and Schwimmer (1988). Later, Rees and Underwood (2002) once again split the two genera, noting that the presence of a labial protuberance or peg is likely to be a taxonomically unreliable feature as it has a functional role in interlocking teeth, and the *L. humblei* was returned to *Lonchidion* along with 12 other species also placed in *Lonchidion*. They emended the diagnosis of *Lonchidion* to small teeth that are mesiodistally longer than they are tall with cusps that are "moderately low to poorly defined" (Rees & Underwood 2002). The roots were described as having numerous foramina, some of which formed a line of pores on the apical edge.

However, *Lonchidion humblei* was written as *Lissodus* once again by Fischer (2008) without explanation. The separation of *Lonchidion* and *Lissodus* was maintained by Rees (2008) and, based on the mix of characters seen in the Acrodontinae and the Lonchidiidae, Rees concluded that *Lissodus* could not be assigned to any family at present and lacked many characters typical of Lonchidiidae. This view was upheld by Cappetta (2012). Here, I use *Lonchidion* as the genus for *Lonchidion humblei* as that is the most recently used genus and has been so for quite some time now, with greater explanation for its use.

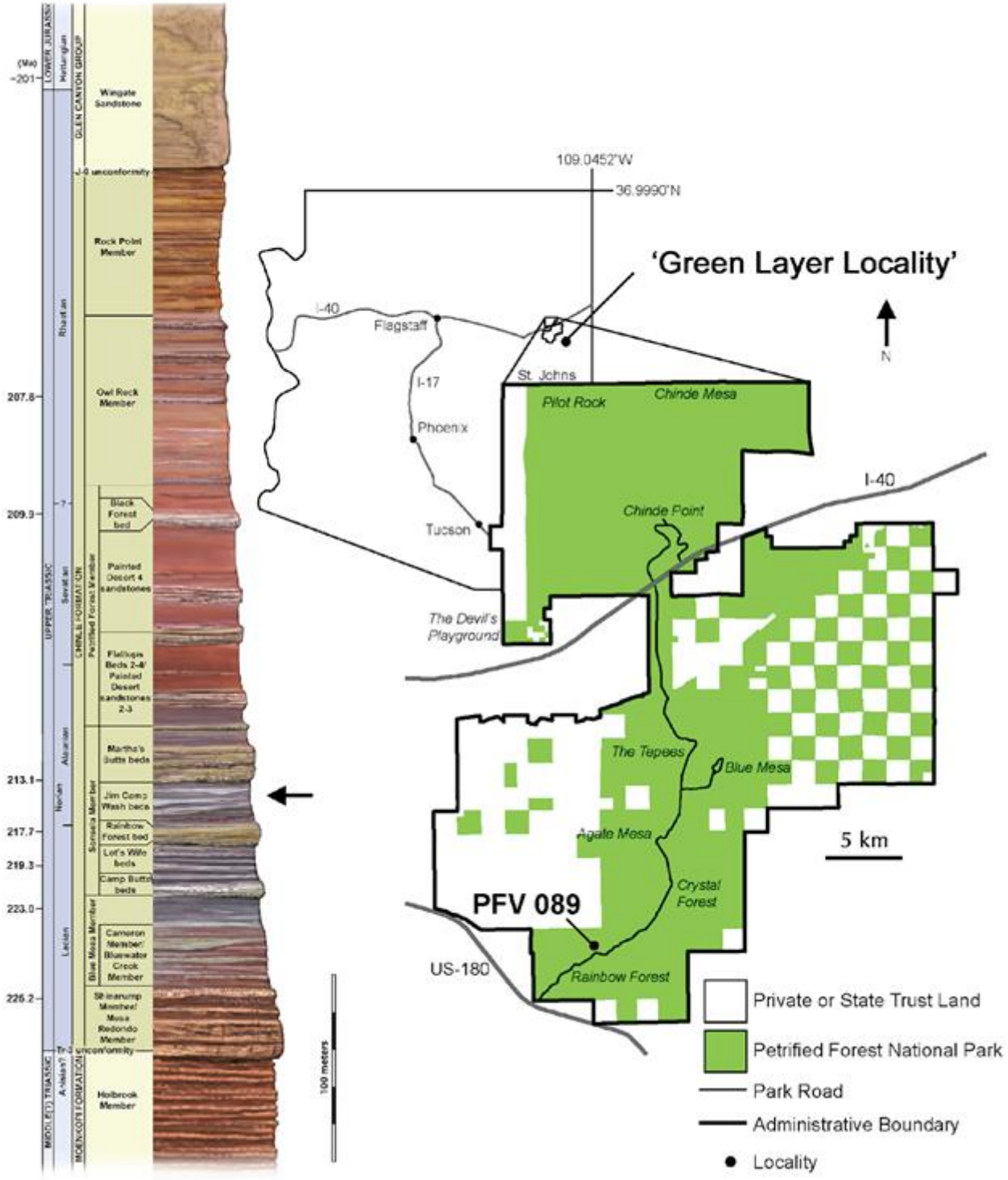
(Ma)
~201
207.8
209.3
213.1
217.7
219.3
223.0
226.2
LOWER JURASSIC
UPPER TRIASSIC
MIDDLE(?) TRIASSIC
Hettangian
Rhaetian
Norian
Adamanian
Revueltian
Apachean
?
?
GLEN CANYON GROUP
CHINLE FORMATION
MOENKOPI FORMATION
Wingate Sandstone
J-0 unconformity
Rock Point Member
Owl Rock Member
Black Forest bed
Painted Desert 4 sandstones
Flattops Beds 2-4/ Painted Desert sandstones 2-3
Martha's Butte beds
Jim Camp Wash beds
Rainbow Forest bed
Let's Wife beds
Camp Butte beds
Sonsela Member
Petrified Forest Member
Blue Mesa Member
Cameron Member/ Bluewater Creek Member
Shinarump Member/ Mesa Redondo Member
unconformity
Holbrook Member
100 meters
109.0452°W
36.9990°N
'Green Layer Locality'
N
I-40
Flagstaff
I-17
Phoenix
Tucson
St. Johns
Pilot Rock
Chinde Mesa
Chinde Point
The Devil's Playground
The Tepees
Blue Mesa
Agate Mesa
Crystal Forest
PFV 089
Rainbow Forest
US-180
5 km
Private or State Trust Land
Petrified Forest National Park
Park Road
Administrative Boundary
Locality

**Figure 1.** Stratigraphic column of the Chinle Formation with an arrow indicating the stratigraphic position of *Lonchidion minimorsus* within the Sonsela Member of the Chinle Formation in the sequence, and map showing the locations of the 'Green Layer Locality' (DMNH 2018-05) and the 'Bowman Site' PFV 089. Modified from Kligman et al. 2020.

## METHODS

Sediment was collected in bulk from the 'Green Layer Locality' and 'Bowman Site' PFV 089 both from the Jim Camp Wash beds of the Sonsela Member of the Chinle Formation (Fig. 1). The 'Green Layer Locality' site is a 2-4 m thick interbedded green and white laminated sandstone (Burch et al. 2024). The 'Bowman Site is a roughly 20 cm thick grey horizon of interfingered conglomeratic lenses with a tan coloured matrix (Kligman et al. 2020). The sediment was screen washed at Petrified Forest National Park to remove sediment (Kligman et al. 2017). After transportation to Virginia Tech, the remaining sediment of the 'Green Layer' material was sieved in sieve sizes 1000, 750, and 90 μm following the method outlined by Kligman et al. (2017) and the residue sorted through under microscope to pick out fossils, including the 275 'Green Layer' teeth noted in this description. Most complete teeth were found in sieve size 1000 μm, and predominantly partial teeth were found in sieve sizes 750 and 90 μm.

Complete tooth crowns from the 'Green Layer' were μCT scanned in the Institute for Critical Technology and Applied Science at Virginia Tech using the SkyScan 1172 μCT. Scan parameters were as follows for the 'Green Layer': copper and aluminium filters, source voltage (kV) 85, source current (uA) 116, Image Pixel Size (μm) 11.15. Parameters for the 'Bowman Site' material were: copper and aluminium filters, source voltage (kV) 76, source current (μA) 131, image pixel size (μm) 10.80. Scans were processed using Materialize Mimics 21.0 (Green

Layer) and 25.0 (Bowman). Models were processed and measured in 3-Matic and Meshlab 2021.07.

**Non-Metric Multidimensional Scaling**

A non-metric multidimensional scaling (NMDS) analysis was conducted in Paleontological Statistics (PAST) (Hammer et al. 2001) to test variation in and between the two populations of the new hybodont. I created six binary characters to capture discrete elements of tooth shape to test this (Table 1). A Gower similarity index was used as it is known to cope well with missing data (Gower 1971).

| | |
|---|---|
| 1 | Labial peg absent (0) or present (1) |
| 2 | Lateral cusp(s) absent (0) or present (1) |
| 3 | Lingual cristae absent (0) or present (1) |
| 4 | Number of cristae two (0) or three (1) |
| 5 | Principle cusp at 90 degrees perpendicular to base (0) or another angle (1) |
| 6 | Labial crest absent (0) or present (1) |

**Table 1.** Characters used in the NMDS analysis

**3D Geometric Morphometrics**

3D geometric morphometric (3DGM) analysis was conducted in R using the method outlined by Fischer et al. (2022). This method drapes a disc of semi-landmarks over the tooth, based on the position of five fixed landmarks. Landmarks were placed on the apex of the tooth,

and the mesial, distal, labial, and lingual sides at the base of the tooth. A generalised Procrustes analysis was performed to remove the confounding influence of size.

**RESULTS**

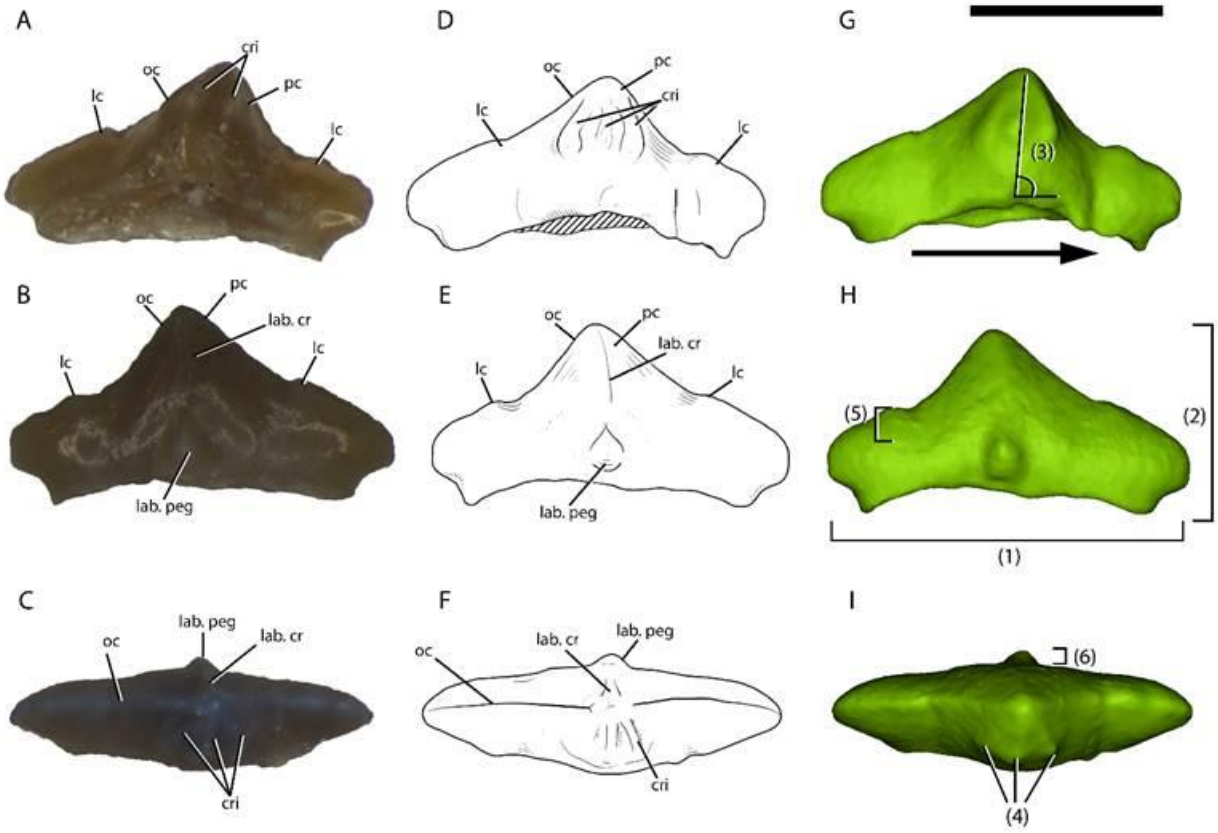


**Figure 2**. Holotype of *Lonchidion minimorsus* n. sp. (DMNH PAL 2018-05-0149) as photographs (A-C), line drawings (D-F), and 3D model from the µCT scan (G-I). Numbers and labels on G-I correspond to characters in Table 1. Cri – cristae, lab.cr – labial crest, lab.peg – labial peg, lc – lateral cusp, oc – occlusal crest, pc – principal crest. Scale bar is 1 mm.

**Systematic Palaeontology**

CHONDRICHTHYES Huxley, 1880

EUSELACHII Hay, 1902

HYBODONTIFORMES Maisey, 1975

HYBODONTOIDEA Owen, 1846

LONCHIDIIDAE Herman, 1977

*LONCHIDION* Estes, 1964

*LONCHIDION MINIMORSUS* sp. nov.

**Etymology**

From the Latin *minima* (smallest), and *morsus* (bite) to become “tiny bite”.

**Holotype**

DMNH PAL 2018-05-0149, tooth crown, the largest of the complete ‘Green Layer’ teeth (Fig. 2).

**Paratypes**

From the ‘Green Layer’, DMNH PAL 2018-05-0150, DMNH PAL 2018-05-0151, DMNH PAL 2018-05-0152, DMNH PAL 2018-05-0153, DMNH PAL 2018-05-0154, DMNH PAL 2018-05-

0156, and DMNH PAL 2018-05-0157 figured here (Fig. 3). DMNH PAL 2018-05-0134, although not complete, is the only known tooth with an attached root.

**Referred Specimens**

274 tooth crowns, with DMNH PAL 2018-05-0160, DMNH PAL 2018-05-0161, DMNH PAL 2018-05-0162, DMNH PAL 2018-05-0163, DMNH PAL 2018-05-0164, DMNH PAL 2018-05-0165, DMNH PAL 2018-05-0166, DMNH PAL 2018-05-0167, DMNH PAL 2018-05-0168, DMNH PAL 2018-05-0169, DMNH PAL 2018-05-0170, DMNH PAL 2018-05-0171, DMNH PAL 2018-05-0172, DMNH PAL 2018-05-0173, DMNH PAL 2018-05-0174, DMNH PAL 2018-05-0175, DMNH PAL 2018-05-0176, DMNH PAL 2018-05-0177, DMNH PAL 2018-05-0178, and DMNH PAL 2018-05-0179 being complete. Additional referred specimens (broken tooth crowns and fragments) are listed in the supplementary information, with some numbers containing multiple fragments. Extra material is present from the 'Bowman Site' PFV 089, 16 partial crowns, some specimen numbers contain multiple teeth: PEFO 42295, PEFO 42103, PEFO 42133, PEFO 42228, PEFO 42267, PEFO 42295.

**Locality and Age**

'Green Layer' locality (Fig.1), Jim Camp Wash Beds, Sonsela Member, Chinle Formation, Arizona. Found southeast of Petrified Forest National Park, the 'Green Layer' is an interbedded green and white sandstone matrix (Burch et al. 2024). This locality can be placed in the Revueltian holochronozone using aetosaur and phytosaur biostratigraphy (Stocker et al. 2019; Kligman et al. 2020) and can be dated to between 218.071 ± 0.088 Ma and 213.870 ± 0.078 Ma based on U-Pb detrital zircon ages of deposits that bracket this locality (Ramezani et al. 2011, Kligman et al. 2020) making it middle Norian in age. The 'Green Layer' has already yielded new

terrestrial vertebrates: a stem anuran (Stocker et al. 2019), a trilophosaurid (Kligman et al. 2020), and a venomous reptile (Burch et al. 2024). The site is highly productive, and study is ongoing.

**Diagnosis**

A species based on isolated tooth crowns. Teeth are small, with most crowns between 1-1.6 mm mesiodistally, rarely exceeding 2 mm (diagnostic character labelled 1 in Figure 2), and are approximately twice as mesiodistally long as they are apicobasally tall (2 in Figure 2). The principal cusp is large and triangular in labial/lingual view, extending upwards, typically at a 90° angle from the base, though this can range from around 70° with the cusp pointing distally (3 in Figure 2). 2-3 cristae radiate from the apex on the lingual side (4 in Figure 2) though a distinct lingual peg is absent as in *Lonchidion babulskii* (Cappetta & Case 1975). The crown is smooth without ornamentation. Lateral cusplets are either absent (fig. 3G-H), or poorly defined, reaching only 25% of the height of the principal cusp when measured from the level of the top of the labial peg (5 in Figure 2), though there is a clear angle change between the occlusal crest of the principal cusp and the rest of the occlusal crest. The labial peg is relatively small or absent, being no more than ~20% of the total labiolingual width at the widest point (6 in Figure 2).

*Lonchidion minimorsus* differs from *Lonchidion breve breve* in the presence of cristae on the lingual side, which the latter lacks (Patterson 1966). In *Lonchidion minimorsus* the central cusp is larger and more well defined than the low cusp of *Lonchidion breve breve.* (Patterson 1966).

The Cretaceous-aged teeth of *Lonchidion babulskii* from New Jersey (Cappetta & Case 1975) are far larger than those of *Lonchidion minimorsus*, reaching 6-7 mm long.

It differs from *Lonchidion breve crenulatum* in that *Lonchidion minimorsus* lacks the crenulations of the occlusal margin and striations on the labial and lingual faces (Patterson 1966)

The teeth of *Lonchidion breve pustulatum* are larger than those of *Lonchidion minimorsus* with the smallest teeth of the subspecies being 1.8 mm, close to the larger teeth of *Lonchidion minimorsus*. *Lonchidion breve pustulatum* has fine, irregular crenulations and small accessory cusplets (Patterson 1966) that are not seen in *Lonchidion minimorsus.*

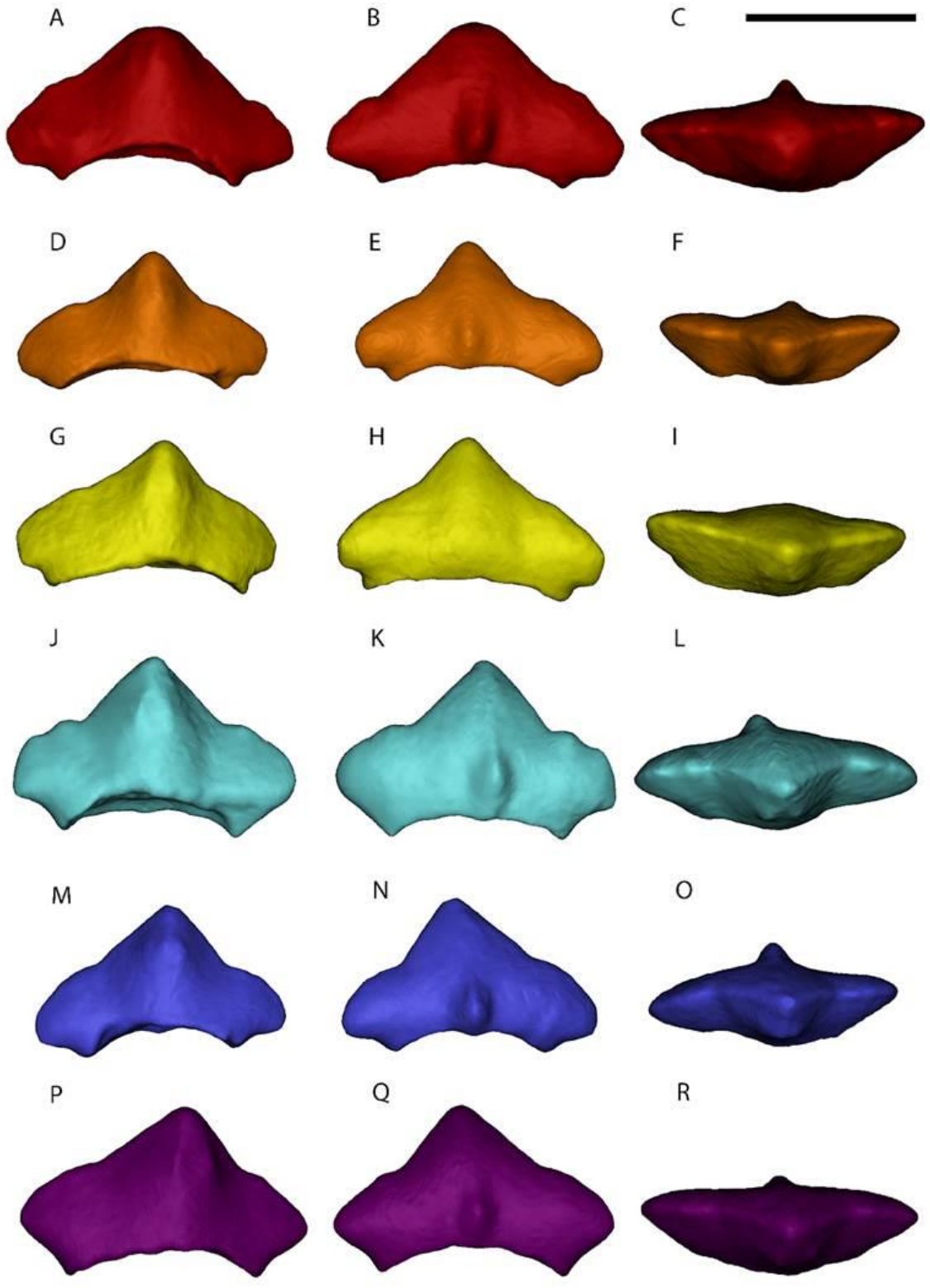
A
B
C
D
E
F
G
H
I
J
K
L
M
N
O
P
Q
R

**Figure 3.** μCT models of select paratype teeth. DMNH PAL 2018-05-0150 in lingual (A), labial (B), occlusal views (C); DMNH PAL 2018-05-0151 in lingual (D), labial (E), occlusal views (F); DMNH PAL 2018-05-0152 in lingual (G), labial (H), occlusal views (I); DMNH PAL 2018-05-0153 in lingual (J), labial (K), occlusal views (L); DMNH PAL 2018-05-0154 in lingual (M), labial (N), occlusal views (O); DMNH PAL 2018-05-0156 in lingual (P), labial (Q), occlusal views (R). Scale bar is 1mm.

**Description**

The teeth of *Lonchidion minimorsus*, like many other hybodontiform teeth, were exclusively found as crowns due to the porosity of the root making it susceptible to being lost during taphonomy (Case 1987), and it being weakly attached to the crown in Mesozoic forms (Koot et al. 2013) or potentially resorbed (Böttcher 2024), hence the vast majority being rootless. This is typical of hybodontiform teeth, of which 90-100% are found without a root in various deposits (Böttcher 2024). The gross shape of the teeth of *Lonchidion minimorsus* with one prominent central cusp that is always taller than the rest of the crown and lateral cusps if present is diagnostic of hybodontiform teeth (Koot et al. 2013). The assignment of *Lonchidion minimorsus* to the group Lonchidiidae (Rees and Underwood 2002) is supported by the small size, greater mesiodistal length than height, well developed labial peg, and poorly defined cusplets in *Lonchidion minimorsus*. Furthermore, the un-ornamented, labiolingually narrow, gracile teeth with a labial protruberence of *Lonchidion minimorsus* are diagnostic of the genus *Lonchidion* (Rees 2008).

There is a small degree of variation among specimens of *Lonchidion minimorsus* most likely indicating the different regions of the mouth each tooth came from, as is typical in hybodontiforms (Ginter et al. 2010) and many chondrichthyans, with differences between lateral cusp (or lack thereof) shape, and labial peg size. Labial pegs are larger in the more anterior teeth and less defined or absent in the more posterior teeth of heterodont taxa in Lonchidiidae (Rees & Underwood 2002). In *Lonchidion minimorsus,* the labial peg and labial crest are rarely absent (Fig. 3 G-H). The mediolateral compression that is apparent in the labial peg of many specimens is typical of the genus *Lonchidion* (Rees & Underwood 2002).

The labial crest of *Lonchidion minimorsus* is weakly visible when present but extends the full height of the crown from the apex to the labial peg (e.g. Fig. 3N). There is a lack of ornamentation or cusplet seen on the labial peg of *Lonchidion minimorsus*, unlike that in *Lonchidion derenzii* (Manzanares et al. 2017) or the type species, *Lonchidion selachos* (Estes 1964). Instead, the peg is rounded and smooth in *Lonchidion minimorsus*. There are also no "nodes" around the labial peg or on the lingual side in *Lonchidion minimorsus*, as in *Lonchidion estesi.* I note, however, that the labial peg has the functional role of interlocking teeth from adjacent tooth files in some Lonchidiidae and *Lissodus* (Rees & Underwood 2002, Rees 2008). This important functional role may make it unsuitable for use in systematics within Lonchidiidae (Rees and Underwood 2002). Around the labial peg, the surface of *Lonchidion minimorsus* is usually convex or straight, in contrast with the Indian taxon *Lonchidion incumbens*, where the crown also overhangs the labial peg (Prasad et al. 2008).

The root of DMNH PAL 2018-05-0134 (fig. 4) is "bean shaped" and shows anaulacorhize (porous) root vascularization with a line of seven large foramina, apicobasically elongated, apically on the convex edge. These foramina are roughly symmetrical. The rest of the

root is also heavily vascularized and has smaller circular foramina on the ventral side that can be seen in the cross section given by the missing labial side. The root extends out from the junction between root and crown almost as far as the full mesiodistal length of the crown. In DMNH PAL 2018-05-0134, the crown is 1.25 times deeper apicobasally than the root at its deepest – this small difference is noted as an anatomical feature in the genus *Lonchidion* (Patterson 1966).

**Figure 4.** DMNH-PAL 2018-05-0134 in lingual view. Scale bar is 1mm.

The teeth of *Lonchidion minimorsus* are the same length as those in *Lonchidion humblei* but the crown in *Lonchidion humblei* does not angle downwards at the mesial and distal edges of the occlusal crest like *Lonchidion minimorsus* does and instead retains a higher crown with a

flatter or even concave root (on the apical surface) (Murry 1981, Murry 1989) than the convex root and crown base of *Lonchidion minimorsus.*

The labial peg of *Lonchidion humblei* is generally more prominent than in *Lonchidion minimorsus* (Murry 1981, Heckert et al. 2007). *Lonchidion humblei* lacks the cristae seen on the lingual side of the crowns of *Lonchidion minimorsus* as are also absent in *Lonchidion breve breve*. There are distinct similarities between *Lonchidion minimorsus* and some of those figured as *Lonchidion humblei* by Heckert (2004) (e.g. NMMNH P-42049). However, as will be explored below, I disagree that these are the same species as *Lonchidion minimorsus*.

**RESULTS**

The teeth of *Lonchidion minimorsus* are highly abundant at the 'Green Layer' locality, and the many specimens allow us to look at variation within this species. From my 3D geometric morphometric analysis, it is clear that there is not a great deal of variation among the 'Green Layer' locality teeth. This especially can be seen in the thin plate splines, which generally show only a small amount of warping of space. Together, the first two principal components (PCs) represent 72.47% of variation between teeth. PC1, accounting for 60.67% of the variation, appears to reflect the mesiodistal length of the teeth, with longer teeth at the negative end. PC2,

accounting for 11.8% of variation, seems to reflect the height of the central

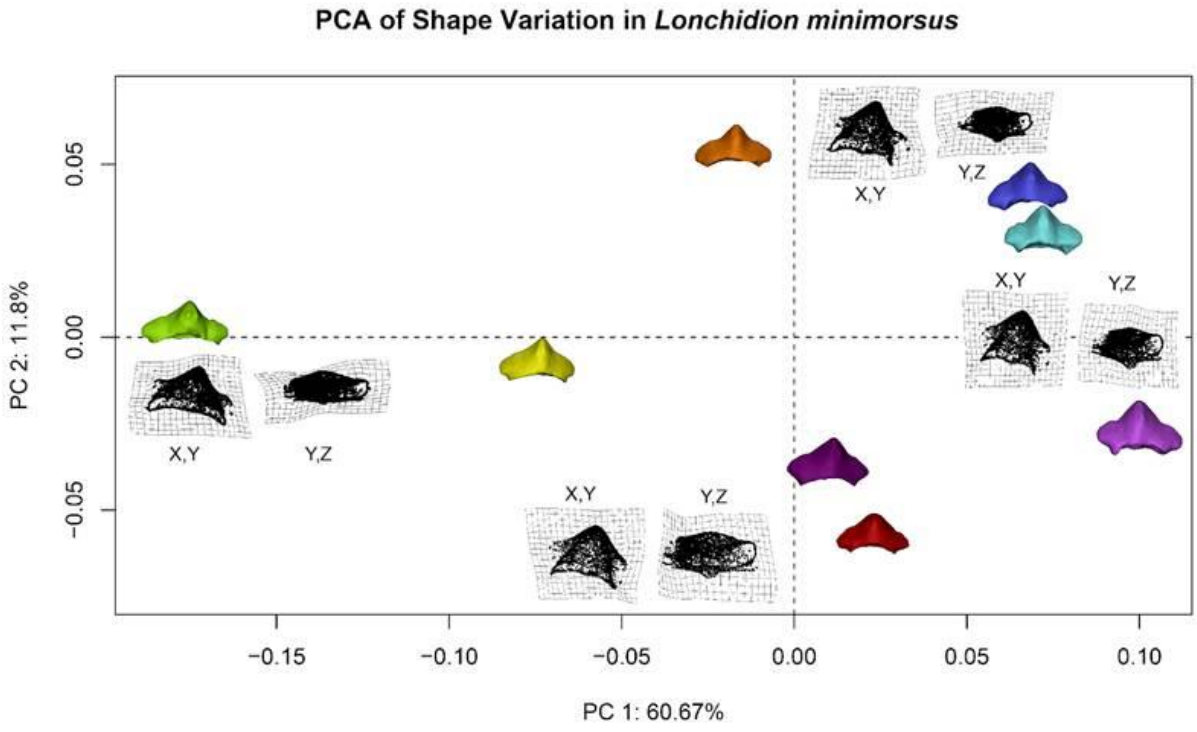


**Figure 5.** Morphospace plot from the 3DGM with thin plate splines at the extremes of the axis. Teeth icons are where those individual specimens plot

cusp, with a taller cusp in the positive. The utility of solely analysing the 'Green Layer' teeth is limited, but ideally, in the future, others may be able to add to this matrix to compare teeth from other localities or species.

Teeth referable to *Lonchidion minimorsus* are also known from broken crowns (Fig.7) from a site within Petrified Forest National Park locality PFV 089 ('Bowman Site') further allowing us to look at variation within two assemblages. I recognise the more fragmentary and less abundant 'Bowman Site' teeth as belonging to *Lonchidion minimorsus* by the presence of a tall principal cusp angled 90° perpendicular from the base, the general presence of a labial peg, a

lack of accessory cusplets, and the presence of two-three cristae on the lingual side. This description matches the diagnosis given here for *Lonchidion minimorsus* and fits within the variation seen in the 'Green Layer' locality teeth. The two populations overlap completely in a non-metric multidimensional scaling (NMDS) analysis (Fig. 6), providing more evidence that they are the same species with a relatively conserved dentition.

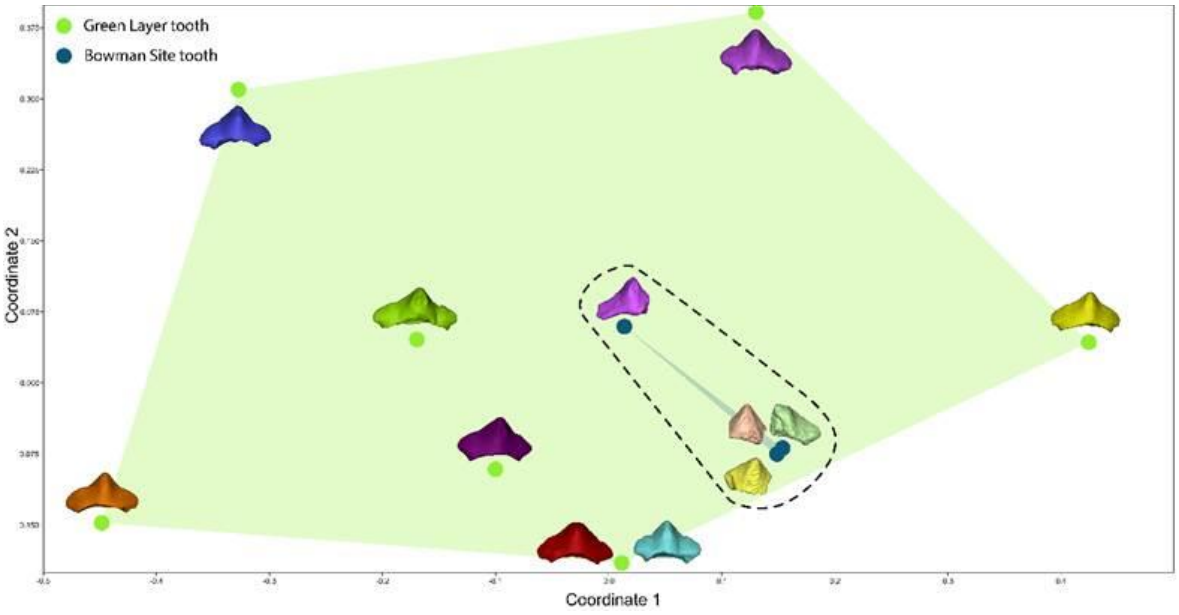


**Figure 6.** NMDS ordination showing variation of 'Green layer' and 'Bowman' locality teeth. Teeth are next to the point that represents them in the same colours as in figures 3 ('Green Layer') and 5 ('Bowman Site'). Teeth are in lingual view. 'Bowman' teeth are highlighted within the dashed line.

## DISCUSSION

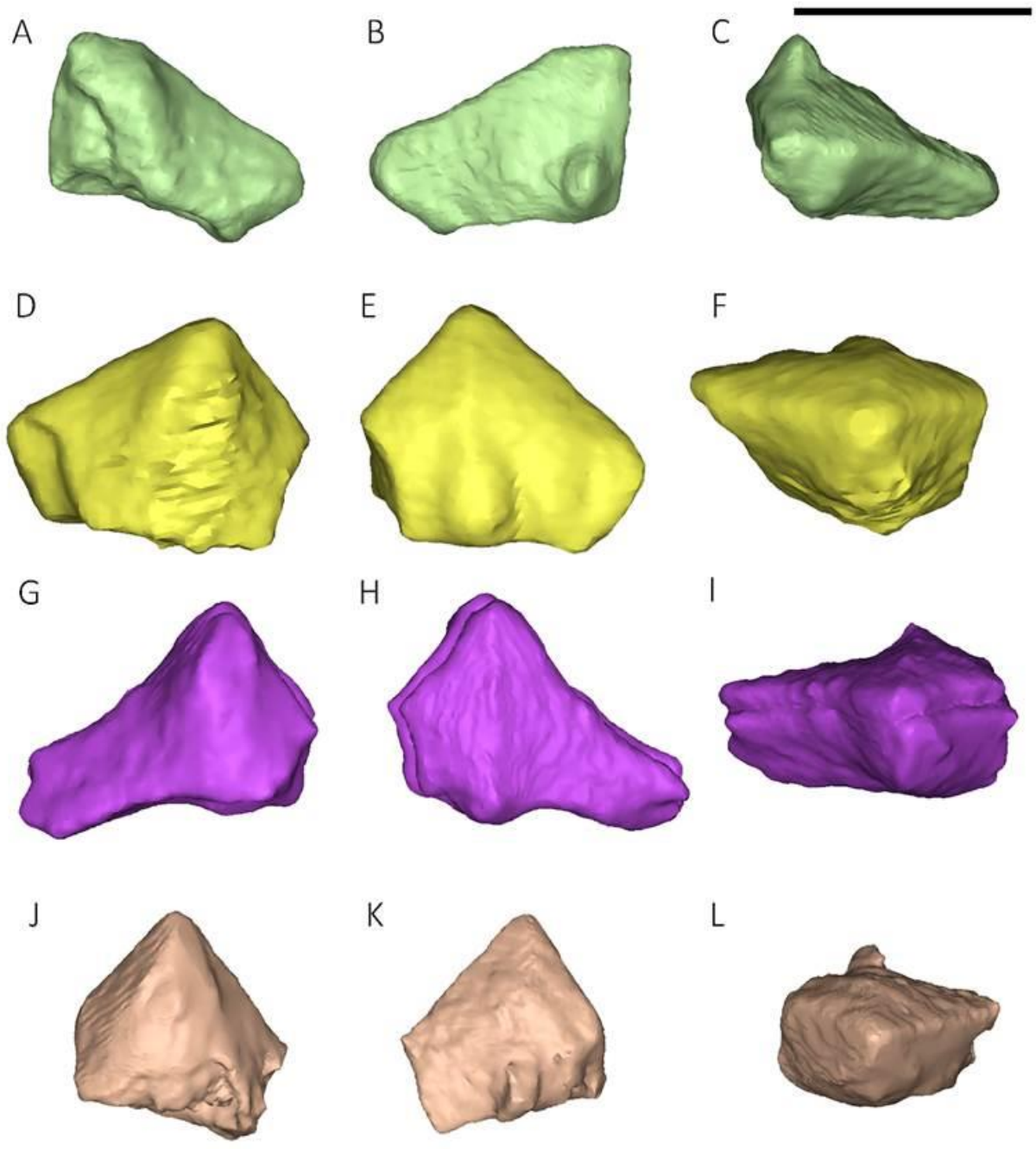


**Figure 7.** µCT models of select Bowman Site teeth. PEFO 42103[a] in lingual (A), labial (B), occlusal views (C); PEFO 42267 in lingual (D), labial (E), occlusal views (F); PEFO42103[b] in

lingual (G), labial (H), occlusal views (I); PEFO 42103[c] in lingual (J), labial (K), occlusal views (L). Scale bar is 1mm.

**Identification**

We assign the teeth of *Lonchidion minimorsus* to hybodontiforms, Lonchidiidae and *Lonchidion* based on the following features. Teeth with one central cusp that is taller than the rest of the crown and any lateral cusps as seen in *Lonchidion minimorsus* is diagnostic of hybodontiforms (Koot et al. 2013). Lonchidiidae teeth are typically small, with a longer length than width, a well-developed labial peg, and poorly defined cusplets (Rees & Underwood 2002), all of which are present in *Lonchidion minimorsus*. Un-ornamented, labiolingually narrow and gracile teeth with a labial protuberance are all diagnostic of the genus *Lonchidion* (Rees 2008) and are all seen in *Lonchidion minimorsus*.

It seems likely that *Lonchidion humblei* is a close relative of *Lonchidion minimorsus*, given their overall gross similarities (general shape, number, location, and shape of cusps) and the presence of *Lonchidion humblei* in the Chinle, including in older sediments (Blue Mesa Member, Adamanian) within Petrified Forest National Park (Heckert et al. 2007).

**Variation**

There appears to be more shape variation in the 'Bowman Site' teeth regarding the mesiodistal length of the teeth. This is likely due to teeth coming from different areas of the mouth than their being separate species as short and deep teeth (eg. PEFO 42267, D-F fig 5) are often from the anterior portion of the mouth in hybodontiforms (Patterson 1966). However, the

NMDS analysis shows that there is more variation in the 'Green Layer' population when looking at discrete characters, though this may be simply a result of having more complete teeth from the 'Green Layer' than the 'Bowman Site'. I did not include all 200 crowns of *Lonchidion minimorsus* because they fall within the variation seen in the chosen tooth crowns in this analysis.

Having two populations of the same taxon suggest that the two localities – the 'Green Layer' and 'Bowman Site' are similar in age and can be biostratigraphically correlated. This is supported stratigraphically given that the two microvertebrate sites are located within the lower portion of the Jim Camp Wash beds of the Sonsela Member, Chinle Formation (Martz & Parker 2010). Similar taxa at both localities, for example the phytosaur *Machaeroprosopus*, and the aetosaurs *Paratypothorax* and *Typothorax* (Parker 2006) also support a similar age. The taxon *Machaeroprosopus* places both sites within the Revueltian holochronozone (Martz & Parker 2017). The presence of abundant *Revueltosaurus* teeth – a taxon indicative of the Revueltian – at both sites further confirms this. The fluvial deposits the two sites *Lonchidion minimorsus* are found within indicate that these were freshwater hybodontiforms. Teeth of *Lonchidion minimorsus* are not known to stratigraphically occur above or below the Sonsela Member. Taken together, the presence of *Lonchidion minimorsus* can be used as another index taxon for the early Revueltian marking the faunal turnover seen at the Adamanian – Revueltian boundary (Parker & Martz 2010).

**Implications for other Chinle Formation hybodontiforms**

The variation and distribution of *Lonchidion minimorsus* have implications for the hybodontiform record in the Chinle Formation and Dockum Group. Until now, *Reticulodus* was the only hybodontiform known from the Sonsela Member or younger sediments within the Chinle Formation of Petrified Forest National Park (Hodnett et al. 2022) whereas *Lonchidion humblei* was recorded in the Blue Mesa Member of the Chinle Formation (Adamanian holochronozone) (Hodnett et al. 2022). The teeth of *Lonchidion minimorsus* found at the 'Bowman Site' PV 089 therefore represent only the second known hybodontiform found within the Sonsela Member and can be used to identify the start of the Revueltian and could be used to differentiate between the Blue Mesa and Sonsela Members in the wider area.

Outside of the Chinle Formation within Petrified Forest National Park, *Lonchidion minimorsus* helps interpret other hybontiform occurrences. A single hybodontiform tooth (NMMNH P 41820), attributed from *Lonchidion humblei,* is reported from the middle – late Revueltian Snyder Quarry in New Mexico, significantly younger than the occurrences of *Lonchidion humblei* in other deposits (Heckert & Jenkins 2005). However, the preservation of this tooth is poor, exhibiting extensive pitting and a rounded and smoothed appearance with a taphonomically worn cusp. This could be a much later occurrence of *Lonchidion minimorsus* or potentially even a different taxon altogether, but it is too worn to be assigned to *Lonchidion humblei* with confidence.

Teeth of *Lonchidion humblei* that reflect the general form of *Lonchidion minimorsus* have been identified from central New Mexico from NMMNH locality 354 (NMMNH P 42049, NMMNH P 31634, NMMNH P 31635) in the Ojo Huelos Member (Heckert 2004). However, I do not consider them to be *Lonchidion minimorsus* based on age, discrete characters, and variation seen within the two populations of *Lonchidion minimorsus* described here.

NMMNH locality 354 appears considerably older than the Sonsela Member sediments in which the specimens described in this paper are found and can be placed in the Adamanian or older based on the presence of *Saurichthys* teeth (Nesbitt pers. com.). These teeth, which in this case previously were identified only as actinopterygian teeth (Heckert 2004), are abundant in Early-Middle Triassic freshwater, marine and brackish deposits, but rare in Late Triassic freshwater sediments (Stack et al. 2025). As freshwater *Saurichthys* is only known from the Blue Mesa Member of the Chinle Formation (Kligman et al. 2017) and the Otischalkian Boren Ranch Beds of the Dockum Group of Texas or from older sediments in the USA (Stack et al. 2025) its presence suggests an older age is most probable for NMMNH locality 354 than the 'Green Layer' locality or the 'Bowman Site' PV 089.

The teeth from NMMNH locality 354 were assigned to *Lonchidion humblei* based on tooth crowns that are "small, low-crowned, lack accessory cusps, and generally possess a prominent labial peg surmounted by a transverse ridge that intersects the otherwise smooth and unornamented occlusal crest" (Heckert 2004 pp 107). In figures (pp 107-108), these teeth appear remarkably similar to those of *Lonchidion minimorsus* in gross shape, the presence of a labial peg, and the lack of accessory cusps. However, both the figures and description lack any cristae as are seen on the lingual side of *Lonchidion minimorsus* teeth. In addition to this, the teeth are extremely small, with many noted to be less than 0.8 mm long and some only reaching 0.5 mm in length. This contrasts with *Lonchidion minimorsus*, which has a minimum size of approximately 1 mm long. The labial peg is also far more prominent in the figured teeth than it is in any *Lonchidion minimorsus* specimens. Based on the limited variation seen in *Lonchidion minimorsus* in size and shape, it is considered unlikely that these represent the same species.

Variation seen in *Lonchidion minimorsus* at the 'Green Layer' locality has implications for *Lonchidion humblei*, which is known from a variable dentition with multiple morphotypes (Murry 1981, Heckert 2004) suggesting that were the 'Green Layer' hybodontiform *Lonchidion humblei* we would find the other morphotypes of this tooth at this site, which we do not. It may be that the variation of discrete shapes seen in *Lonchidion humblei* is characteristic of the species, whereas we see more continuous variation in *Lonchidion minimorsus* with only slight differences among the individual teeth in things such as the presence or absence of lateral cusplets (which are already small when they are present) or the mesiodistal length. Given the extensive sampling of 'Green Layer' locality sediments thus far, uncovering and continuing to uncover hundreds of crowns that fit within the variation seen in *Lonchidion minimorsus,* along with the distinct *Reticulodus* (Murry & Kirby 2002, Voris & Heckert 2017), represented by rectangular crushing tooth plates which can easily range from near square to at least four times long as they are wide at this site, it seems highly unlikely that any new hybodontiform morphotypes in significant numbers to match those we see will be recovered.

Another possibility is that the similar teeth noted by Heckert 2004 (e.g. Fig. 90) are not *Lonchidion humblei*. It is true that they do not fully reflect those teeth figured in the original description, having much more ventrally angled crowns with a U-shaped base as opposed to those described by Murry (1981), which retain a high angle of the mesial and distal corners of the crown and flat bases. Some morphotypes noted by Murry (1981) do not have a central cusp at all and many have crenulations and minute accessory cusps, which do not match either *Lonchidion minimorsus* or the teeth figured by Heckert (2004) pp 107-108.

Many of the referred specimens in previous publications lack specimen numbers and are difficult or impossible to reevaluate (e.g. Murry 1989).

## CONCLUSIONS

*Lonchidion minimorsus* is a new species of hybodontiform known only from the Jim Camp Wash Beds of the Sonsela Member of the Chinle Formation. The occurrence of *Lonchidion minimorsus* at both the 'Green Layer' locality and the 'Bowman Site' PFV 089 within Petrified Forest National Park further strengthens the link between these two localities as having been deposited at similar times. The loss of *Lonchidion humblei* before the Revueltian and the appearance of *Lonchidion minimorsus* above the Adamanian-Revueltian boundary suggests that chondrichthyans were part of the faunal turnover during this time. These specimens further expand the known diversity of hybodontiforms from the Late Triassic of western North America.

## ACKNOWLEDGMENTS

I thank J. Socha for access to and training, and B. Kligman for training me on the μCT scanner. The Virginia Tech Paleobiology Group conducted fieldwork at the 'Green Layer Locality', processed the material, handpicked the specimens and provided useful discussion. V. Yarborough aided with photomicroscopy. Thank you to Matthew Smith for access to PEFO specimens. Thanks are given to Dr.Valentine Fischer for providing R code and discussion

## REFERENCES

1. Błażejowski, B. 2004. Shark teeth from the Lower Triassic of Spitsbergen and their histology. *Polish Polar Research* **25(2)**: 153-167.
2. Böttcher, R. 2024. Root resorption during tooth replacement in sharks – a unique character of the Hybodontiformes (Chondrichthyes, Elasmobranchii). *Palaeodiversity* **17(2)**: 121-194.
3. Burch, H.E., Eddins, H.S., Stocker, M.R., Kligman, B.T., Marsh, A.D., Parker, W.G. & Nesbitt, S.J. 2024. A small venomous reptile from the Late Triassic (Norian) of the southwestern United States. *PeerJ* **12**: e18279.
4. Cappetta, H. 2012. Chondrichthyes. Mesozoic and Cenozoic Elasmobranchii: Teeth. In: Schultze, H. P. (Ed.). *Handbook of Paleoichthology, Vol. 3E*. Verlag Dr. Friedrich Pfeil, München, 512 pp.
5. Case, G.R. 1987. A new selachian fauna from the late Campanian of Wyoming (Teapot Sandstone Member, Mesaverde Formation, Big Horn Basin). *Palaeontographica Abteilung A* **197**: 1-37.
6. Case, G.R. & Schwimmer, D.R. 1988. Late Cretaceous fish from the Blufftown Formation (Campanian) in western Georgia. *Journal of Paleontology* **62 (2)**: 290–301
7. Duffin, C. J. 1985. Revision of the hybodont selachian genus Lissodus Brough (1935). *Palaeontographica (A)* **188(4–6)**:105–152.
8. Estes, R. 1964. Fossil vertebrates from the Late Cretaceous Lance Formation eastern Wyoming. *University of California Publications in Geological Sciences* **49**: 1- 187.
9. Everhart, M.J. 2011. Occurrence of the hybodont shark genus *Meristodonoides* (Chondrichthyes; Hybodontiformes) in the Cretaceous of Kansas. *Transactions of the Kansas Academy of Science* **114(1-2)**: 33-46.

10. Fischer, J. 2008. Brief synopsis of the hybodont form taxon *Lissodus* Brough, 1935, with remarks on the environment and associated fauna. – *Paläontologie, Stratigraphie, Fazies* (16), Freiberger Forschungshefte, C **528**: 1–23.
11. Fischer, J.A., Axsmith, B.J. & Ash, S.R. 2010. First unequivocal record of the hybodont shark egg capsule *Palaeoxyris* in the Mesozoic of North America. *Neues Jahrbuch für Geologie und Paläeontologie* **255**: 327-244.
12. Ginter, M. 2022. The biostratigraphy of Carboniferous chondrichthyans. *Geological Society, London, Special Publications* **512**: 769-790.
13. Ginter, M., Hampe, O. and Duffin, C. 2010. Chondrichthyes (Paleozoic Elasmobranchii: teeth). Handbook of Paleoichthyology, Vol. 3D. Verlag Dr. Friedrich Pfeil, München, 165 pp.
14. Gower, J.C. 1971. A general coefficient of similarity and some of its properties. *Biometrics* **27**: 857-874.
15. Hammer, Ø., Harper, D., Ryan, P. 2001. PAST-Palaeontological statistics software package for education and data analysis. *Palaeontologia Electronica* **4(1)** 1-9.
16. Hay, O.P. 1902. Bibliography and catalogue of the fossil Vertebrata of North America. *US Geological Survey Bulletin* **179***:* 1-868.
17. He, T., Sone, M., Hirayama, R., Yoshida, M., Komatsu, T., Khamha, S. & Cuny, G. 2017. First hybodont shark assemblage from the Cretaceous of Malaysia: updated report. *Research and Knowledge* **3(2)**: 69-70.
18. Heckert, A.B. 2004. Late Triassic microvertebrates from the lower Chinle Group (Otischalkian – Adamanian: Carnian), southwestern USA. *New Mexico Museum of Natural History and Science Bulletin* **27**: 1-170.

19. Heckert, A.B., Ivanov, A. & Lucas, S.G. 2007. Dental morphology of the hybodontid shark *Lonchidion humblei* Murry from the Upper Triassic Chinle Group, USA. *New Mexico Museum of Natural History and Science Bulletin* **41**: 45-48.

20. Heckert, A. B. and Jenkins, H. S. 2005. The microvertebrate fauna of the Upper Triassic (Revueltian) Snyder Quarry, north-central New Mexico. In Lucas, S. G., Zeigler, K. E., Lueth, V. W. and Owen, D. E eds. *New Mexico Geological Society, 56th Field Conference Guidebook, Geology of the Chama Basin* 319 – 334. Albuquerque : Starline Printing.

21. Herman, J. 1977. Les Sélaciens des terrains néocrétacés and paléocènes de Belgique et des contrées limitrophes. Eléments d'une biostratigraphic intercontinentale. *Mémoires pour servir à l'explication des Cartes géologiques et Minières de la Belgique* **15**: 1-401.

22. Hodnett, J-P.M., Tweet, J.S. & Santucci, V.L. 2022. The occurrence of fossil cartilaginous fishes (Chondrichthyes) within the parks and monuments of the National Park Service. *New Mexico Museum of Natural History and Science Bulletin* **90**: 183-208.

23. Huxley, T.H. 1880. On the application of the laws of evolution to the arrangement of the Vertebrata, and more particularly of the Mammalia. *Proceedings of the Scientific Meetings of the Zoological Society of London* **43**: 649–662.

24. Johns, M.J., Albanesi, G.L. & Voldman, G.G. Freshwater shark teeth (Family Lonchidiidae) from the Middle-Upper Triassic (Ladinian – Carnian) Paramillo Formation in the Mendoza Precordillera, Argentina. *Journal of Vertebrate Paleontology* **34(3)**: 512-523.

25. Kaye, F.T., & Padian, K. 1994. Microvertebrates from the *Placerias* Quarry: a window on Late Triassic vertebrate diversity in the American southwest. *In* N.C. Fraser and H.-D.

Sues (eds.), In the Shadow of the Dinosaurs: Early Mesozoic Tetrapods. Cambridge University Press, New York. pp. 171-196.

26. Kligman, B.T., Parker, W.G. & Marsh, A.D. 2017. First record of *Saurichthys* (Actinopterygii) from the Upper Triassic (Chinle Formation, Norian) of western North America. *Journal of Vertebrate Paleontology* **37(5)**: e1367304

27. Kligman, B.T., Marsh, A.D., Nesbitt, S.J., Parker, W.G. & Stocker, M.R. 2020. New trilophosaurid species demonstrates a decline in allokotosaur diversity across the Adamanian-Revueltian boundary in the Late Triassic of western North America. *Palaeodiversity* **13(1)**: 25-37.

28. Koot, M.B., Cuny, G., Tintori, A. & Twitchett, R.J. 2013. A new diverse shark fauna from the Wordian (Middle Permian) Khuff Formation in the interior Haushi-Huqf area, Sultanate of Oman. *Palaeontology* **56**: 303-343.

29. Maisey, J.G. 1975. The interrelationships of phalacanthous selachians. *Neues Jahrbuch für Geologie und Paläontologie Monatshefte* **9**: 553–567.

30. Manzanares, E., Pla, C., Martínez-Pérez, C., Ferrón, H. & Botella, H. *Lonchidion derenzii*, sp. nov., a new lonchidiid shark (Chondrichthyes, Hybodontiforms) from the Upper Triassic of Spain, with remarks on lonchidiid enameloid. *Journal of Vertebrate Paleontology* **37**(1): 1-5.

31. Marsh, A.D. & Parker W.G. 2020. New dinosauromorph specimens from Petrified Forest National Park and a global biostratigraphic review of Triassic dinosauromorph body fossils. *PaleoBios* **37**: 1-56.

32. Martz, J.W. & Parker, W.G. 2010. Revised lithostratigraphy of the Sonsela Member (Chinle Formation, Upper Triassic) in the southern part of Petrified Forest National Park, Arizona. *PLoS ONE* **5(2):** e9329.

33. Murry, P.A. 1981. A new species of freshwater hybodont from the Dockum Group (Triassic) of Texas. *Journal of Paleontology* **55(3)**: 603-607.

34. Murry, P.A. 1989. Geology and paleontology of the Dockum Formation (Upper Triassic), West Texas and eastern New Mexico, *in* Lucas, S.G. and Hunt, A.P., eds., Dawn of the Age of Dinosaurs in the American Southwest: Albuquerque, New Mexico Museum of Natural History pp. 102-148.

35. Murry, P.A. and Kirby, R.E. 2002. A new hybodont shark from the Chinle and Bull Canyon Formations, Arizona, Utah, and New Mexico. *Upper Triassic Stratigraphy and Paleontology: New Mexico Museum of Natural History and Science Bulletin* **21**: 87–106.

36. Owen, R. 1846. Lectures on the comparative anatomy and physiology of the vertebrate animals, delivered at the Royal College of Surgeons of England in 1844 and 1846. Part 1. Fishes. Longman, London, 308 pp.

37. Parker, W.G. 2006. The stratigraphic distribution of major fossil localities in Petrified Forest National Park, Arizona. In Parker, W.G., Ash, S.R. & Irmis, R.B. eds. A Century of Research at Petrified Forest National Park: Museum of Northern Arizona Bulletin **62**: 46-61.

38. Parker, W.G. & Martz, J.W. 2010. The Late Triassic (Norian) Adamanian-Revueltian tetrapod faunal transition in the Chinle Formation of Petrified Forest National Park, Arizona. *Earth and Environmental Science Transactions of the Royal Society of Edinburgh* **101**: 231-260.

39. Patterson, C. 1966. British Wealden Sharks. *Bulletin of the British Museum (Natural History)* **2(7)**: 251-350.

40. Prasad, G.V.R., Singh, K., Parmar, V., Goswami, A. & Sudan, C.S. 2008. Hybodont shark teeth from the continental Upper Triassic deposits of India. pp. 413–432 in G. Arratia, H.-P. Schultze, and M.V.H. Wilson (eds.), Fishes 4–Homology and Phylogeny, Proceedings of the international meeting Miraflores de la Sierra, 2005, Verlag Dr. Friedrich Pfeil, Münichen, Germany.

41. Ramezani, J., Hoke, G. D., Fastovsky, D. E., Bowring, S. A., Therrien, F., Dworkin, S. I., Atchley, S. C. & Nordt, L. C. 2011. High-precision U-Pb zircon geochronology of the Late Triassic Chinle Formation, Petrified Forest National Park (Arizona, USA): Temporal constraints on the early evolution of dinosaurs. *Geological Society of America Bulletin* **123**: 2142–2159.

42. Rees, J. 2008. Interrelationships of Mesozoic hybodont sharks as indicated by dental morphology – preliminary results. *Acta Geologica Polonica* **58(2)**:217-221.

43. Rees, J. & Underwood, C.J. 2002. The status of the shark genus *Lissodus*, Brough, 1935, and the position of nominal *Lissodus* species within the Hybodontoidea (Selachii). *Journal of Vertebrate Paleontology* **22**: 471-479.

44. Rees, J. & Underwood, C.J. 2008. Hybodont sharks of the English Bathonian and Callovian (Middle Jurassic). *Palaeontology* **51(1):**117-147.

45. Stack, J., Nesbitt, S.J., Stricklin, M.L. & Stocker, M.R. 2025. A new species of the ray-finned fish *Saurichthys* (Actinopterygii) from the Dockum Group of Texas (Upper Triassic, Norian) highlights the late appearance of elongate jaws in neopterygians. *Journal of Vertebrate Paleontology* **44(5)**: e2470026.

46. Stumpf, S., López-Romero, F.A., Kindlimann, R., Lacombat, F., Pohl, B. & Kirwet, J. 2021. A unique hybodontiform skeleton provides novel insights into Mesozoic chondrichthyan life. *Papers in Palaeontology* **7(3)**: 1479-1505
47. Voris, J.T. & Heckert, A.B. 2017. Ontogenetic heterodonty in *Reticulodus synergus* (Chondrichthyes, Hybodontiformes) from the Upper Triassic of the southwestern U.S.A., with a redescription of the genus. *Journal of Vertebrate Paleontology* **37(4)**: e1351980
48. Williamson, T.E., Kirkland, J.I. & Lucas, S.G. 2016. Selachians from the Greenhorn Cyclothem ("middle" Cretaceous: Cenomanian-Turonian), Black Mesa, Arizona, and the paleogeographic distribution of Late Cretaceous selachians. *Journal of Paleontology* **67(3)**: 447-474.
49. Zangerl, R. 1981. Chondrichthyes I: Paleozoic Elasmobranchii in Schultze, H.P. ed. *Handbook of Paleoichthyology***.** Stuttgart, Gustav Fischer Verlag, p. 114

## APPENDICES

### Supplemental Figures

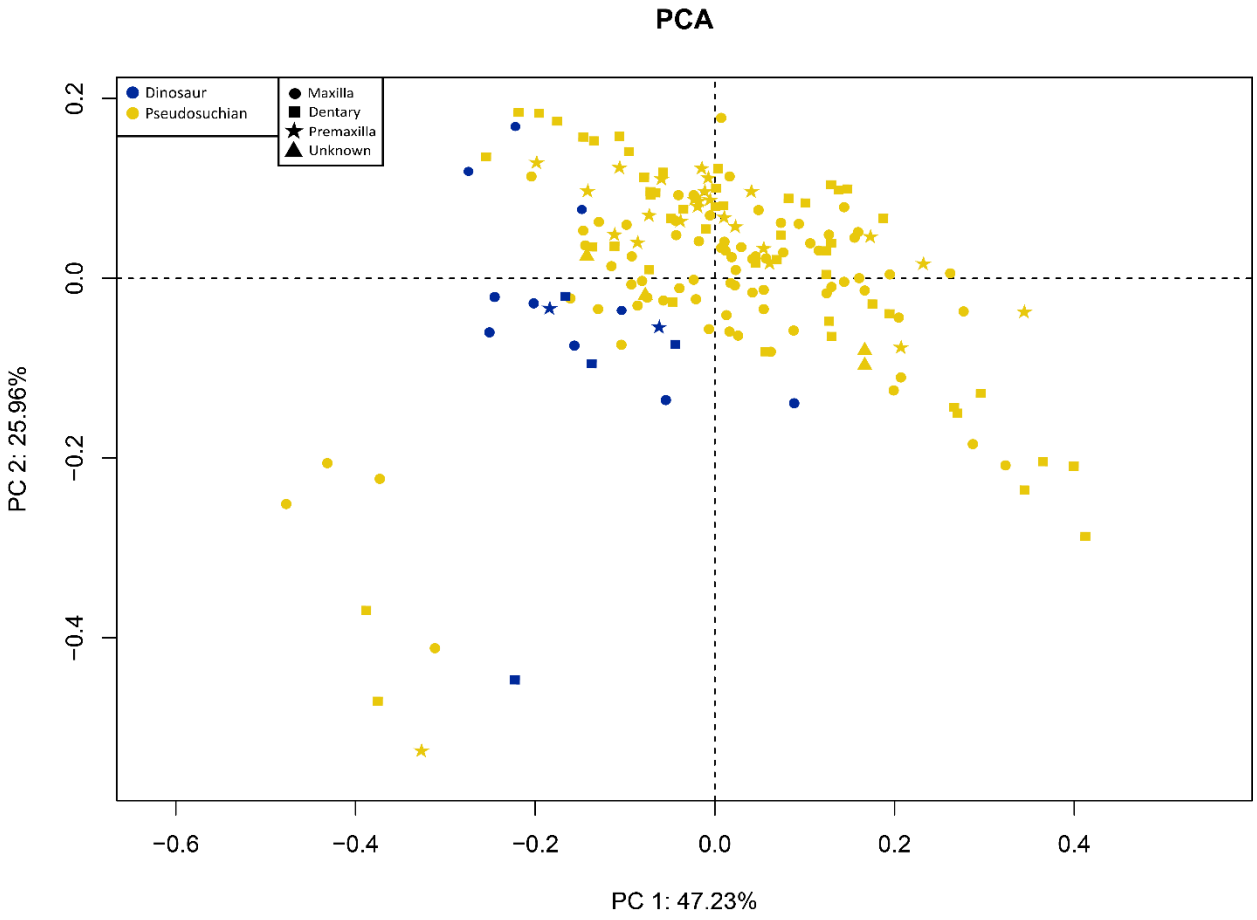


**Supplemental Figure 1.** The same PCA as Chapter 2 Figure 28, but with the major clades of dinosaurs and pseudosuchians highlighted.

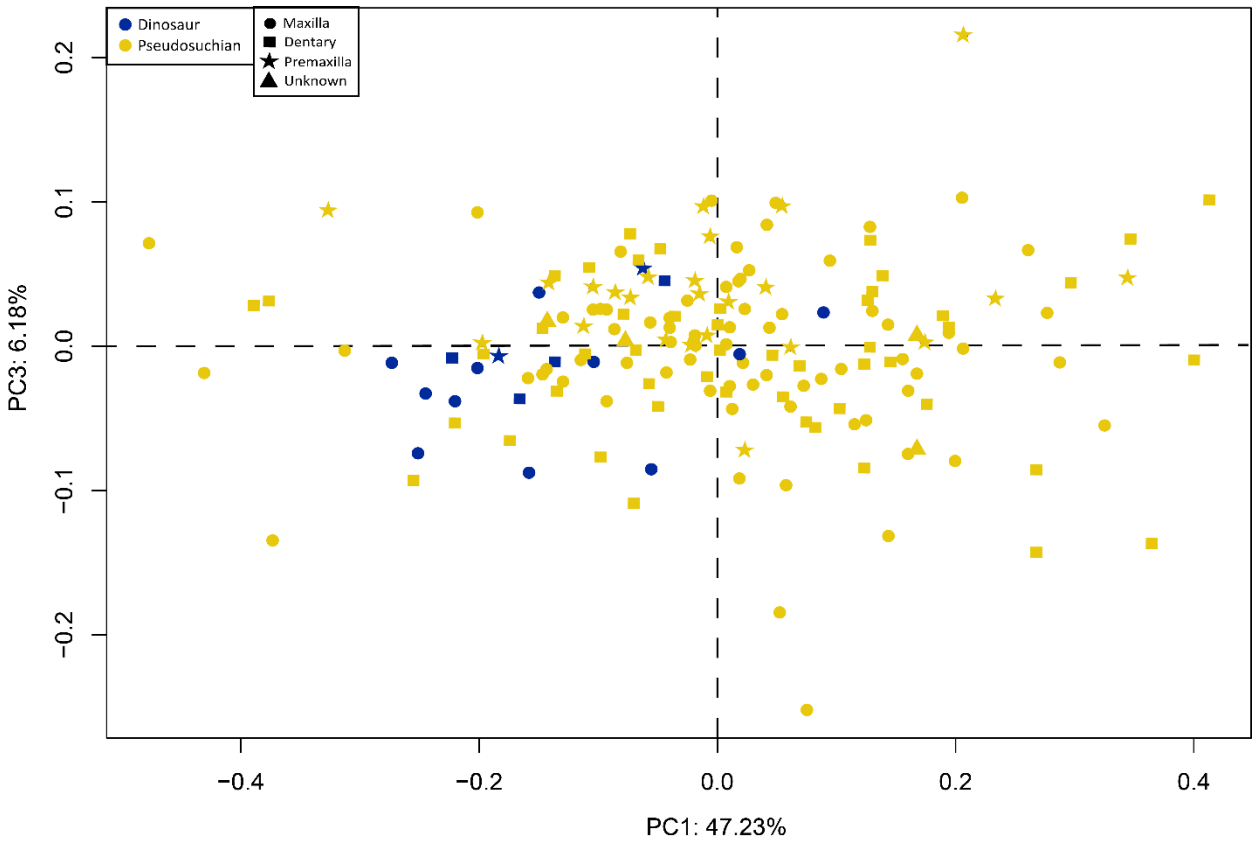


**Supplemental Figure 2.** The same PCA as Chapter 2 Figure 29, but with the major clades of dinosaurs and pseudosuchians highlighted.

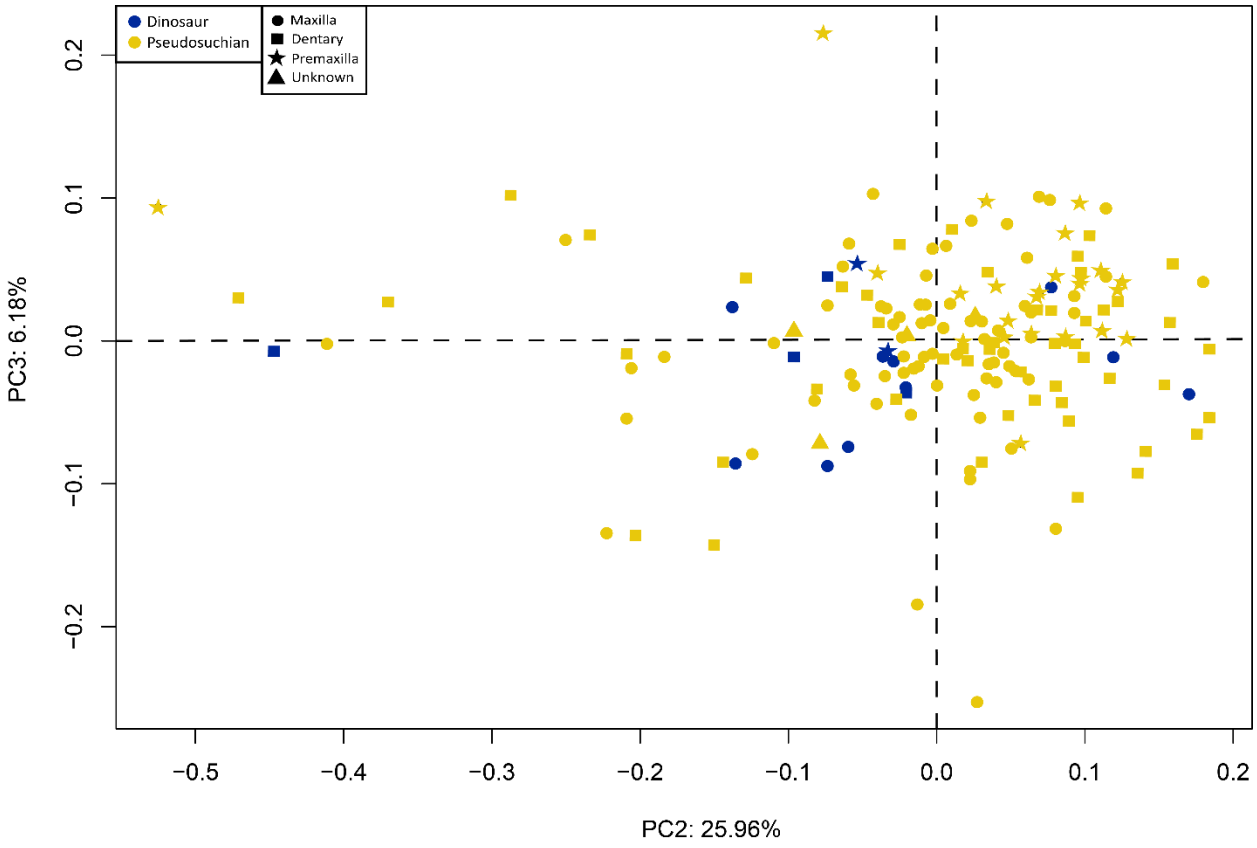


**Supplemental Figure 3.** The same PCA as Chapter 2, Figure 30, but with the major clades of dinosaurs and pseudosuchians highlighted.

**Code for all chapters**

### Simplified HD3DGM with pseudolandmarking script ###

### Written by V.Fischer 2022 ###

############################################################

```
#=========================================================#

#====================== Libraries ======================#

#=========================================================#

install.packages("geomorph")

install.packages("readxl")

install.packages("Morpho")



#Read and treat 3D data

library(geomorph)

library(readxl)

library(Morpho)



#=========================================================================
============#

#====================== Import 3D models and fixed landmarks
======================#
```

```
#=============================================================================
============#

setwd("[INSERT WORKING DIRECTORY]")



template <- read.ply(file='template2.ply') #,ShowSpecimen=FALSE)

data <- as.data.frame(read_excel("specimen_info.xlsx",na="NA")) #DF: not sure what this does



#Import all meshes with .pts data (fixed landmarks)

ptslist <- dir(pattern='.pts')

taxa_list <- substr(c(ptslist),1,nchar(c(ptslist))-4)



#Create mesh3d objects named as the ply files, it can be very long depending on the number of
files

meshlist <- list()

for(i in 1:length(taxa_list)){

  meshlist[[i]] <- try(assign(taxa_list[i],read.ply(file=paste(taxa_list[i],".ply",sep=""),
ShowSpecimen=FALSE)))
```

```
  print(paste(round(100*(i/length(taxa_list)),1),"%"))
}
names(meshlist) <- taxa_list

#Create array with all fixed landmarks of all specimens and the template
# ! very strangely enough, the coordinates exported from Checkpoint as .pts need to be multiplied by 10!
to_patch<-array(dim=c(5,3,length(ptslist)))

for(i in 1:length(ptslist)){
  to_patch[,,i]<-as.matrix(read.table(file=ptslist[i],skip=2,row.names=1))
}
dimnames(to_patch)[[3]] <- taxa_list

#============================================================#
#====================== Create the atlas ====================#
#============================================================#
```

```
###    Place the five fixed landmarks on the template or reuse the .nts file

template_lands <- digit.fixed(template,5,center=FALSE) #to place the landmarks on the dome if not done yet

template_lands <- as.matrix(read.table(file="template.nts",skip=2)) # or directly load a file



### Place the surface semi-landmarks on the template using a pseudo-landmarking method

#automatically create surface landmarks by randomly sampling 2000 coordinates of the point cloud of the template: this method draws from the pseudolandmark approach and applies it to surface landmarking

temp_points <- t(template$vb)[,1:3]

temp_points <- temp_points[temp_points[,"zpts"]>0.01,]



sample <- sample(1:nrow(temp_points),2000,replace=FALSE)

template_surface_sample <- temp_points[sample,]
```

```
#check if the template is ok

shade3d(template,col="grey")

spheres3d(template_surface_sample,radius=0.01,color="blue")




###    Create Atlas/template

atlas <- createAtlas(template,template_lands,template_surface_sample)

plotAtlas(atlas,cols=c("#FF0D68","#23CC8F"),legend=FALSE)




#=========================================================================
==#

#====================== Patching, sliding, and GPA ======================#

#=========================================================================
==#



###Patching
```

```
#Patch!

patched <- placePatch(atlas, to_patch, path="./")

#checkLM(patched, path="./", atlas=atlas, pt.size=1)



fixed <- 1:5 #in our protocol we have 5 fixed landmarks

surface <- c(1:nrow(patched))[-fixed]



#OPTIONAL: visualisation of individual teeth with their patches

shade3d(template,col="#f2d09b")

spheres3d(patched[,,1],radius=c(rep(1,5),rep(0.5,2000)),color=c(rep("#FF0D68",5),rep("#23CC8
F",nrow(patched[,,1]))))

spheres3d(patched[,,"Aetosaur_PEFO_49321_Max_Tooth_5"],radius=c(rep(1,5),rep(0.5,2000)),
color=c(rep("#FF0D68",5),rep("#23CC8F",nrow(patched[,,1]))))



###Slide and General Procrustes Analysis directly with geomorph

GPA <- gpagen(patched,surfaces=surface,ProcD=FALSE)
```

```
#Check if position of 3DLM appear correct

spheres3d(GPA$coords[,,"Aetosaur_PEFO_49321_Max_Tooth_5"],radius=c(rep(0.001,5),rep(0.
001,2000)),color=c(rep("#FF0D68",5),rep("#23CC8F",nrow(patched[,,1]))))




#=========================================================#

#====================== Morphospace ======================#

#=========================================================#


###PCA and plot basic morphospace

PCA <- gm.prcomp(GPA$coords)

summaryPCA <- summary(PCA)

PCAplot <- plot(PCA, main="PCA", cex = 0.5) ;

text(PCA$x,labels=rownames(PCA$x),adj=c(0.5,1), cex = 0.15)



#plot axis 1 against axis 3
```

```
plot(PCA$x[, 1], PCA$x[, 3], cex = 0.5, xlab = "PC1", ylab = "PC3", pch = 19);

text(PCA$x[, 1], PCA$x[, 3], labels = rownames(PCA$x), adj = c(0.5, 1), cex = 0.15)

#plot(PCA, axis1 = 1, axis2 = 3) ; text(PCA$x,labels=rownames(PCA$x),adj=c(0.5,1), cex =
0.15)

#above blanked out gives % of each component, not sure how to add into newer stuff



#=======================================# by DavideFoffa

#library(geomorph)



#setwd("C:\\Users\\david\\Desktop\\EmilyKeeble_code\\test")

#template <- read.ply(file='test2.ply') #,ShowSpecimen=FALSE)

#fixed.lms1 <- digit.fixed(spec = template, fixed = 5) # allows you to place landmarks

#write.pts(fixed.lms1, filename = "test2.pts") # writes down a pts file.



###### ANOVA by Nicholas Campione #######



## ANOVA in geomoph
```

```
install.packages("xlsx") #installs the package (only need to do this once)

library(xlsx) #access package

metadata <- read.xlsx("ch1metadata.xlsx", sheetIndex = 1) #read metadata into R, sheet 1

anova.data <- geomorph.data.frame(GPA, Age = metadata$Age, Genus = metadata$Genus,
DFA.train = metadata$Train) #sets up the data needed to run ANOVA (i.e., procD.lm)

anova <- procD.lm(coords ~ Age, data = anova.data) #runs the ANOVA

summary(anova) #generate summary of results


Gpairwise <- pairwise(anova, groups = metadata$Genus) #pairwise comparison between genera

summary(Gpairwise)


anova2 <- procD.lm(coords ~ Tooth_type, data = anova.data)

summary(anova2)

Tpairwise <- pairwise(anova, groups = metadata$Tooth_type)

summary(Tpairwise)


#### Shape analysis ####
```

```
GPA$consensus

ref <- mshape(GPA$coords)

plotRefToTarget(ref, GPA$coords [,,1], method = "points") #plots consensus shape against how it's deformed

toothlinks <- matrix(c(1,rep(2:16, each=2),1), nrow = 16, byrow = TRUE)

toothlinks

plotRefToTarget(ref, GPA$coords[,,1],

        gridPars = gridPar(tar.pt.bg = "blue", tar.link.col="blue",

                tar.link.lwd = 2), method = "points", links = toothlinks) #links exterior points, grey = consensus, blue = how it's changed

PCA$shapes$shapes.comp1$min

plotRefToTarget(ref, PCA$shapes$shapes.comp2$min,

        gridPars = gridPar(tar.pt.bg = "blue", tar.link.col="blue",

                tar.link.lwd = 2), method = "points", links = toothlinks) #shows minimum of PC1 shape

plotRefToTarget(ref, PCA$shapes$shapes.comp2$max,
```

```
gridPars = gridPar(tar.pt.bg = "blue", tar.link.col="blue",

                   tar.link.lwd = 2), method = "points", links = toothlinks) #shows maximum
```

of PC1 shape

```
#PC2

plotRefToTarget(ref, PCA$shapes$shapes.comp2$min, method = "TPS") #creates warp plot of
```

minimum shape

```
plotRefToTarget(ref, PCA$shapes$shapes.comp2$max, method = "TPS")



#PC3

plotRefToTarget(ref, PCA$shapes$shapes.comp3$min, method = "TPS")

plotRefToTarget(ref, PCA$shapes$shapes.comp3$max, method = "TPS")
```

**Additional Specimen Numbers of *Lonchidion minimorsus***

| |
|---|
| PAL 2018-05-0180 |
| PAL 2018-05-0181 |
| PAL 2018-05-0182 |
| PAL 2018-05-0183 |
| PAL 2018-05-0184 |
| PAL 2018-05-0185 |
| PAL 2018-05-0186 |

| |
|---|
| PAL 2018-05-0187 |
| PAL 2018-05-0188 |
| PAL 2018-05-0189 |
| PAL 2018-05-0190 |
| PAL 2018-05-0191 |
| PAL 2018-05-0192 |
| PAL 2018-05-0193 |
| PAL 2018-05-0194 |
| PAL 2018-05-0195 |
| PAL 2018-05-0196 |
| PAL 2018-05-0197 |
| PAL 2018-05-0198 |
| PAL 2018-05-0199 |
| PAL 2018-05-0200 |
| PAL 2018-05-0201 |
| PAL 2018-05-0202 |
| PAL 2018-05-0203 |
| PAL 2018-05-0204 |
| PAL 2018-05-0205 |
| PAL 2018-05-0206 |
| PAL 2018-05-0207 |
| PAL 2018-05-0208 |
| PAL 2018-05-0209 |
| PAL 2018-05-0210 |
| PAL 2018-05-0211 |
| PAL 2018-05-0212 |
| PAL 2018-05-0213 |
| PAL 2018-05-0214 |
| PAL 2018-05-0215 |

| |
|---|
| PAL 2018-05-0216 |
| PAL 2018-05-0217 |
| PAL 2018-05-0218 |
| PAL 2018-05-0219 |
| PAL 2018-05-0220 |
| PAL 2018-05-0221 |
| PAL 2018-05-0222 |
| PAL 2018-05-0223 |
| PAL 2018-05-0224 |
| PAL 2018-05-0225 |
| PAL 2018-05-0226 |
| PAL 2018-05-0227 |
| PAL 2018-05-0228 |
| PAL 2018-05-0229 |
| PAL 2018-05-0230 |
| PAL 2018-05-0231 |
| PAL 2018-05-0232 |
| PAL 2018-05-0233 |
| PAL 2018-05-0234 |
| PAL 2018-05-0235 |
| PAL 2018-05-0236 |
| PAL 2018-05-0237 |
| PAL 2018-05-0238 |
| PAL 2018-05-0239 |